IMPROVEMENT OF RHEOLOGICAL, MECHANICAL AND INTERFACE PROPERTIES OF SOLID ROCKET MOTOR LINER

A THESIS SUBMITTED TO
THE GRADUATE SCHOOL OF NATURAL AND APPLIED SCIENCES
OF
MIDDLE EAST TECHNICAL UNIVERSITY

BY

ONURCAN ASLAN

IN PARTIAL FULFILLMENT OF THE REQUIREMENTS
FOR
THE DEGREE OF MASTER OF SCIENCE
IN
POLYMER SCIENCE AND TECHNOLOGY

FEBRUARY 2021

Approval of the thesis:

IMPROVEMENT OF RHEOLOGICAL, MECHANICAL AND INTERFACE PROPERTIES OF SOLID ROCKET MOTOR LINER

submitted by **ASLAN ONURCAN** in partial fulfillment of the requirements for the degree of **Master of Science** i**n Polymer Science and Technology, Middle East Technical University** by,

Prof. Dr. Halil Kalıpçılar
Dean, Graduate School of **Natural and Applied Sciences** _____

Prof. Dr. Necati Özkan
Head of the Department, **Polymer Science and Technology** _____

Prof. Dr. Necati Özkan
Supervisor, **Polymer Science and Technology** _____

Dr. Gürkan Atınç Yılmaz
Co-Supervisor, **TUBITAK SAGE** _____

Examining Committee Members:

Prof. Dr. Cevdet Kaynak
Metallurgical and Materials Eng, METU _____

Prof. Dr. Necati Özkan
Polymer Science and Technology, METU _____

Prof. Dr. Ali Çırpan
Chemistry, METU _____

Assoc. Prof. Dr. İrem Erel Göktepe
Chemistry, METU _____

Assoc. Prof. Dr. Eda Ayşe Aksoy
Pharmacy, Hacettepe Uni. _____

Date: 11.02.2021

I hereby declare that all information in this document has been obtained and presented in accordance with academic rules and ethical conduct. I also declare that, as required by these rules and conduct, I have fully cited and referenced all material and results that are not original to this work.

Name, Last name : Onurcan Aslan

Signature :

ABSTRACT

IMPROVEMENT OF RHEOLOGICAL, MECHANICAL AND INTERFACE PROPERTIES OF SOLID ROCKET MOTOR LINER

Aslan, Onurcan
Master of Science, Polymer Science and Technology
Supervisor : Prof. Dr. Necati Özkan
Co-Supervisor: Dr. Gürkan Atınç Yılmaz

February 2021, 103 pages

This study aims to improve the mechanical, rheological, and interface properties of the currently used liner formulation (referred to as the standard liner) based on carbon black filled polyurethane structure. Two types of carbon black powders (Thermax N-991 and Printex-U) were used as fillers in Hydroxyl-Terminated Polybutadiene (HTPB) - Isophorone Diisocyanate (IPDI) based polyurethane liner. Three different dispersing agents (alkylammonium salt of a high molecular-weight copolymer, high molecular-weight copolymer with pigment affinic groups, and hydroxyl functional silicone modified polyacrylate) were used in this study. Alkylammonium salt of a high molecular-weight copolymer dispersing agent was determined the most effective according to rheological and mechanical test results and particle size analyses. The particle size was lowered from 521 nm to 392 nm for Thermax N-991 and from 550 nm to 263 nm for Printex-U when the dispersant agent (alkylammonium salt of a high molecular-weight copolymer) was used.

The tensile strength and the elongation at break values of the standard polyurethane liner were 1.3 MPa and 270 percent, respectively, and they were improved to 1.77 MPa and 370 percent, respectively, when 10 weight percent of Printex-U were added in the polyurethane liner. Furthermore, the tensile strength and the elongation at break values of the polyurethane liner were improved to 1.88 MPa and 410 percent, respectively, with the addition of 2 weight percent of alkylammonium salt of a high molecular weight copolymer dispersing agent based on the amount of carbon black. The viscosity of the carbon black filled liner formulation was also decreased about two folds; thus, the pot-life of the polyurethane liner was extended up to 53 percent by adding the dispersing agent. Moreover, the effective dispersion of carbon black particles made the polyurethane liner more resistant to the plasticizer migration at the interface.

It is concluded that the use of alkylammonium salt of a high molecular weight copolymer dispersing agent improves mechanical, rheological, and interface properties of the polyurethane liner containing 10 weight percent of Printex-U carbon black.

Keywords: Liner, Dispersing Agent, Mechanical Properties of Liner, Rheological Properties of Liner, Liner-Propellant Interface

ÖZ

KATI ROKET MOTORU ASTARININ REOLOJİK, MEKANİK VE ARAYÜZ ÖZELLİKLERİNİN İYİLEŞTİRİLMESİ

Aslan, Onurcan
Yüksek Lisans, Polimer Bilim ve Teknolojisi
Tez Yöneticisi: Prof. Dr. Necati Özkan
Ortak Tez Yöneticisi: Dr. Gürkan Atınç Yılmaz

Şubat 2021, 103 sayfa

Bu çalışma, karbon siyahı dolgulu poliüretan esaslı mevcut kullanılan astar formulasyonunun (standard astar olarak adlandırılmış) mekanik, reolojik ve arayüz özelliklerine göre geliştirilmesini amaçlamaktadır. Hidroksil Uçlu Polibutadien (HTPB) - İzoforon Diizosiyanat (IPDI) esaslı poliüretan astarda dolgu maddesi olarak iki tip karbon siyahı tozu (Thermax N-991 ve Printex- U) kullanılmıştır. Bu çalışmada, üç farklı dispersiyon ajanı (yüksek molekül ağırlıklı kopolimerin alkilamonyum tuzu, pigment afinik gruplu yüksek moleküler ağırlıklı kopolimer, hidroksil uçlu silikon modifiye poliakrilat) kullanılmıştır. Yüksek molekül ağırlıklı kopolimerin alkilamonyum tuzunu içeren dispersiyon ajanının reolojik, mekanik test sonuçları ve partikül boyutu analizlerine göre en etkili olduğu belirlenmiştir. Dispersiyon ajanı (yüksek molekül ağırlıklı kopolimerin alkilamonyum tuzu) kullanıldığında partikül boyutu Thermax N-991 için 521 nm'den 392 nm'ye ve Printex-U için 550 nm'den 263 nm'ye düşürülmüştür.

Standart poliüretan astar 1.3 MPa gerilme mukavemetine ve yüzde 270 kopma uzamasına sahiptir ve bu özellikler, poliüretan astara ağırlıkça yüzde 10 Printex-U eklenmesiyle sırasıyla 1.77 MPa ve yüzde 370'e yükseltilmiştir. Ayrıca, yüksek molekül ağırlıklı kopolimerin alkilamonyum tuzunu içeren dispersiyon ajanının karbon siyahı miktarına göre ağırlıkça yüzde 2 ilavesi, bu değerleri sırasıyla 1.88 MPa ve yüzde 410'a yükseltmiştir. Dispersiyon ajanı eklenmesi karbon siyahı dolgulu poliüretan astarın akmazlığını yaklaşık iki kat azaltmış; böylece kap ömrü yüzde 53'e kadar uzatılmıştır. Ayrıca, karbon siyahı taneciklerinin etkili bir şekilde dağılması, astarı plastikleştirici göçüne karşı daha dayanıklı yapmıştır.

Yüksek molekül ağırlıklı kopolimerin alkilamonyum tuzunu içeren dispersiyon ajanının kullanımı, ağırlıkça yüzde 10 Printex-U karbon siyahı içeren poliüretan astarın mekanik, reolojik ve arayüz özelliklerini geliştirdiği sonucuna varılmıştır.

Anahtar Kelimeler: Astar, Dispersiyon Ajanı, Astarın Mekanik Özellikleri, Astarın Reolojik Özellikleri, Astar-Yakıt Arayüzü

To My Family

ACKNOWLEDGMENTS

I would like to express my sincere gratitude to my supervisor Prof. Dr. Necati Özkan, for his expertise and guidance throughout the study. I am also very grateful to my co-supervisor, Dr. Gürkan Atınç Yılmaz, for his assistance.

This study was carried out at The Scientific Council of Turkey- Defense Industries and Development Institute (i.e., TUBİTAK SAGE) in the Propellant and Explosive Department. I would like to thank TUBİTAK SAGE for its financial support. I would like to thank my colleagues in the Department of Propellant and Explosive, especially Dr. Değer Çetin, Head of the Department, and Assoc. Prof. Dr. Taner Atalar, for their close interest during the study.

I am very grateful to Anıl Tatlıdilli, Tuğçe Sabir, Gökçe Özlü, Setenay Ünçe and Dr. Oktay Acar for their help about DMA, FTIR and Mechanical analysis in this study.

Finally, I would like to express appreciation to my father, İsmail Aslan, and my mother, Nursel Aslan, for being with me all time and my fiance Ayşegül Balcan for her unlimited support.

TABLE OF CONTENTS

LIST OF TABLES

TABLES

LIST OF FIGURES

FIGURES

LIST OF ABBREVIATIONS

ABBREVIATIONS

A	Area
AFM	Atomic Force Microscopy
AP	Ammonium Perchlorate
ASTM	American Society and Testing of Materials
ATR	Attenuated Total Reflection
BET	Brunauer, Emmett, and Teller
C	Carbon
CB	Carbon Black
CNT	Carbon Nanotube
CO_2	Carbon dioxide
DA	Dispersing Agent
DA-1	Dispersing Agent-1
DA-2	Dispersing Agent-2
DA-3	Dispersing Agent-3
DBTDL	Dibutyltin dilaurate
DCM	Dichloromethane
DLS	Dynamic Light Scattering Analysis
DMA	Dynamic Mechanical Analysis
DOA	Dioctyl Adipate
FeAA	Iron acetylacetonate
FESEM	Field Emission Scanning Electron Microscopy
FTIR	Fourier Transform Infrared
H	Hydrogen
HDI	Hexamethylene Diisocyanate
HTPB	Hydroxyl Terminated Polybutadiene
IDP	Isodecylpelargonate

IPDI	Isophorone Diisocyanate
ISO	International Organization of Standardization
LOI	Limiting Oxygen Index
MAPO	tris(1-2(methyl) aziridine) phosphine oxide
MDI	Methylene diphenyl diisocyanate
MEK	Methyl Ethyl Ketone
MILP	Metal-Insulator-Liner-Propellant
MWCT	Multi-Wall Carbon Nanotube
MT	Medium Thermal
N	Nitrogen
NASA	The Aeronautics and Space Administration
NSA	Nitrogen Surface Area
O	Oxygen
OI	Oxygen Index
PdI	Polydispersity Index
R	Radical
RCG	Regular Color Gas Black
SEM	Scanning Electron Microscope
SWCNT	Single Wall Carbon Nanotube
STANAG	Standardization Agreement
T	Thickness
TDI	Toluene Diisocyanate
TEA	Triethanolamine
TEM	Transmission Electron Microscopy
TGA	Thermal Gravimetric Analysis
TMP	Trimethylolpropane
TPB	Triphenyl Bismuth
VST	Vacuum Stability Test

LIST OF SYMBOLS

SYMBOLS

%	Percent
°C	Celcius
cals	Calories
cm	Centimeter
E'	Storage Modulus
E″	Loss Modulus
g	Gram
h	Hours
Hz	Hertz
k	Reaction Rate Constant
kN	Kilonewton
kV	Kilovolt
l	Liter
L	Length
mg	Milligram
min	Minutes
mL	Milliliter
mm	Millimeter
mmHg	Millimeters of Mercury
MPa	Megapascal
nD	Refractive Index
nm	Nanometer
P	Poise
Pa	Pascal
rpm	Revolutions per Minute
s	Second

t	Time
tan(δ)	Ratio of Loss Modulus to Storage Modulus
T	Temperature
Tg	Glass Transition Temperature
W	Watt
W	Width
wt	Weight
η	Viscosity
σ	Standard Deviation

CHAPTER 1

INTRODUCTION

A solid rocket motor works as a propulsive unit. The basic concept of propulsion is that potential energy is converted to kinetic energy. A large volume of hot gases generated during the propellant burning is ejected through the nozzle, and gas pressure produces thrust at high speed. (Rodić, 2007). The rocket motor primarily consists of four parts that are propellant, motor case, nozzle, and igniter (see Figure 1-1).

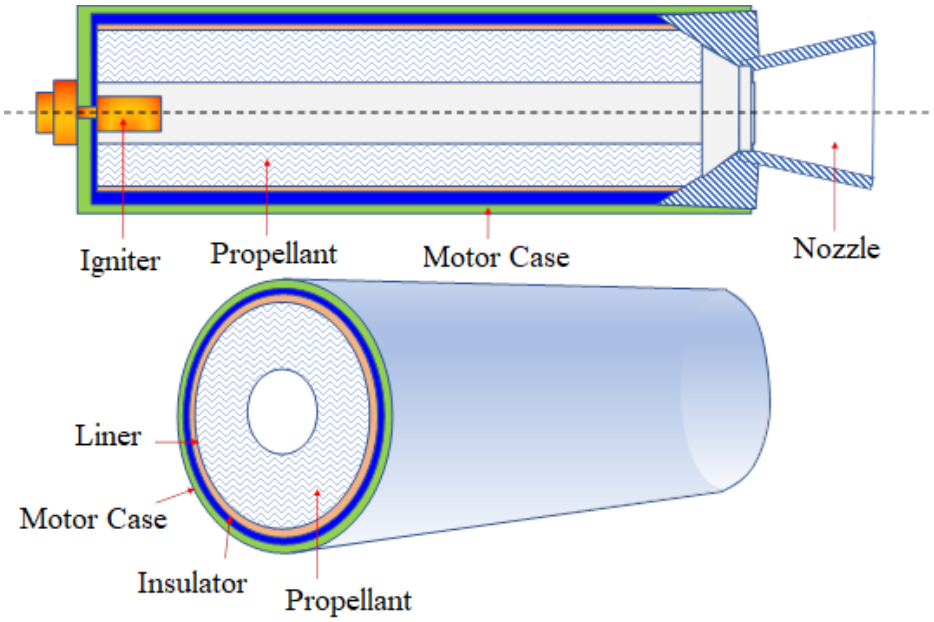

Figure 1-1. Schematic illustration of a Solid Rocket Motor

The motor case is the outer part of the rocket motor that acts as a combustion chamber and is commonly made up of steel, steel alloy, aluminum, or composite material. The propellant, insulator, and liner stay bonded together in the motor case. Igniter locating at the head or the end of the motor provides starting the propellant

burning. In the nozzle part, the combustion of propellant gases is convergent at the narrow side and released throughout the atmosphere at the broadside.

1.1 Propellant

In this thesis, a polyurethane-based solid propellant is used. A solid propellant is a composite material that an oxidizer particle is embedded in the polymer binder, which also acts as a fuel. A solid oxidizer is mixed with a liquid binder, and the mixture hardens during curing by the cross-linking of polymer chains in the binder.

Solid propellants must meet strict mechanical and chemical criteria to ensure safety during both operation and storage. The propellant must deform elastically to avoid cracking within the propellant grain. The propellant cracks cause a higher surface area that increases the burning rate; thus, the rocket motor fails due to over pressurization throughout the casing (Hamilton et al., 1994). Besides, a crack may be formed due to different thermal expansion coefficients of the propellant and motor case (Douglass, 1973). A propellant must be designed to serve temperatures ranging from -65°C to 150°C (Douglass, 1973). Properties of a propellant depend mainly on the following parameters (Oberth & Bruenner, 1969);

- Properties of the binder matrix
- Particle size and particle size distribution of solids
- Quality of interphase between solid particles and polymer binder matrix
- Storage conditions such as temperature and moisture

Typical ingredients of composite solid propellants are fuel binder, oxidizer, plasticizer, curing agent, crosslinking agent, and bonding agent. The ingredients are used in a specific amount since they have a profound effect on propellant performance.

1.2 Insulator

An Insulator provides thermal insulation that protects the motor case from high-temperature combustion gases. The insulation materials are commonly inert, non-combustible elastomeric materials (Giants, 1991). The insulator is bonded to the inner side of the motor case with an adhesive primer. The bonding between the motor case and insulator must be robust since the insulator transmits load between the case and the propellant. The insulator thickness ranges between 1 mm to 3 mm depending on the rocket motor design, configuration, and burning time. The following properties require for the insulator (Krishnamurthy & Varghese, 2017);

- Low thermal conductivity [4-5x10^{-4} cal/(s .cm.°C)]
- Low erosion rate (0.1-0.2 mm/s)
- Compatible with the motor case, liner, and propellant
- High flame retardancy and flexibility

Nitrile Rubber, Chloroprene Rubber, and EPDM Rubber (Ethylene-Propylene-Diene Ter-polymer) are most frequently used as an insulator material in the motor case.

1.3 Liner

Liner is a thin layer of elastomeric material applied uniformly on the insulator to bond both the insulator and the propellant. The interface between the propellant and insulator must be strong enough since the interface should resist the stresses and strains lead by the thermal contraction and pressurization of propellant and acceleration loads (Toulemonde et al., 2018). Hence, the liner must have good mechanical properties such as tensile and shear strength. The liner also works as an inhibitor. While combustion reaches the liner, it inhibits the combustion to prevent the motor case from an explosion. Moreover, the liner should have a higher ductility than the propellant; therefore, it prevents crack formation in the propellant during

storage and transportation (Toulemonde et al., 2018). Significant features of the liner should be as follows;

- Liner should have low viscosity to be applied easily, such as spray application
- Liner thickness may be up to 1mm
- Liner should endure high temperatures
- Liner should have a useful pot life
- Liner should have a reliable aging characteristic

The Carbon Black filled polyurethane liner formulation was used in this study. The ingredients and their functions were given in Table 1-1. Pinto reported that the same binder and isocyanate are used to produce propellant and liner to ensure chemical compatibility since it provides better adhesion and higher cohesive strength (Pinto, 2006). Hence, the propellant used in this study has a similar polymer structure to the liner.

Table 1-1. Ingredients of the liner and its functions

Chemical	**Function**
HTPB	Binder
IPDI	Curing Agent
DBTDL	Catalyst
TEA	Crosslinking Agent
MAPO	Bonding Agent
IDP	Plasticizer
Carbon Black	Reinforcing Filler

1.4 Ingredients and Their Functions

1.4.1 Binder

HTPB is used as an organic binder (Figure 1-2). In the propellant, HTPB binds the oxidizer and metallic fuel to form a polymer matrix that withstands thermal and mechanical stresses. The binder is one of the materials that determine the mechanical properties of the propellant and the liner. HTPB binder reacts with a curing agent to form a crosslinked polymer, which provides a matrix to bind all solid ingredients. HTPB is commonly used in propellant and liner formulations due to its low glass transition temperature (Tg), approximately -70°C. HTPB also provides high combustion performance due to the high hydrocarbon units (CH_2) and C/H ratio in its backbone. The sufficiently low viscosity of HTPB is an important advantage for handling during the mixing process.

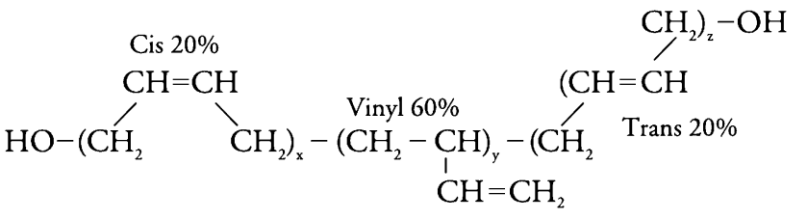

Figure 1-2. The chemical formula of Hydroxyl Terminated Polybutadiene (Krishnamurthy & Varghese, 2017)

HTPB polymers are prepared by hydrogen peroxide initiated free-radical polymerization of 1,4-butadiene or anionic polymerization of butadiene (Mahanta & Pathak, 2012). The functionality and the microstructure of HTPB depend on the methods chosen. The anionic process gives higher vinyl, cis contents, and lower trans content than the free-radical manufacturing method. The free-radical technique of producing HTPB gives more than two functionalities, while the anionic process gives two or less functionality (Ajaz, 1994). Since hydroxyl groups are highly reactive, they can rapidly react with isocyanate, and they are also exposed to air oxidation,

causing the propellant's hardening (Oberth & Bruenner, 1969). The effect of microstructure on the properties of HTPB is summarized in Table 1-2.

Table 1-2. Effect of configurations on the properties of HTPB

Configurations	**Viscosity (η)**	**Glass Transition Temperature (T_g)**	**Mechanical Properties**
Cis	Lowers η	Decreases	More flexible
Trans	Increases η	Increases	Less flexible
Vinyl	Increases η	Increases	Less flexible

1.4.2 Plasticizer

Isodecyl pelargonate (IDP) is used as a plasticizer in the liner and propellant formulations. IDP is non-reactive and non-volatile liquids having low molecular weight, approximately 300 g/mole (Figure 1-3). The function of IDP plasticizer is to reduce the viscosity; therefore, propellant and liner can be easily processed. Besides, it enhances the flexibility of polymers and lowers T_g.

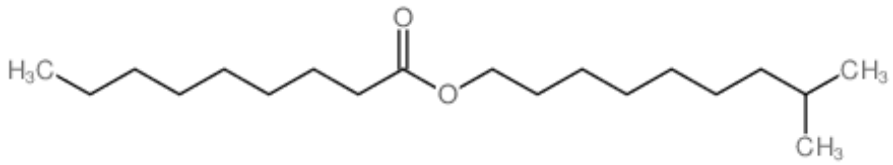

Figure 1-3. Molecular Structure of IDP (*PubChem*, n.d.)

The plasticizer cannot affect the crosslink density since it cannot react with the binder. It penetrates into the polymer matrix and establishes attractive polar forces

between the chain segments (Figure 1-4). It reduces the cohesive forces between polymer chains; therefore, the mobility of the chain increases, so T_g decreases.

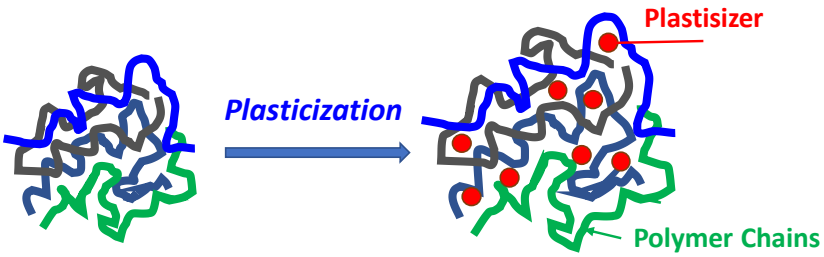

Figure 1-4. Representative scheme of the effect of plasticizer

1.4.3 Crosslinking Agent

Crosslinking is the formation of bridging between linear polymer chains, and as a result, three-dimensional network structure is obtained. In this thesis, Triethanolamine (TEA) is used for crosslinking in the liner and propellant formulations (Figure 1-5).

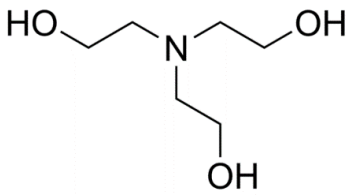

Figure 1-5. Molecular Structure of Triethanolamine (TEA) (*PubChem*, n.d.)

Whether the crosslinking reaction occurs or not depends on the reactivity of the binder and curing agent. In other words, the binder and curing agent should have bi-functionality, and one or both of them should also have some tri-functional molecules. While curing reaction occurs, uncrosslinked linear polymers still contain either reactive functional groups or double bonds on the backbone. The crosslinking agent reacts with active groups of the pre-polymer, and then curing takes place resulting in a crosslinked polymer (Krishnamurthy & Varghese, 2017). If the crosslinking agent is not used in this case, only linear coupling of the pre-polymer is

synthesized. The degree of crosslinking depends on the ratio of the bi-functional to the tri-functional molecules present in the system. The crosslinking agent used in a small amount may improve the mechanical properties of propellant and liner.

1.4.4 Curing Agent

Curing agents consist of isocyanate groups defined as the "R-N=C=O" formula. Since isocyanate groups are extremely electrophilic, they rapidly react with nucleophilic groups such as hydroxyl, amino, carboxyl. There are two types of polyisocyanates; aromatic such as TDI and aliphatic polyisocyanates such as IPDI. The aromatic nature, coupled with the ortho-para effect, makes TDI more reactive; however, alicyclic nature, combinations of primary and secondary isocyanate groups, makes IPDI less reactive (Ajaz, 1994) (see Figure 1-6). Thus, less reactivity brings about longer pot life, giving an advantage for processing. Furthermore, a polyurethane with higher strength is produced using aliphatic isocyanates (Manjeet & Raminder, 2017). Hence, IPDI is used in this thesis.

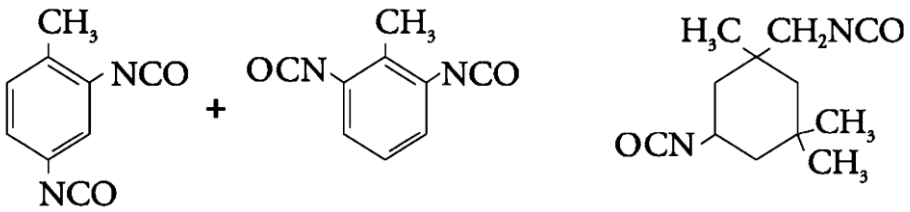

TDI IPDI

Figure 1-6. The chemical formula of TDI and IPDI (*PubChem*, n.d.)

There are two types of reactions that are primary and secondary. Primary reactions are relatively faster and occur at relatively lower temperatures compared to secondary reactions. The primary reactions of isocyanates are shown in Figure 1-7.

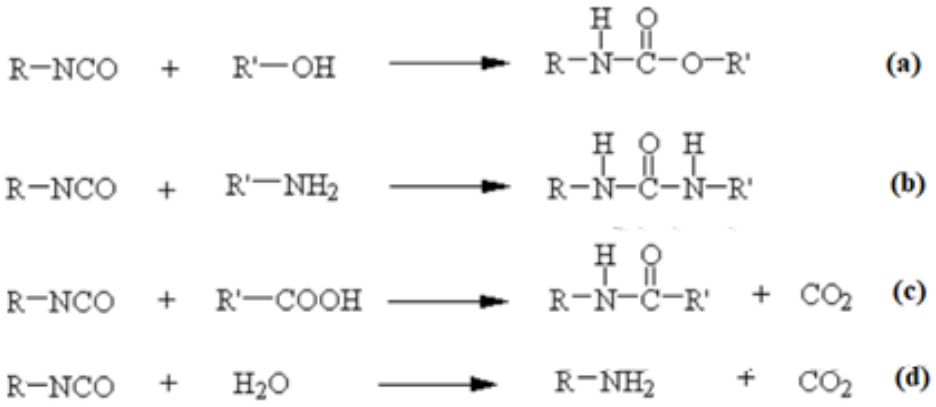

Figure 1-7. Primary Reactions of Isocyanate a) Urethane, b) Urea, c) Amide, d) Amine (Hepburn, 1992)

Isocyanates react with the secondary amino group of urethanes, ureas, and amide, forming Allophanates, Biurets, and Acyl Ureas, respectively, as shown in Figure 1-8. The secondary reactions of isocyanate lead to cross-linking.

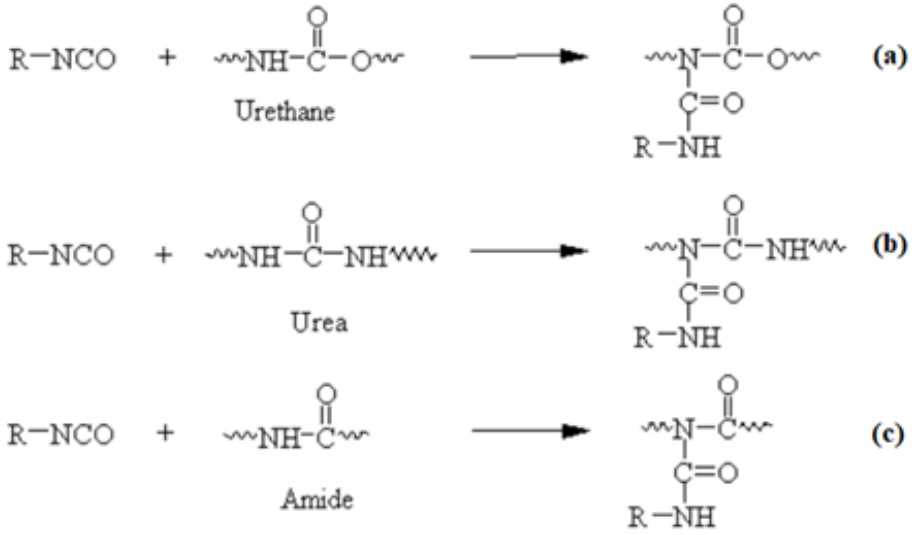

Figure 1-8. Secondary Reactions of Isocyanate a) Allophanate, b) Biuret, c) Acyl Urea (Hepburn, 1992)

For the liner and propellant production, the urethane linkage formed between isocyanates of IPDI and the hydroxyl groups of HTPB. Curing reaction between HTPB and IPDI occurs two-step polymerization known as second-order reaction

(Kincal & Özkar, 1997). In step 1, two moles of secondary NCO groups reacted with two OH groups in one-mole HTPB. In step 2, the primary NCO groups reacted with OH groups in HTPB and formed a polyurethane structure. The speed of the curing reaction is affected by mixing temperature, mixing time, and catalyst usage.

1.4.5 Bonding Agent

Bonding agents are used in both liner and propellant formulations. They are mainly used to improve the bonding between binder and oxidizer by secondary ion-polar attraction to incorporate oxidizer particles into the binder matrix. Hence, the bonding agent can improve the mechanical properties of liner and propellant since it forms chemical and physical bonds that depend on the type of bonding agents. There are many types of bonding agents having functional groups such as an aziridine, hydroxyl, amino, and cyano (Yadav et al., 2020);

In the liner formulation, a bonding agent with an aziridine functional group is commonly used since it bonds to Ammonium Perchlorate (AP) in the propellant at the liner-propellant interface. Pinto uses MAPO (tris(1-2(methyl) aziridine) phosphine oxide) as a bonding agent, and he states that MAPO improves adhesion strength through two mechanisms: the ring-opening reaction of the imine ring with hydroxyl groups of propellant binder and by hydrogen forces between MAPO from the liner and AP from the propellant (Pinto, 2006) (see Figure 1-9)

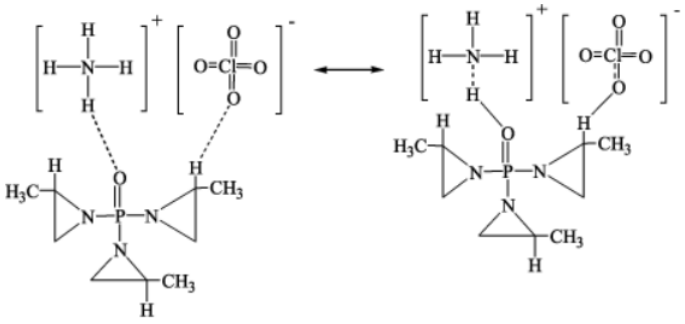

Figure 1-9. Intermolecular interaction between AP (NH_4ClO_4) and bonding agent MAPO (Hori et al., 1985)

In this thesis, MAPO is used as a bonding agent in the CB-filled polyurethane liner formulation. Chen et al. state that the propellant and liner bonding strength gets improved until a particular amount of MAPO, but the excessive amount would cause low tensile strength since the bonding agent reduces crosslink density. Gercel et al. studied aziridine-type bonding agents, and they reported that tensile and shear strength increased up to 2wt.% of bonding agent in the liner formulation (Gercel et al., 2001).

1.4.6 Filler

Filler materials are used to reinforce the binder in the liner formulation. The filler must be inert and have high thermal degradation since the liner is exposed to high temperatures during combustion. Besides, the filler used in the liner formulation should have a flame retardant characteristic. Although many types of fillers are used in liner formulations, such as titanium dioxide, asbestos, carbon nanotube, etc., carbon black powder is used as a filler in this thesis. Ross et al. reported that carbon black provided better mechanical and thermal properties to the HTPB based polyurethane liner among the other fillers such as calcium carbonate, zinc oxide, and nanoclay (i.e., Cloisite 20A) (Ross et al., 2017).

1.4.7 Other Substances

A catalyst may be used in the liner to decrease curing time. However, it is unnecessary to use a catalyst in propellant formulation since it may harden the propellant higher than the desired level; therefore, cracks may be formed during the storage period. Lewis acid catalysts such as iron acetylacetonate (FeAA), dibutyltin dilaurate (DBTDL), or Triphenyl Bismuth (TPB) are commonly used. FeAA causes a short pot life. Curing is slowed when TPB is used; therefore, it may cause settling of solid particles (Hui et al., 2017). Dibutyltin dilaurate (DBTDL) has better catalytic

effects on polyurethane (Hui et al., 2017). Thus, DBTDL is used as a catalyst in the CB-filled polyurethane liner used in this thesis.

Antifoaming agents, antioxidants, desensitizing agents, and other stabilizers may also be used in liner and propellant formulations.

1.5 Design Parameters of Liner

The typical polyurethane material can be designed with three main parameters that are isocyanate index (NCO/OH), triol/diol, and Plasticizer/Polymer ratios. The formulation of a liner should be designed based on the design parameters of the propellant (Giants, 1991).

1.5.1 Isocyanate Index

Isocyanate Index is the ratio of total NCO functional groups in isocyanate to total OH functional groups in the composition, such as a binder and crosslinking agent. It is commonly indicated as NCO/OH ratio. NCO/OH formula can be seen as follow;

$$\frac{NCO}{OH} = \frac{\dfrac{\text{Functionality of Isocyanate } (F_I)}{\text{Molecular Weight of Isocyanate } (MW_I)}}{\dfrac{\text{Functionality of Binder } (F_B)}{\text{Molecular Weight of Binder}(MW_B)} + \dfrac{\text{Functionality of Triol } (F_T)}{\text{Molecular Weight of Triol } (MW_T)}} \qquad (1)$$

Isocyanate index directly affects the mechanical properties of polyurethane. The higher isocyanate index provides a remarkable increase in hardness and modulus but decreases elongation and small change in a swelling ratio, making propellant service life shorter (Villar et al., 2011). Moreover, the excess amount of NCO groups provides faster chain extension rates, and then softer material is obtained.

1.5.2 Triol/Diol Ratio

Triol/Diol ratio is an essential parameter that affects the crosslink density of the polyurethane material. Hence, the mechanical and thermal properties of liner and propellant are improved by increasing the crosslink density. Triol/Diol ratio is calculated as triol equivalents divided by diol equivalent. The formula can be seen as follow;

$$\frac{\text{Triol}}{\text{Diol}} = \frac{\dfrac{\text{Functionality of Trifunctional Polyol } (F_T)}{\text{Molecular Weight of Trifunctional Polyol } (MW_T)}}{\dfrac{\text{Functionality of Difunctional Polyol } (F_D)}{\text{Molecular Weight of Difunctional Polyol } (MW_D)}} \quad (2)$$

1.5.3 Plasticizer/Polymer Ratio

The Plasticizer/Polymer ratio must be considered while designing both liner and propellant formulation since plasticizer affects mechanical and thermal properties, especially glass transition temperature (T_g). An optimum amount of plasticizer must be used in the liner and propellant formulation due to plasticizer migration. The polymer in this calculation consists of a binder, curing agent, crosslinking agent, bonding agent, plasticizer, and other polymeric additives if they are used.

1.6 Application of Liner

A liner formulation is prepared and then applied to the insulator or motor case by spraying or brushing. Since the liner thickness must be uniform throughout the motor case, spraying is a suitable choice for the application. However, the brushing may also be used if the diameter of the motor case is too narrow for the spraying process.

Spray application depends on the viscosity of the liner and the power of the pump that sprays the liner at a specific pressure. If the liner has a high viscosity, spraying may not be utilized, so the liner should be diluted with a solvent. Many solvents such as Dichloromethane (DCM), Toluene, Methyl Ethyl Ketone (MEK), Hexane, and

Ethyl Acetate, DCM can be used due to solving HTPB. Before the liner application, primer adhesive is applied to the insulator. Then, the liner diluted with solvent is applied, and the motor case should be axially rotated at the curing temperature until the liner reaches tacky state form, termed as a partly polymerized state that exhibits stickiness. During this time, the solvent evaporates, and a thin layer of liner is achieved. After completing the liner application, the propellant is casted in the rocket motor. Then, the rocket motor containing propellant is cured at a specific temperature.

1.7 Interface Properties Between Propellant and Liner

The interface properties have high importance to provide structural integrity of the rocket motor. Although chemical bonding, physical adsorption, interdiffusion, and mechanical interlocking play a key role in interface adhesion according to adhesive theories, chemical bonding and interdiffusion are considered as dominant mechanisms (please see Figure 1-10, Figure 1-11) (Giants, 1991). The chemical bonding takes place after the propellant casting. Since the liner is partially cured, free –NCO groups of the liner react with free –OH groups of the propellant across the interface (see Figure 1-10). In the propellant formulation, NCO/OH ratio is less than 1.0, while in the liner, the ratio is higher than 1.0 (Giants, 1991). Besides, the bonding agent in the liner improves adhesion strength due to bond with the oxidizer (i.e., AP) in the propellant. Kakade et al. studied the effect of oxidizer on interface properties, and they state that adhesion strength decreases as the percentage of oxidizer increases; however, NCO/OH ratio plays a vital role for interface strength (Kakade et al., 2003). The wettability of solid particles in the propellant and the liner are also essential to form a strong bond. Thus, the propellant and liner should be mixed well during production to increase the wettability of solid particles.

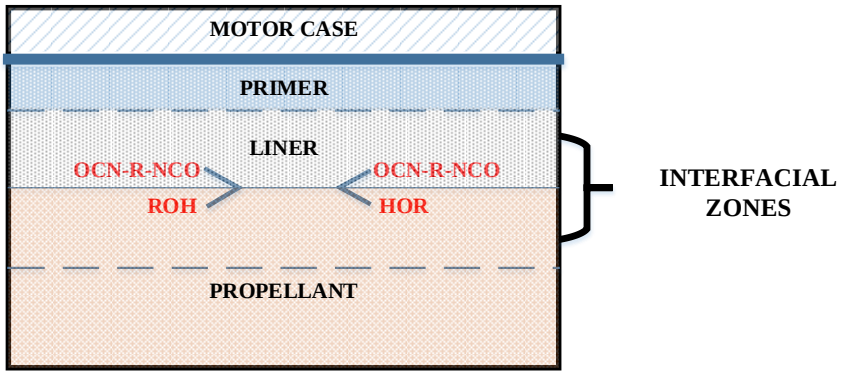

Figure 1-10. The cross-sectional view of a solid rocket motor

Interdiffusion is defined as the migration of molecules from high concentration regions to low concentration regions (see Figure 1-11a). Although liner and propellant formulation affects interdiffusion, chemical similarities between the liner and propellant may decrease interdiffusion effectively. The polarity of the molecules also affects the adhesion mechanism (Figure 1-11b).

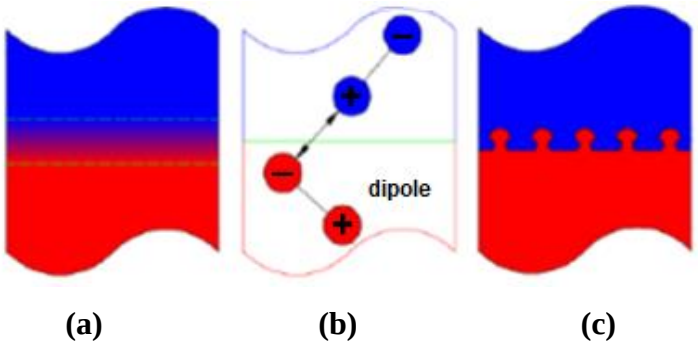

Figure 1-11. Adhesive mechanisms: (a) Interdiffusion, (b) Polarity action (c), Mechanical interlocking (Zhou et al., 2016)

In general, the plasticizer migrates from propellant to liner, which causes the liner to soften, the propellant becomes harder. Meanwhile, other chemicals may migrate from the liner into the propellant. The migration rate and path depend on chemical properties such as molecular weight and chemical concentration in the liner and

propellant formulations. Migration can affect the following properties (Vogelsanger et al., 1996);

- The mechanical properties of the propellant, liner, and insulator
- The bonding strength between the propellant, liner, and insulation
- The burn rate characteristics

Migration proceeds during the storage period of a rocket motor; therefore, it affects rocket motor service life. However, slight migration of plasticizer from propellant to liner is usually beneficial for adhesion since it brings about polymer-polymer interpenetration. Thus, mechanical interlocking occurs at the interface (Figure 1-11c)

1.7.1 Failure Analysis

The primary failure mechanism of the propellant-liner interface is the interface de-wetting between the liner and AP in the propellant at the interface. Tensile and shear test specimens are standard test methods to measure the bonding characteristics of propellant-liner interface. Gercel et al. describe the mode of failure in Table 1-3.

Table 1-3. Description of Failure Modes (Gercel et al., 2001)

Failure Mode	**Description**	**Appearance**
CFP	Cohesive failure from the propellant	The failure occurred from the propellant up to 1,6 mm depth from the interface
CFI	Cohesive failure at the interface	The failure occurred from the propellant as a thin film
AF	Adhesive failure	The failure occurred from neither propellant nor liner
CFL	Cohesive failure from the liner	The failure occurred from the liner

After the test is performed, the appearance of the fracture surface indicates perfect adhesion if cohesive failure from the propellant (CFP) is observed. However, the failure modes depend on bonding strength and storage conditions such as temperature and moisture.

1.8 The Scope of This Work

This study aims to improve the currently used liner formulation (referred to as the standard liner) according to its mechanical, rheological, and interface properties. Mechanical and interface properties of liner provide structural integrity for the rocket motor during the operation conditions. Moreover, the rheological properties of liner are also important during the preparation stage of solid rocket motors.

The standard liner formulation is a carbon black filled HTPB-IPDI based polyurethane liner. The standard liner has 1.3 MPa tensile strength and 270% elongation at break. The improvement of the standard liner was studied using dispersing agents, carbon black type, and loading. However, the improvement should be made at the lowest level of carbon black loading so that adhesion strength can not be decreased. In fact, high filler loading decreases polymer amount in the liner formulation; therefore, adhesion strength may be affected due to a decrease in free functional groups in the liner. For this purpose, the polyurethane liner formulations were prepared using two types of carbon black powders (i.e., Thermax N-991 and Printex U) with different loading percent. Thus, it is aimed to determine specific liner formulations whose mechanical properties are better or close to the standard carbon black filled polyurethane liner. Then, it is considered that the use of dispersing agent improves mechanical and rheological while not reduce adhesion strength. In fact, the effective dispersion provides limiting plasticizer migration that causes crack formation at the liner-propellant interface. For this purpose, three different dispersing agents such as alkylammonium salt of a high molecular-weight copolymer, high molecular-weight copolymer with pigment affinic groups, hydroxyl

functional silicone modified polyacrylate are used in this study. It is aimed to find a suitable type of dispersing agent and its amount used in the liner formulations.

At the end of the study, the specific amount of dispersing agent is desired to improve the rheological, mechanical, and interface properties by effectively dispersing carbon black powders in the polyurethane liner formulation.

CHAPTER 2

LITERATURE REVIEW

Liner and propellant are viscoelastic materials having both viscous and elastic properties. Since their processing procedure is basically to embed the particle in a polymer binder, particle properties affect the physical and mechanical properties. The particle characteristics are mainly based on the surface area, aspect ratio, dimension, and particle size.

2.1 Elastomer

Elastomers exhibit rubber-like behavior. In the raw form of elastomers are generally liquid or viscous. Elastomers have a backbone of either carbon or silica atoms to which other elements such as hydrogen or functional groups such as methyl groups are attached. The following characteristics are required for the elastomer's structure to exhibit rubbery behavior (Carraher & Craver, 2000).

- The polymer chains must be flexible
- There should be sites on the backbone where the polymer chain can be crosslinked

Elastomers flow under stress in the raw form, and then they are cured. During the curing process, crosslinks are formed between polymer chains. There are two types of curing processes. The first one is that curing is induced by chemicals such as hardeners, curing agents, and sulfur (i.e., sulfur vulcanization). The second one is that curing is induced by external factors such as light, heat, and radiation (Carraher & Craver, 2000). However, curing reactions can be fastened by heat or pressure that depends on the reaction mechanism. The curing of the polyurethane liner used in this

thesis is induced by heat. Figure 2-1 shows the structure of polymer chains before and after curing.

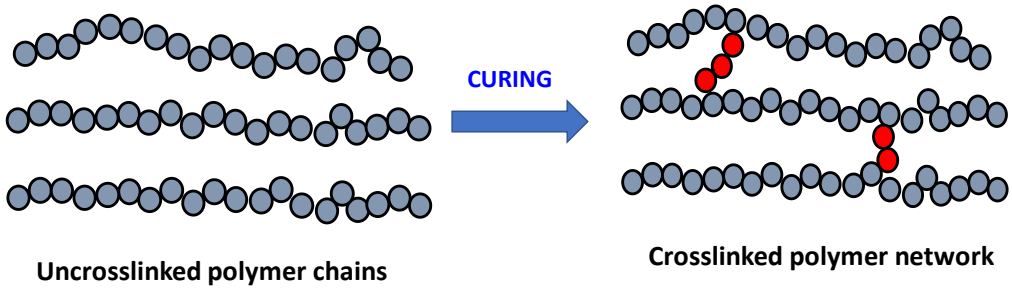

Figure 2-1. The structure of cross-linked polymer chain

After the curing process, a crosslinked polymer is called either thermoset material or elastomer, depending upon the degree of crosslinking. The lightly crosslinked material is termed an elastomer. Hence, the polyurethane liner can be considered as an elastomer.

2.2 Filler

Filler materials are particles added to polymer binder that can improve specific properties. They can be classified as functional fillers and reinforcing fillers. Functional fillers enhance particular properties such as electrical conductivity, crystallization rate, etc., while reinforcing fillers increase mechanical properties such as tensile stress or strain, elastic modulus, stiffness, etc. (Ullmann, 2016). Fillers can be solid inorganic or organic materials. Typical filler materials can be shown in Table 2-1.

Table 2-1. Common Types of Fillers (Pegoretti & Dorigato, 2019)

Inorganics		**Organics**	
Chemical Family	**Common Examples**	**Chemical Family**	**Common Examples**
Oxides	SiO_2, Sb_2O_3, ZnO, etc	Carbon, Graphite	Carbon/Graphite Fibers and Flakes, CNTs, and CB
Hydroxides	$Al(OH)_3$, $Mg(OH)_2$	Natural Polymers	Cellulose Fibers, Wood Flour, Starch, etc
Salts	$CaCO_3$, $CaSO_4$, etc	Synthetic Polymers	Polyamide, Polyester, Aramid
Silicates	Talc, MMT, Asbestos, etc		
Metals	Boron, Steel		

Fillers are also classified as their scales and dimensions. Three main groups are the macro scale, microscale, and nanoscale. The scale depends on particle size, and the ranges of particle size are defined by the scale as follow (Cao, 2004);

- Macro –anything greater than ~100 micrometers.
- Micro – 100 micrometers to 100 nanometers
- Nano – 100 nanometers to 1 nanometer (at least one dimension)

The dimensional classification depends on particle shape, essentially dimensional topology. Dimensional classification can be seen as follows (see Figure 2-2);

- One-dimensional (e.g., Carbon Nanotubes, Fibers)
- Two-dimensional (e.g., Nanoclay, Graphene)

- Three-dimensional (e.g., Carbon Black Particles)

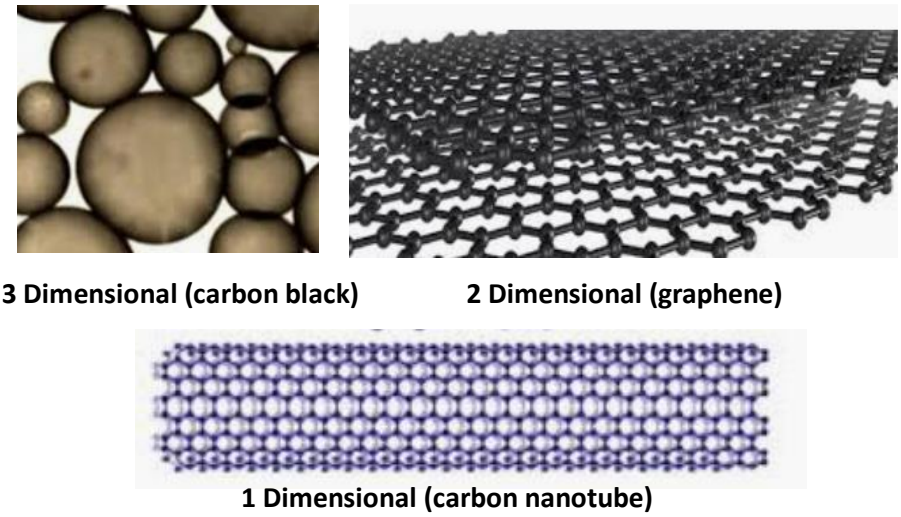

Figure 2-2. Classification of fillers (Koo, 2016)

2.2.1 Carbon Black Particles

Carbon black is a colloidal form of elemental carbon. It is produced by the thermal decomposition or the partial combustion method using oil or gas as a hydrocarbon fuel (Kelsall et al., 2005). There are many types of carbon black used; therefore, it is classified by the manufacturing process. The processing conditions can be controlled by the following variables (Cao, 2004);

- Reaction Time
- Temperature
- Water Quenching

Short reaction time and high-temperature results in a high structure and a smaller particle size for carbon black particles produced. After the production, the following characteristics are essential for the classification of carbon black.

- Size of the particles

- Shape or Morphology (Aspect Ratio)
- Crystal Structure
- Agglomeration

The smallest individual building block formed is called a primary particle, as shown in Figure 2-3. Cluster of the primary particles coalesce together to form aggregates. The larger secondary agglomerates are formed from the primary particles that flocculate together. Van der Waals forces attraction held the agglomerates together (Kraus, 1977). In fact, the size distribution of carbon black particles can be determined using the Dynamic Light Scattering Technique (DLS) or Laser Diffraction Technique. The particle size of carbon black commonly ranges from 10 nm to 500 nm in the industry.

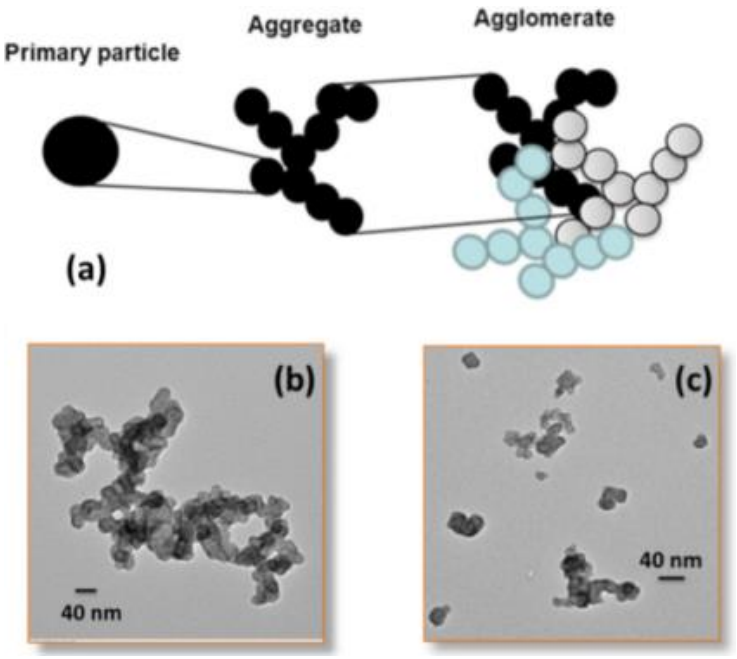

Figure 2-3. Sketch of (a) a carbon black primary particle, aggregates, and agglomerates, (b) TEM image of ‘‘high structure’’ carbon black, (c) TEM image of ‘‘low structure’’ carbon black (Qi et al., 2013)

The pH of carbon black is another classification parameter since the pH is relevant to functional groups on the carbon black particle surface. For example, Thermax N-991 Carbon Black (pH 9-10) has a higher pH value than Printex-U (pH 4-5) (these carbon black particles are used in this thesis). The surface activity of carbon black affects surface interaction with the polymer. Kraus states that carbon blacks with a high surface activity provide high reinforcement to rubber (Kraus, 1977).

Carbon black powders such as Thermax N-991 having low surface area and shape factors bring about a low tendency to agglomerate. On the contrary, carbon black filler such as Printex-U having high surface area and shape factor brings about a high tendency to agglomerate. The fundamental relation between structure, particle size, and surface area can be seen in Figure 2-4.

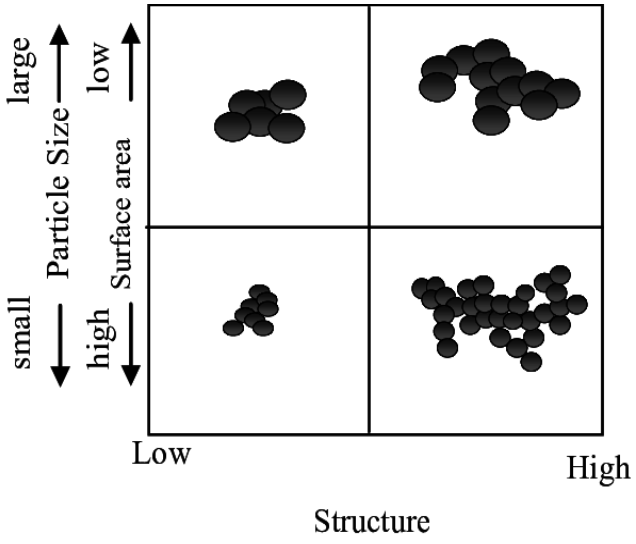

Figure 2-4. The relation between particle size, surface area, and structure of carbon black (Donnet et al., 1993)

2.2.1.1 Types of Carbon Black Particles

In ASTM D1765 standard, carbon black is classified into specific categories, as shown in Table A-1 in Appendix A. According to the standard, the definition consists

of a prefix letter followed by a three-digit number. The prefix indicates the type of cure, with N designated for normal and S for slow. Besides, the particle size of carbon black decreases as the first number after the prefix letter increases. The name of the class depends on the manufacturing method of carbon black.

2.2.1.2 Effect of Carbon Black Particles on Reinforcement

The particle size of filler has a strong effect on the reinforcement of composite materials. The reinforcement strength is summarized in Table 2-2.

Table 2-2. Effect of particle size on reinforcement

Size (nm)	Strength
1000-5000	Small reinforcement
<1000	Medium reinforcement
<100	Strongest reinforcement

Herd et al. state that small reinforcing particles have a more excellent adhesion between the filler and the rubber since small particles have a higher surface area. In other words, carbon black with a smaller particle size adhere well to the polymer matrix due to the higher surface area; therefore, higher reinforcement is obtained (Billmeyer, 1984). However, the processability becomes difficult as the particle size decreases (Kakade et al., 2001).

2.3 Preparation of Polymer Composite Material

There are various methods used to prepare polymer composite material. The most common methods are solution processing, in-situ polymerization, melt processing, and extrusion. Selecting a suitable method depends on filler type and characteristic, desired final product, and the matrix material (thermoset or thermoplastic). The methods are schematically indicated in Figure 2-5.

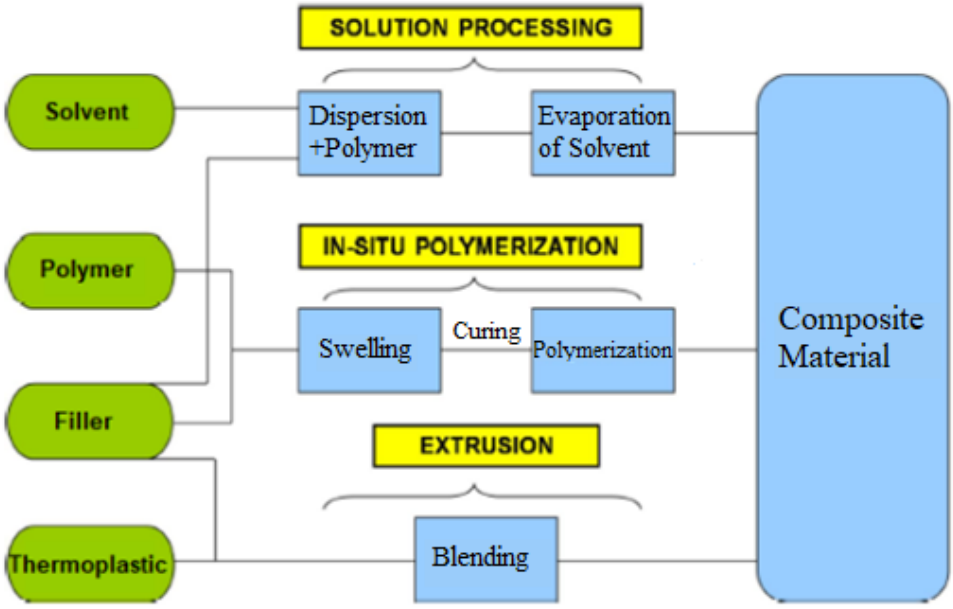

Figure 2-5. Flowchart of processing methods of polymer composite material

The melt processing method is used for thermoplastic materials. The viscous thermoplastic liquid is blended with a filler, and then the mixture solidifies on cooling to form a composite material.

In situ polymerization method is used to prepare thermoset and elastomer materials. It involves mixing a filler with polymer and polymerizing them by addition or condensation polymerization reaction.

Solution processing is another method used for preparing composites. The polymer is dissolved in a suitable solvent to obtain a polymer solution, and filler particles are dispersed in the polymer solution. After dispersion, the solvent is evaporated to form a composite material. Ultrasonication or homogenizer is generally employed to obtain a homogeneous distribution.

2.4 Dispersing Agents as an Additive

Fine particles must be well dispersed to achieve efficient reinforcement of the composite material. Since fine particles tend to agglomerate due to attractive van der

Waals forces between particles, dispersing agents can modify the particle-polymer interface and prevent particles from aggregating. The molecules of dispersing agents cover the particles entirely or partially; therefore, prevent particles from re-agglomerating by acting as a barrier to attractive van der Waals forces. Dispersing agents must be present in an adequate amount in the system; otherwise, re-agglomeration can occur (Esmaeilpour et al., 2016).

- **Electrostatic repulsion** between the particles is only working in the water-based application. If two particles having the same charge approach each other, they repel each other. As a result, Columbian repulsion allows charged particles to remain stable in the system (see Figure 2-6).

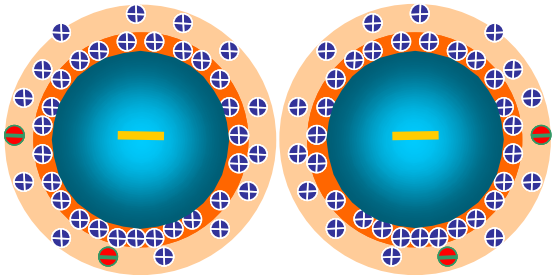

Figure 2-6. Representation of electrostatic stabilization (Agbo et al., 2017)

- **Steric stabilization** works for both water-based and solvent-based systems. It depends on the adsorption layer of polymer chains on the surface of the particles. If polymers fully cover the particles' surface, particles are sterically stabilized; therefore, particle-particle contact is difficult (see Figure 2-7).

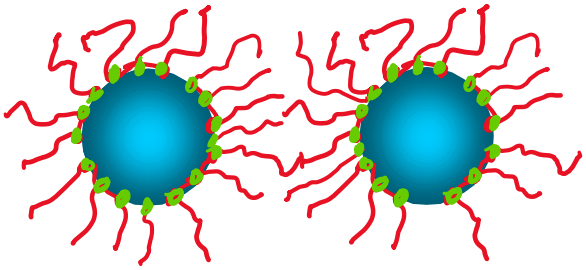

Figure 2-7. Representation of steric stabilization (Agbo et al., 2017)

Many factors are known to play an essential role in the stability of particles (Sethi, 2014);

- Nature of dispersing agent
- The concentration of the dispersing agent
- Type of interaction
- Mixing process

There are two main types of dispersing agents: surfactants (surface active agents) and polymeric dispersing agents. The main differences between the dispersing agents are the molecular weight. In fact, surfactants are generally low molecular weight. They are usually used in water-based solutions, while the polymeric dispersing agents are high molecular weight and commonly used alone or in solvent-borne systems (Pirrung et al., 2002).

Polymeric dispersing agents stabilize particles by steric stabilization mechanism. They have a specific anchor group that can strongly adsorb onto the particle surface. They consist of sufficiently long polymer chains that provide steric stabilization in the medium (see Figure 2-8).

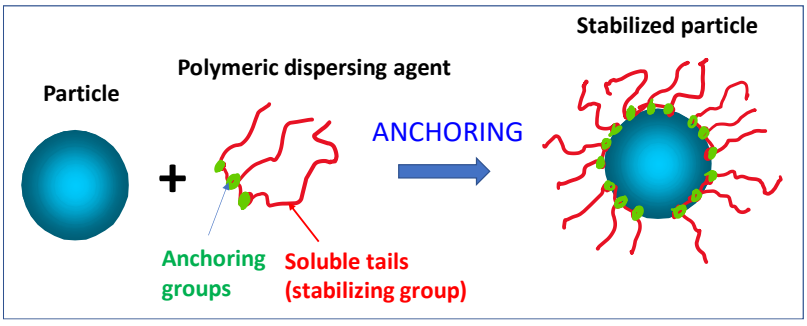

Figure 2-8. Steric stabilization using a polymeric dispersing agent

The concentration of the dispersing agent can be determined by quantitative analysis. The surface area of the particle affects the amount of dispersing agent used. If an excessive amount is used, the protective barrier thickness is reduced (see Figure 2-9). Polymeric dispersing agents are usually used as a concentration of 1.0-60.0wt.% of

solid particles (Harbers P., 2020). Figure 2-9 (b) shows the optimum amount of the dispersing agent, and this case brings about the lowest viscosity and maximum stability.

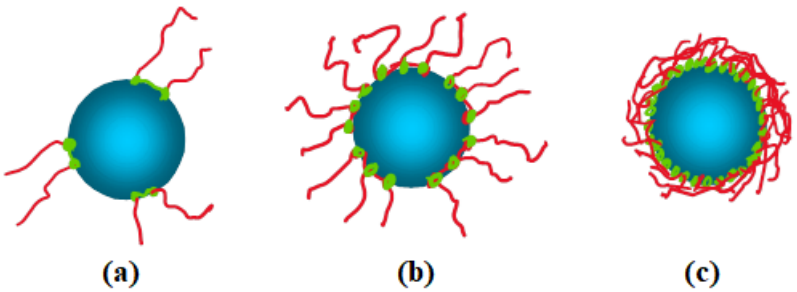

Figure 2-9. Interaction of dispersing agent amount of (a) too little, (b) optimum (c), excessive (Harbers P., 2020)

There are many types of mixing processes during particle dispersion: ultrasonication, calendaring, ball milling, and shear mixing. Those can be used alone, or some of them can be combined. Ultrasonication is a useful tool for dispersion in a liquid medium; researchers have been extensively studied and reported a successful approach (Sethi, 2014). The disadvantage of ultrasonication is that local hotspots may form, therefore causing particle agglomeration. Ultrasonication equipment can be classified into two types, which are bath sonicators and probe sonicators. Probe ultrasonication is an efficient method to separate particles due to transferring energy directly to particles (Sethi, 2014).

2.5 Flame Retardancy

Flame retardant systems are purposed to inhibit or stop the polymer combustion process. The flammability of a material is not an intrinsic property, such as density and heat capacity. Flame retardancy depends on the chemical or physical properties of the agents and mode of action. Carbon-based particles such as carbon black, carbon nanotube, and graphene are typical examples that provide flame retardancy. When carbon-based particles are added to a polymeric material, they produce an

intumescent char, accumulating on the surface. At the same time, the polymer is degraded, providing insulation to the underlying materials and partially protecting it from the action of the flame (Norouzi et al., 2015). Particles with a high aspect ratio and better dispersion provide better mechanical properties to the composite material and better flame retardancy characteristics (Kashiwagi et al., 2008). The flame retardancy can be tested by Cone Calorimeter ASTM D284, Limiting Oxygen Index (LOI) ASTM D2863, and UL 94 flammability test.

2.6 Previous Works About Thesis Subject

To our best knowledge, we did not find any research work on the usage of dispersing agents for solid rocket motor liner formulation. However, dispersing agents such as alkylammonium salt of a high molecular-weight copolymer and high molecular-weight copolymer with pigment affinic groups were widely used in carbon-based filled composite materials. The studies in the literature were summarized below.

Esfahani et al. were used alkylammonium salt of a high molecular weight copolymer as a compatibilizer in graphite nanosheet filled silicone rubber. They have observed that the use of alkylammonium salt of a high molecular weight copolymer decreased the electrical conductivity; therefore, they stated that this was evidence of better dispersion of graphite nanosheets. In addition, the interaction between graphite nanosheets and alkylammonium salt of a high molecular weight copolymer was verified using FTIR analysis in their study. They also observed that storage modulus increased when alkylammonium salt of a high molecular weight copolymer was used in graphite nanosheet-filled silicone rubber.

Zhao & Duan used an alkylammonium salt of a high molecular weight copolymer as a dispersing agent in a composite material containing a single-wall carbon nanotube (i.e., SWCNT) and epoxy resin. They used the dispersing agent 0.9 wt.% of the total formulation. They have observed that the flexural property of the composite improved from 400 MPa to 460 MPa since the dispersing agent improved the

dispersion of SWCNTs. Glass transition temperature of the composite material slightly increased from 188 ºC to 188.5 ºC, the authors interpreted the result as an insignificant. Moreover, tan(δ) decreased from 0.11 to 0.08 when the dispersing agent was used in the composite. As a result, they concluded that using an alkylammonium salt of a high molecular weight copolymer dispersing agent improved the dispersion of SWCNT, which has also been verified using SEM images in their study.

Korayem et al. studied the dispersion of Multi-Wall Carbon Nanotube (i.e., MWCNT) using dispersing agent having high molecular-weight copolymer with pigment affinic groups. They initially studied the dispersion of MWCNT in ethanol solution using UV-Vis Analysis. They observed the stability of 1 wt.% MWCNT in ethanol solution mixed with 2 wt.% dispersing agent, and it was to yield well-dispersed CNTs in ethanol solution. Then, they used 0.2wt.% of the dispersing agent in the composite material containing 0.1 wt.% MWCNT and 97.7 wt.% Araldite. They reported that the use of dispersing agent having high molecular-weight copolymer with pigment affinic groups enhanced tensile strength and Young's modulus about 10% without reducing the elongation at breakage.

Hauptman et al. studied the influence of dispersing agent having high molecular-weight copolymer with pigment affinic groups on the electrical conductivity of carbon black particles in a binder. They found that the dispersing agent reduced the electrical conductivity of carbon black particles and the electrical conductivity remained the same at high dispersing agent addition. They also studied FTIR analysis and observed very weak chemical bonds. They stated that the dispersing agent with high molecular weight copolymer with pigment affinic groups acted mostly as a spacer between carbon black particles. They concluded that the dispersing agent provided a homogeneous and stable dispersion of carbon black (CB) particles both in the liquid phase and binder.

Esmaeilpour et al. studied the effectiveness of OH-functional silicone modified polyacrylate on the surface chemical and physical characteristics of polyurethane

coatings. They reported that 5.0 mol% of OH-functional silicone modified polyacrylate provided better surface features that higher water contact angle was improved from 67º to 100º. The result was also supported by FESEM and AFM results.

Xia & Song characterized carbon nanotube (i.e., CNT) based polyurethane composite. The TEM results showed that the dispersing agent having high molecular-weight copolymer with pigment affinic groups effectively stabilized the SWCNT and MWCNT in the polyurethane. They used 50wt.% of the dispersing agent based on CNTs. The samples were prepared by in-situ polymerization, and they reported that better thermal and mechanical properties were obtained when samples were prepared by ball milling rather than mechanical stirrer.

Loos et al. studied the effect of dispersing agents on the properties of carbon nanotube-filled epoxy systems. They used many types of block-copolymer dispersing agents, and one of them was the dispersing agent having high molecular-weight copolymer with pigment affinic groups. The 0.075wt.% of MWCNT was added to the epoxy matrix, and the composite material was prepared using a mechanical mixer and ultrasonication. The amount of dispersing agent was not reported in their study. The Young's modulus of MWCNT filled epoxy was increased from 2.64 to 3.06 Gpa, and the elongation at break was increased from 8.62% to 10.60% when the dispersing agent having high molecular-weight copolymer with pigment affinic groups was used. The dispersion quality of MWCNT was also investigated using SEM images; as a result, the dispersing agent provided the wetting of the nanotubes, and mechanical properties were increased. They also stated that the dispersing agent wrapped around MWCNT, and this was expected to influence the charge migration between epoxy and MWCNT so that electrical conductivity could be decreased.

CHAPTER 3

EXPERIMENTAL

3.1 Material Used

Carbon black was used as a filler in HTPB-IPDI based polyurethane liner since carbon black has both mechanical reinforcement and flame retardancy abilities. Two different types of carbon black (Printex U (RCG type) and Thermax N991 (MT type) were used.

Three different types of dispersing agents were used to prevent carbon black agglomeration in this study. The selection of a dispersing agent was made according to compatibility with the binder and the carbon black powders used in this study.

The polyurethane structure of the liner and propellant are similar. HTPB binder was supplied from TOTAL, France, under the R-45M product name. The molecular weight of the HTPB binder used in this study was 2800 g/mole, and the hydroxyl value was 0.77 meq/g. HTPB binder is a liquid form with a viscosity of about 5000 centipoises at room temperature. The curing agent IPDI was supplied from FLUKA Company. The molecular weight of IPDI used in this study was 222 g/mole with –NCO value of 8.89 meq/g. The trifunctional crosslinking agent TEA (Triethanolamine) was taken from MERCK, Germany, and its hydroxyl value was 22.11 meq/g. The plasticizer used in this study was IDP (Isodecyl pelargonate) supplied from Platifay Kimya. The bonding agent used in the carbon black (CB) filled polyurethane liner was MAPO ((Tris(1-2(methyl) aziridine) phosphine oxide) delivered from MACH-I Company, USA. DBTDL (Dibutyltin Dilaurate) was used as a curing catalyst supplied from MERCK, Germany. Desmodur RE was used as an adhesive primer applied to the insulator. It was provided from Covestro, Germany.

A carbon black filler named Printex-U is supplied as a powder form from Orion, Germany. Carbon black named Thermax N-991 was supplied as a powder form from Cancarb, Canada. According to their technical documents, the average particle size of Printex-U is 25nm, and that of Thermax N-991 is 300 nm., The BET Surface Areas of Printex-U and Thermax N-991 are 110 m^2/g and 9.0 m^2/g, respectively.

All dispersing agents used in this study were supplied from BYK company, Germany. One of the dispersing agents was alkylammonium salt of a high molecular-weight copolymer under the BYK-9076 product name (i.e., DA1) (see. Figure 3-1a). The other was a high molecular-weight copolymer dispersing agent having pigment affinic groups under the BYK-9077 product name (i.e., DA2) (see. Figure 3-1b). These dispersing agents were generally used to stabilize carbon black particles. Silicone-modified polyacrylate under the BYK 3700 product name (i.e., DA3) was also used as a dispersing agent, which also acts as a surface modifier (see. Figure 3-1c).

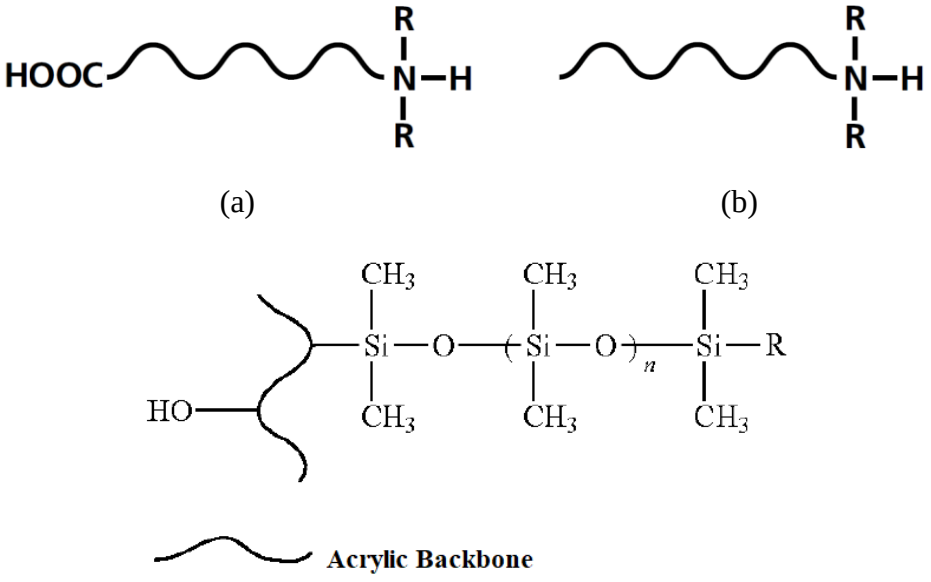

Figure 3-1. Basic molecular structure for (a) DA1 (Esfahani et al., 2012), (b) DA2, (c) DA3 (Tang et al., 2014)

3.2 Preparation of Carbon Black Filled Polyurethane Liner

The carbon black powders were dried at 90°C in an oven for 18 hours before the polyurethane liner preparation, and other ingredients except for TEA and DBTDL were conditioned for 18 hours at 50°C temperature. The NCO/OH ratio was fixed to 1.1, the Triol/Diol ratio was 0.054, and the Plasticizer/Polymer ratio was 6.8 for the CB-filled polyurethane liner formulation. Haska et al. reported that better mechanical properties were obtained for the polyurethane liner when the isocyanate index was selected between 1.1 and 1.2, and the Triol/Diol ratio was 0.054 (Haska et al., 1996). The CB-filled polyurethane liner samples used in this study are summarized in Table 3-1 and Table 3-2.

Table 3-1. The CB-filled polyurethane liner formulations depending on the type and the percent amount of carbon black powders

Carbon Black Type	**% Amount of Carbon Black in the Polyurethane Liner Formulation**		
	2wt.%	**5%**	**10%**
Printex-U	P2	P5	P10
Thermax-N991	T2	T5	T10
Printex-U + Thermax-N991	-	-	PT10

Table 3-2. The CB-Filled Polyurethane Liner formulations depending on the type and amount of Dispersing Agents

Dispersing Agents	**% Amount of Dispersing Agent**	**CB filled Polyurethane Liner Formulations**		
		P10	T10	PT10
DA1	1	P10+DA1X1	T10+DA1X1	PT10+DA1X1
	2	P10+DA1X2	T10+DA1X2	PT10+DA1X2
	3	P10+DA1X3	T10+DA1X3	PT10+DA1X3
	4	P10+DA1X4	T10+DA1X4	PT10+DA1X4
DA2	1	P10+DA2X1	T10+DA2X1	PT10+DA2X1
	2	P10+DA2X2	T10+DA2X2	PT10+DA2X2
	3	P10+DA2X3	T10+DA2X3	PT10+DA2X3
	4	P10+DA2X4	T10+DA2X4	PT10+DA2X4
DA3	1	P10+DA3X1	T10+DA3X1	PT10+DA3X1
	2	P10+DA3X2	T10+DA3X2	PT10+DA3X2
	3	P10+DA3X3	T10+DA3X3	PT10+DA3X3
	4	P10+DA3X4	T10+DA3X4	PT10+DA3X4

3.2.1 Preparation of Carbon Black Filled Polyurethane Liner via Mechanical Stirrer

The polyurethane liner was produced as batch production. 1000 g of polyurethane liner mixture was produced using a mechanical stirrer (Heidolph Hei-Torque Precision 400). Four Blade Mixing Impeller was used during the production. A water bath was set to 50°C to provide a stable temperature during production. All components of the CB-filled polyurethane liner were weighted in a 2-liter beaker starting from smaller quantity components. Then, the polymer mixture was stirred at 500 rpm for about 15 minutes by the mechanical stirrer. Then, the carbon black was added, and the mixture was stirred for 60 minutes. Uniform mixing is essential to obtain a CB-filled polyurethane liner with desired properties. Then, the curing agent

(IPDI) was added, and the mixture was stirred for 10 minutes. After adding the curing agent, the pot life of CB filled polyurethane liner is approximately 2 hours. During the pot life, the CB-filled polyurethane liner was poured into test specimen molds. The CB-filled polyurethane liner was also applied onto the mechanical test specimens by brushing, and test specimens were cured at 65°C for 14 hours to achieve a partially cured liner (i.e., tacky state). Then, it was totally cured at 65°C for about six days.

3.2.2 Preparation of Carbon Black Filled Polyurethane Liner via Ultrasonication

The CB-filled polyurethane liner was also produced using an ultrasonication process. At first, the CB-filled polyurethane liner was produced without adding isocyanate. Then, it was mixed with ethyl acetate with a ratio of 1:1. Ethyl Acetate was used due to its low boiling point (65°C) and high volatility; furthermore, it can dissolve the HTPB binder. Then, the mixture was ultrasonicated. The temperature was controlled by cooling with liquid nitrogen during the ultrasonication process to prevent re-agglomeration. After the ultrasonication, isocyanate was added, and the mixture was stirred by a mechanical stirrer for about 5 minutes at 300 rpm. Subsequently, the mixture was poured into the test specimen, and the solvent was removed by using a vacuum oven at 25°C. The solvent removal process was carried for 18 hours duration under a 500-600 mmHg vacuum. The test specimen was then taken to cure in an oven at 65°C for about six days without a vacuum. NanoLinker Ultrasonic Homogenizer NL-400 having a 13 mm diameter titanium alloy tip was used for the ultrasonication process.

3.3 Preparation of the Propellant

The propellant formulation was fixed in this study. The NCO/OH ratio was lower than the CB-filled polyurethane liner due to effectively adhere to the liner. Triol/Diol

and Plasticizer/Polymer ratios were higher than the liner. The propellant was cured with the CB-filled polyurethane liner, having curing conditions of 65°C temperature for about six days. The propellant samples used in this study are described in Table 3-3.

Table 3-3. The Propellant Samples

Sample	Description
RP	The propellant sample is taken 5mm away from the propellant-liner interface
I1	The propellant sample is taken from propellant- **P10 liner** interface
I2	The propellant sample is taken from propellant- **P10+DA1X2** liner interface

3.4 Characterization Techniques

3.4.1 Particle Size Analysis

Laser Diffraction and Dynamic Light Scattering Techniques were used to characterize the size of particles used in this thesis. BET Surface Area Analysis was also done to verify the surface area of Printex-U and Thermax N991 carbon black powders. In addition, SEM analyses were also done to identify the size of the primary particles.

3.4.1.1 Laser Diffraction Analysis

The mean particle sizes of Printex-U and Thermax N991 carbon blacks were determined using the HORIBA LA-960S Laser Particle Size Analyzer instrument. The ethyl acetate solvent was used as the dispersion medium, and its refractive index (n_D) was taken as 1.372 at room temperature. The refractive index of carbon black

samples was taken as 1.730 at room temperature. 2 mg carbon black was put in the 400 mL beaker. Then, 250-300 mL of the ethyl acetate solvent was poured into the beaker. The mixture was ultrasonicated according to the conditions given in Appendix B. Meantime, 300 mL of the ethyl acetate solvent was poured into the reservoir of the Laser Particle Size Analyzer instrument. After the ultrasonication was finished, the mixture was poured into the reservoir drop by drop using a disposable pipette until the back transmittance reaches %96-%97 level. The mean particle sizes were determined from the volume-based particle size distribution data. The test results comply with ISO 13320:2009 (Particle Size Analysis-Laser Diffraction Methods).

3.4.1.2 Dynamic Light Scattering (DLS) Analysis

Malvern Zetasizer instrument was used to measure the z-average size of the carbon black samples. 1mg of carbon black powder was put into a 250 mL beaker, and approximately 200 mL of Methyl Ethyl Ketone (MEK) solvent was poured into the beaker. Then, the mixture was sonicated at 100 W ultrasonic power for 1 minute. Then, the proper amount of the mixture was poured into a glass cuvette using a disposable pipette. The cuvette was put in the Zetasizer instrument, and the test was started. The test was carried out at METU Central Laboratory.

3.4.1.3 BET Analysis

The BET instrument (Quantachrome Corporation, Autosorb-6) was used to determine the specific surface area (m^2/g) of carbon black powders. Before analysis, the carbon black samples were conditioned in the oven at 90°C for 18 hours. Nitrogen was used as an adsorbate gas, and the outgassing temperature was fixed at 65°C. The test was conducted using the multipoint approach, and the calculation was based on the BET theory. The test was conducted at METU Central Laboratory.

3.4.2 SEM Analysis

A scanning electron microscope (SEM) was used to observe the agglomerate size of carbon black powders (Printex U and Thermax N991). The carbon black dispersion quality in the CB-filled polyurethane liner formulation was also monitored by using SEM. JSM-6400 Electron Microscope instrument (METU METE SEM Laboratory) was used at 20 kV and 300000X magnification, and ZEISS EVO 40 instrument (Ankara University, SEM Laboratory) was operated at 20 kV and 20000X magnification.

3.5 Mechanical Tests

The tensile testing of the CB-filled polyurethane liner samples was conducted using dogbone-shaped samples. The notation of these liner samples is given in Table 3-1 and Table 3-2. The Metal-Insulator-Liner-Propellant (MILP) test specimens are described in Table 3-4. The same propellant formulation was used while MILP test specimens were prepared.

Table 3-4. MILP Test Samples

Sample	Description
MILP-1	The test specimen was prepared using **P10 liner**
MILP-2	The test specimen was prepared using **P10+DA1X2 liner**
MILP-3	The test specimen was prepared using **P10+DA1X2-S liner**

3.5.1 Tensile Properties

Mechanical properties of the CB-filled polyurethane liner samples were measured using dogbone test specimens to study the effects of carbon black content and

particle size. Test conditions such as pretreatment, temperature, and humidity were kept constant for all test specimens. Instron 5965 Universal Testing Instrument with a 5kN load cell was used with the Bluehill Universal Software.

After the CB-filled polyurethane liner was produced, 60±5g of the liner was cast into rectangular Teflon molds with 140mm x 95mm dimensions. The Teflon mold must be kept in the oven at 65°C for at least 2 hours before casting; otherwise, bubbles could be formed in the test specimen. After casting, the liner sample in the Teflon mold was cured in the oven at 65°C for about six days. The cured liner sample was then removed from the Teflon mold and cut manually into the dog-bone shaped according to ASTM D412 (Standard Test Methods for Vulcanized Rubber and Thermoplastic Elastomers-Tension). The dimension of dogbone-shaped test specimen can be seen in Figure 3-2.

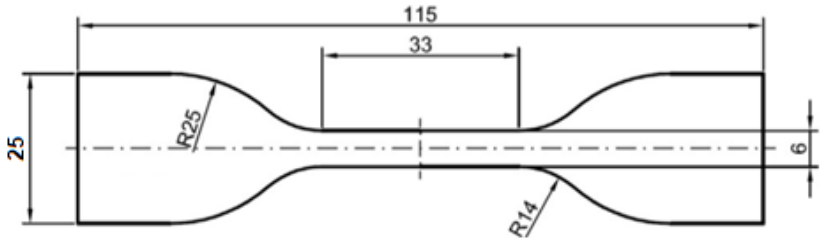

Figure 3-2. Schematic of Tensile Test Specimen

Before the tensile testing, the width and thickness of the test specimens were measured by a caliper, and the data was entered into the software of the instrument. The tensile tests were carried out at room temperature (23±2°C) using 50 mm/min crosshead speed. At least three specimens from each CB-filled polyurethane liner composition were tested under the same conditions.

3.5.2 Metal-Insulator-Liner-Propellant (MILP) Tensile Test

The bonding performance between the insulator-liner-propellant was analyzed by using MILP Tensile Test specimens. After the test, the types of failure were also observed.

The EPDM Rubber (Ethylene-Propylene-Diene Terpolymer) insulator having 50mm(L)x25mm(W)x2mm(T) dimensions have been applied onto the steel metal blocks. The primer Desmodur RE was then applied to the insulator using a brush and dried for 15 minutes. The CB-filled polyurethane liner was then applied with the thickness of 0.40±0.1mm to the insulator using a brush, and the metal blocks were cured at 65°C for approximately 14 hours. The liner reached partially cured form; in other words, the liner surface was sticky. At this time, two metal blocks were assembled reciprocally by using a special mold. The propellant was casted between two metal blocks, and the test mold was cured at 65°C for about six days. After curing, the mold was disassembled. The test specimen is illustrated in Figure 3-3 and Figure 3-4.

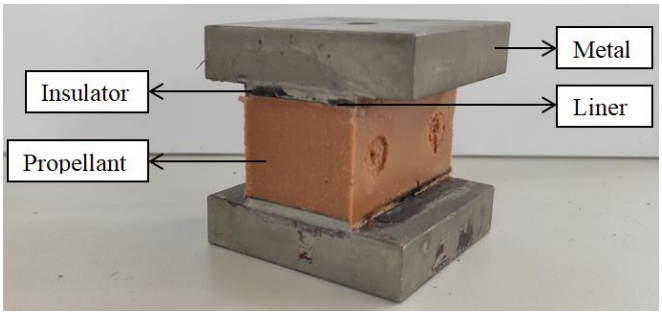

Figure 3-3. MILP Tensile Test Specimen

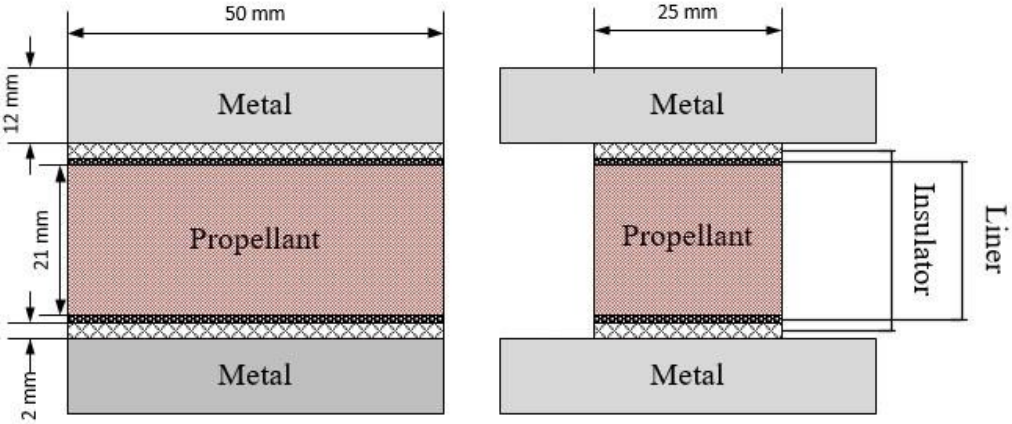

Figure 3-4. 2D Sketch of MILP Tensile Test Specimen

Ten specimens were prepared for each sample. Five samples were kept in a vacuum bag for six months at room temperature, and the other samples were tested after the curing period. Before the test, the length between two metal blocks, the width, and the thickness of test specimens were measured by a caliper. The stress-strain curves of the specimens were analyzed. Finally, the types of failure observed were reported as shown in Table 1-3.

3.5.3 Metal-Insulator-Liner-Propellant (MILP) Double Lap Shear Test

This method was used to determine the adhesive ability of CB-filled polyurethane liner to the propellant by comparing shear strengths.

The EPDM Rubber insulator having 25mm(L) x 25mm(W) x2mm(T) dimensions have been applied on the steel metal strips having 100mm(L)x25mm(W)x2mm(T) dimensions. The liner application and sample preparation were the same as Metal-Insulator-Liner-Propellant (MILP) Tensile Test. A typical test specimen is illustrated in Figure 3-5 and Figure 3-6.

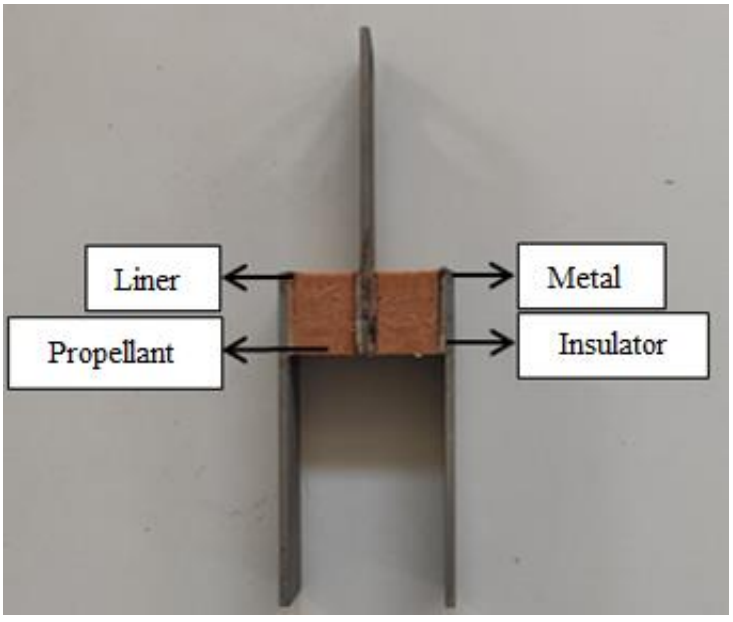

Figure 3-5. MILP Shear Test Specimen

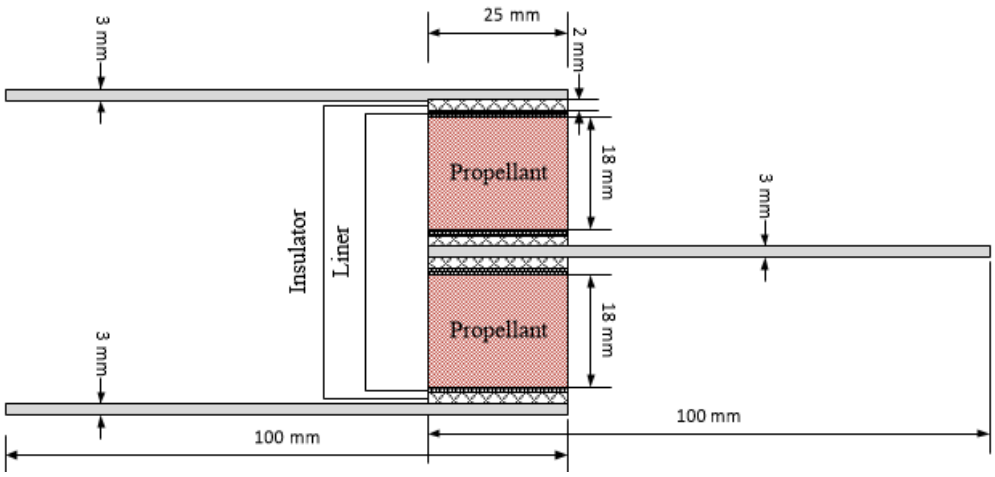

Figure 3-6. 2D Sketch of MILP Shear Test Specimen

Ten specimens were prepared for each sample. Five samples were kept in vacuum bags for six months at room temperature, and the others were tested after the curing period. Before the experiment, the length between two metal blocks, width, and thickness of the test specimen was measured by a caliper, and the data was entered into the instrument's software. The specimen was tested using the Instron 5965 Universal Testing Instrument, in which crosshead speed was set as 1.0 mm/min. The load was applied to the sample in the plane of the liner that slides in the opposite directions. Those forces reflect the total stress exerted through the liner. The stress-strain curves of the specimens were analyzed. The observed types of failure for the specimens were summarized in Table 1-3.

3.6 Viscosity Measurements

Brookfield Viscometer DV-2T instrument was used to understand the effect of filler loading, filler particle size, and dispersing agent on the viscosity of CB-filled polyurethane liner. The test was conducted using the LV-4 spindle due to the high viscosity measurement range (between 1000 cP and 2 Million cP). The viscosity of liner samples that did not contain isocyanate was measured at room temperature (23±2°C).

The CB-filled polyurethane liner material behaves as a shear-thinning material. The power-law parameters of the samples were calculated from the viscosity against shear rate data for the samples using Equation (3):

$$\eta = k\,\dot{\gamma}^{n-1} \qquad (3)$$

The following expression can give the temperature dependence of k:

$$k = A \exp\left(-\frac{E}{RT}\right) \qquad (4)$$

Combining the equations (3) and (4), a formula describing the dependence of viscosity on shear rate and temperature can be obtained:

$$\eta = A \exp\left(-\frac{E}{RT}\right)\dot{\gamma}^{n-1} \qquad (5)$$

In these equations, A is constant; $\dot{\gamma}$ is a shear rate; n is the power-law index; E is the activation energy for the viscous flow; T is test temperature, and R is the gas constant. The viscosity measurements were carried out at 25°C, 35°C, 50°C, and 65°C temperatures, and the constant speeds were used from 5 rpm to 40 rpm with 5 rpm increments. The water bath was used to adjust the test temperatures during the measurements.

3.7 Vacuum Stability Test

Vacuum Stability Test (VST) was performed to study the chemical compatibility of dispersing agents with the propellant. STABIL Vacuum Stability Test (VST) Instrument supplied from the OZM Research Company was used in this study. Electronic pressure transducers measure gas pressure produced by decomposition and evaporation. The instrument software calculates gas volume from the gas pressure. The test must comply with the STANAG 4556 standard (Explosives: Vacuum Stability Test) and STANAG 4147 (Chemical Compatibility of Ammunition Components with Explosives (Non-Nuclear Applications).

For the chemical compatibility test, 5 g of the propellant, 5 g of the liner containing dispersing agent, and 5 g of the mixture (2,5 g propellant and 2,5 g liner) were put in the glass tubes separately. Electronic transducers were placed on the glass tubes, and then the glass tubes were vacuumed. The samples in evacuated glass test tubes were placed into the heating block and held at 100°C for 40 hours. Then, instrument software calculates the volume of gas evolved at the end of the test. The test result must obey the equation (6) to interpret the samples as chemically compatible.

$$V_{mix}-(V_{propellant}+V_{liner})<5\ cm^3 \qquad (6)$$

3.8 Limiting Oxygen Index (LOI) Test

LOI method is used to determine the flammability of polymers. The test is defined as the minimum concentration of oxygen need in a nitrogen-oxygen mixture during the combustion of the specimen. The LOI test conforms to ASTM D2863, Standard Test Method for Measuring the Minimum Oxygen Concentration to Support Candle-Like Combustion of Plastics (Oxygen Index) in this study.

The CB-filled polyurethane liner specimens with 140±1 mm (L) x 52±1 mm (W) x 4±1 mm (T) were prepared for the LOI test. A test specimen was then placed vertically in a mixture of oxygen and nitrogen flowing upwards through a transparent chimney and ignited with a propane gas flame. Then, the oxygen level was reduced slowly until the specimen stopped burning. The oxygen index and the burning time were reported, and also the burned distance was calculated. The test was carried out at 20±2°C temperature and 65±4% relative Humidity. Each sample was repeated 20 times, and the average result was reported with a standard deviation. The test was performed in BUTEKOM R&D Center.

3.9 Dynamic Mechanical Analysis (DMA)

The viscoelastic properties of the CB-filled polyurethane liner samples were studied using DMA Q850 (TA Instruments) and Metravib DMA 450+ test instruments. The test specimen dimensions for the CB-filled polyurethane liner were 5±0.5 mm (W) x 2±0.5 mm (T) x 20±1 mm (L). The test specimens were tested from -100 °C to 80 °C with a heating rate of 5 °C/min. Tests were done using the tensile mode at 10 Hz frequency and %0.01 strain amplitude. Storage Modulus, Loss Modulus, and glass transition temperature (Tg) of the samples were monitored. In addition, the curing of CB-filled polyurethane liner specimens was followed by complex viscosity vs. time graph using a Metravib DMA 450+ instrument. Liquid test apparatus was used (see Figure 3-7), and the tests were performed for 24 hours isothermally at 65°C that is the curing temperature of the liner. The test was carried at 30 Hz frequency.

Figure 3-7. Liquid test apparatus for DMA (Metravib, n.d.)

3.10 TGA Analysis

The thermal gravimetric analyses (TGA) of samples were performed using TGA Q500 (TA Instrument). TGA analyses were done for the propellant samples and the propellant samples taken from the liner-propellant interfaces. TGA curves were obtained from room temperature to 500 °C with a heating rate of 10 °C/min under a

nitrogen atmosphere. The samples were taken from MILP Tensile test specimen kept in vacuum bags for six months at room temperature since the plasticizer was migrated during this period. The sample weight must not exceed 1 mg due to the explosion risk. The test was mainly done to detect plasticizer migration.

3.11 Fourier Transform Infrared (FTIR) Analysis

FTIR Analysis was used to identify the migration mechanism of the liner-propellant interface. The propellant samples were measured using Perkin Elmer Spectrum 100 instrument. The absorption spectrum was recorded in the wavenumber range from 4000 cm^{-1} to 400cm^{-1}. FTIR was set up to record in the ATR mode. The samples were taken from MILP Tensile test specimen kept in vacuum bags for six months at room temperature since the plasticizer was migrated during this period. The spectrum graph in which the peaks overlap iterated the curve-fitting process by adjusting the peak high and width to achieve the best Gaussian-shaped. Curve fitting was performed using Origin software. According to the Lambert-Beer law, a curve area is directly proportional to the concentration of the substance. The change in the selected band area was divided by the area of the reference band to identify the concentration difference. The intensity of the absorption band at 1640 cm^{-1} for the C=C stretching for the HTPB-IPDI reaction remains constant during the curing reaction, and the peak is used as a reference (Kincal & Özkar, 1997).

CHAPTER 4

RESULTS AND DISCUSSION

4.1 Characterization of Carbon Black Particles

As shown in the SEM pictures (see Figure 4-1), Thermax N991 and Printex-U carbon black powders are nearly spherical and show some aggregate regions. However, Printex-U powders have a higher tendency to form agglomerates due to their smaller primary particle size. The primary particle sizes of Printex-U powders range from 35 nm to 55 nm, and those of Thermax N991 powders range from 255 nm to 433 nm. According to Figure 4-1, it can be stated that the particle size of carbon black samples conform to ASTM D1765 (Standard of Classification of Carbon Black) indicated in Table A-1**.**

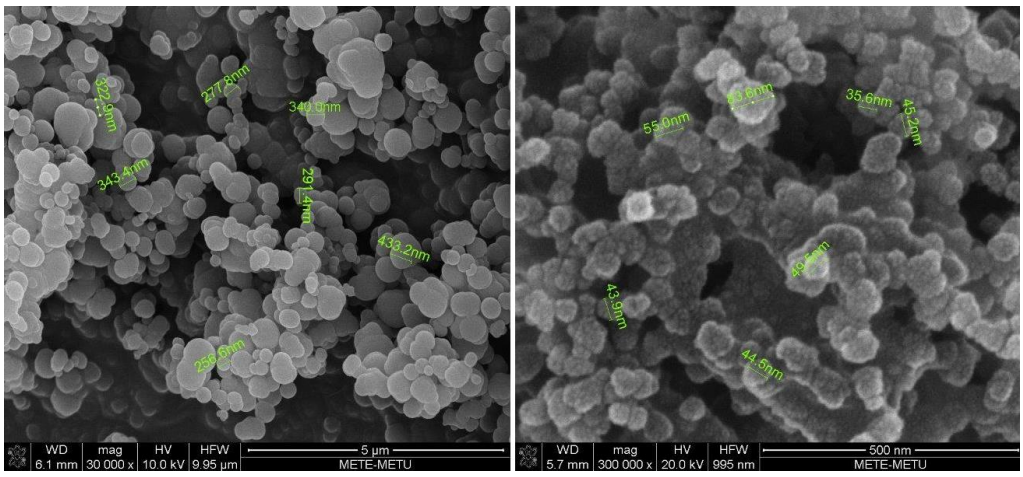

(a) **(b)**

Figure 4-1. SEM images for carbon back samples (a) Thermax N991 (b) Printex-U powders

SEM images can provide information about the primary particle size and particle morphology. In addition, the agglomerate size and particle size distribution of the

carbon black powders were determined using Laser Diffraction Analysis and Dynamic Light Scattering Analysis (DLS). The results of the DLS analysis are given in Table 4-1.

Table 4-1. The DLS results for the carbon black powders

Result	Thermax N991	Printex-U
Z-Average Mean Size (nm)	388.9	224.4
Polydispersity Index (PdI)	0.916	0.220

The Z-average is intensity-based mean particle size, and the polydispersity index (PDI) is related to the width of the distribution. As seen in Table 4-1, the z-average particle mean size was measured as 224.4 nm. The z- average mean particle size of Thermax N991 was found as 388.9 nm. When the primary particle size observed in SEM images and the z-average particle mean size were compared, it is possible to state that Printex-U had a higher tendency to agglomerate since the average particle size reached 30nm to 224.4nm in an aqueous medium. However, Thermax N991 has a low tendency to agglomerate since the z- average mean particle size of Thermax N991 was found as 388.9 nm and close to the primary particle size observed in the SEM analysis.

Carbon black powders were also characterized by the multi-point BET analysis given in Table 4-2.

Table 4-2. Multipoint BET result of Carbon Black samples

Result	Thermax N991	Printex-U
Multipoint BET (m^2/g)	9.058	91.32

According to Table 4-2, Printex-U powders had a higher surface area than Thermax N991 powders due to their smaller primary particle size. The BET surface area of carbon black powders conform to the BET results given in the Technical Data Sheet (TDS) of Printex-U and Thermax N991.

The nanoparticles generally agglomerate due to their high surface energy, making them more active for adsorption of other species or interacting with each other (Koo, 2016). Thus, the formation of agglomerate diminishes the surface energy, and the particle turns to stabilized form. In this case, Printex-U carbon black powders have a high surface area, so that they have more free valence atoms on their surfaces than Thermax N991. For this reason, Printex-U carbon black powders show a high tendency to agglomerate than Thermax N991.

Agglomerates are accumulations of particles connected by attractive physical interactions such as van-der-Waals forces. Hence, the aggregate size can be decreased using a suitable dispersing agent that interacts with the surface of the particle. Three different dispersing agents with various concentrations were used to disperse the carbon black powders. The mean particle sizes of the carbon black powders dispersed using various dispersing agents with different concentrations given in Figure 4-2 and Figure 4-3.

Figures 4.2 and 4.3 suggest that the optimum concentration of dispersing agents was 2wt.% based on the carbon black content**.** A higher amount of dispersing agent causes re-agglomeration of the particles. In fact, **i**ncreasing the concentration of the dispersing agents enables more hydrophobic chains of copolymer molecules to attach to the carbon black surface and causes a gradual increase of free copolymer molecules in the solution. The increased free copolymer in the solution finally leads to micelle formation. The higher concentrations induce an uncompensated force that results in a depletion attraction between particles, leading to the agglomeration of carbon black particles (Hauptman et al., 2011).

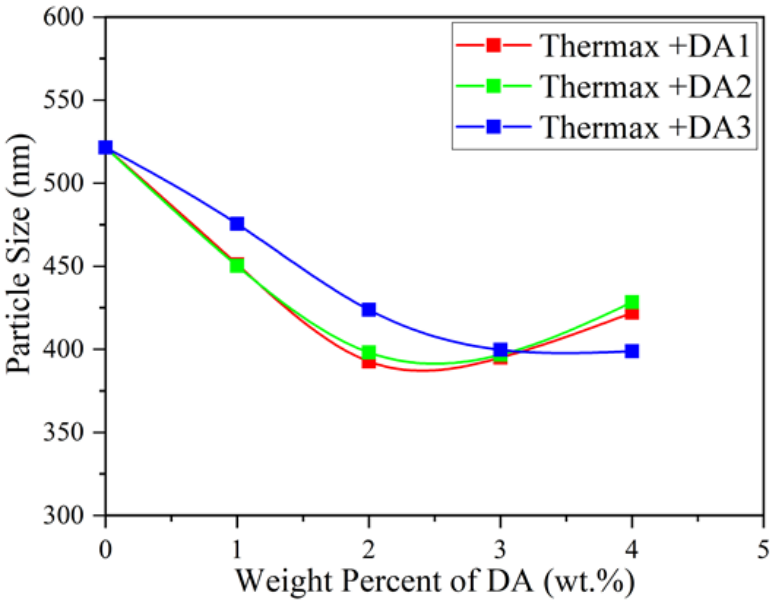

Figure 4-2. The effect of dispersing agents on the particle size of Thermax N991 Carbon Black

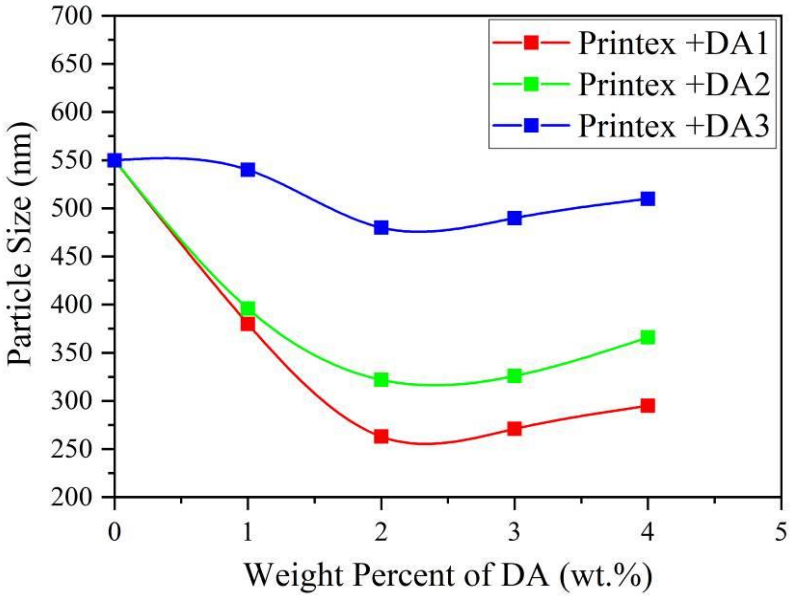

Figure 4-3. The effect of dispersing agents on the particle size of Printex-U Carbon Black

As shown in Figure 4-2, the minimum mean particle size was obtained for Thermax N991 using DA1 and DA2. The particle size was decreased from 521 nm to 392 nm for Thermax N991. On the other hand, the minimum particle size was also obtained using DA1 for Printex-U. The particle size is decreased from 550 nm to 263 nm for Printex-U.

The maximum amount of dispersing agent adsorbed on the carbon black (CB) surface depends on its head groups and tail lengths. It was shown that the secondary amine groups of DA1 and DA2 support the proton exchange between head groups of the dispersing agent and acid groups on the CB surface. Thus, the surface charge is generated to give long-range electrostatic repulsion forces between CB particles. Then, the net effect of the forces improved the stability of the dispersion.

DA1 consists of secondary amine groups as well as carboxylic functionalities. The presence of a carboxylic group on the structure of DA1 provides two side interactions; therefore, it can react with both acidic and basic functional groups. DA2 is a solution of polyester block copolymer consisting of secondary amine groups and interact with acid groups. DA1 and DA2 generate a uniform electrical charge on the carbon black surface; therefore, electrostatic stabilization is formed. The resulting repulsion effect and the steric stabilization prevent the flocculation, and the average particle size can be decreased. However, DA3 may reduce the surface activity of the polymeric materials by accumulating on the surface; thus, it does not directly interact with the particle surface. As a result, DA3 may not effectively decrease the average particle size of carbon black particles.

The stabilization effect of carbon black particles was observed by a sedimentation test. Printex-U powder is used due to its smaller particle size and high tendency to agglomerate. Printex-U samples were mixed with Ethyl Acetate solvent in beakers. Dispersing agents were added into the beakers with 2wt.% based on CB. The sedimentation behavior for these samples was observed after 24 hours.

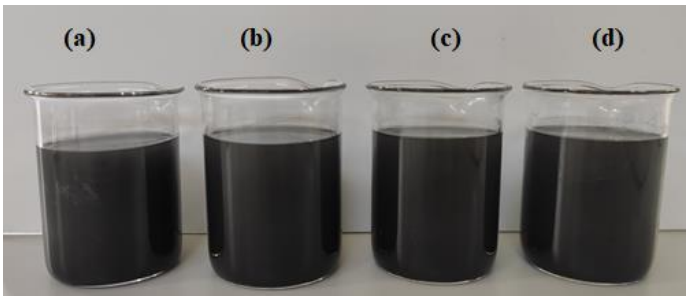

Figure 4-4. Effect of different dispersing agents (a: no dispersing agent; b: DA1; c: DA2; d: DA3) on the stability at t=0

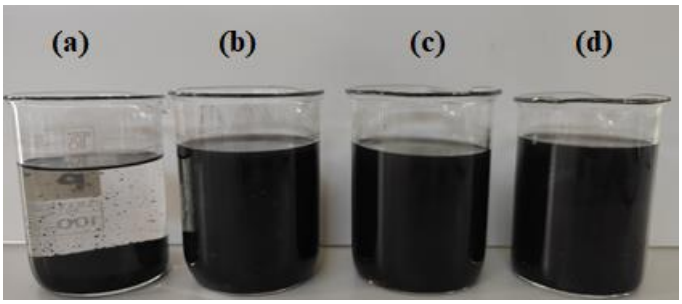

Figure 4-5. Effect of different dispersing agents (a: no dispersing agent; b: DA1; c: DA2; d: DA3) on the stability at t=24 hours

DA1, DA2, and DA3 are polymeric dispersing agents with pigment affinitive groups that attach to the pigment surface and therefore ensure adsorption of the dispersing agents. The polymer segments are also responsible for compatibility in organic solvents and are the first contact between two particles. If the particles become close to each other, the polymer chains start to interpenetrate, therefore increasing the local concentration of polymer chains. As a result, the solvent molecules start to migrate into the interpenetrating polymer layers zone and re-separate the two particles again. In this way, a balance is achieved between attraction and repulsion. The thickness of the adsorbed polymer layer determines whether the distance between the particles is large enough to overcome the London van-der-Waals attraction forces between the molecules (Pirrung et al., 2002). In this way, all the dispersing agents can stabilize the carbon black particles, as shown in Figure 4-5.

4.1.1 Ultrasonication Study

The smaller aggregates usually cannot be broken up since the primary particles in these smaller aggregates are firmly bound to each other; thus, it is practically impossible to break them apart (Napper, 1984). Hence, the ultrasonication energy is necessary to decrease the particle size of aggregates. Printex-U CB was used to identify ultrasonication parameters such as the ultrasonication power, duration time, and start/wait period since it was found to have a high tendency to agglomerate. DA1 dispersing agent was used as 2wt.% based on Printex-U CB amount in this study.

The ultrasonication optimization results can be seen in Appendix B. The results show that 300 W ultrasonication power with 5 minutes duration and 7 seconds/3seconds start/wait period gives optimum results based on the mean particle sizes. The volume-weighted mean size (D[4:3]) of Printex-U agglomerates was found as 195nm at those ultrasonication parameters. In comparison, the D[4:3] of Printex-U agglomerates without ultrasonication process was found as 263 nm. The ultrasonication parameters determined were also used for further studies related to the mechanical properties.

4.2 Rheological Properties of Carbon Black Filled Polyurethane Liner

The rheological properties of the CB-filled polyurethane liner formulations containing 2wt.%, 5wt.%, 10wt.% of the carbon black powders were characterized. The other parameters such as NCO/OH ratio, Triol/Diol ratio, and Plasticizer/Polymer ratio were kept constant for the polyurethane liner formulations. The effect of particle size and CB powder loading on rheological properties is discussed.

4.2.1 Effect of Carbon Black Loading on Viscosity of Carbon Black Filled Polyurethane Liner

The viscosity of the liner formulations that do not contain isocyanate can be seen in Figure 4-6. The results show that the CB powder type and loading directly affect the viscosity as expected. Since the smaller particle size has a higher surface area, they adsorb more polymer on the surface; therefore, the viscosity increases. Highest loading of Printex-U particles that can allow processable polyurethane liner formulation was found as 10 wt.% (see Figure 4-6). Thus, 10 wt.% of powder loading was kept constant for further studies to show the effect of CB particle size on the properties. PT10 is a binary mixture produced by mixing 5wt.% of Thermax N991 and 5wt.% of Printex-U. Since Printex-U and Thermax N991 have a theoretically big and small particle size, the effect of particle packing on the properties is discussed using PT10 formulation. In fact, particle packing depends on the voids between larger particles filled by smaller particles, thereby reducing the volume of voids (Furnas, 1931).

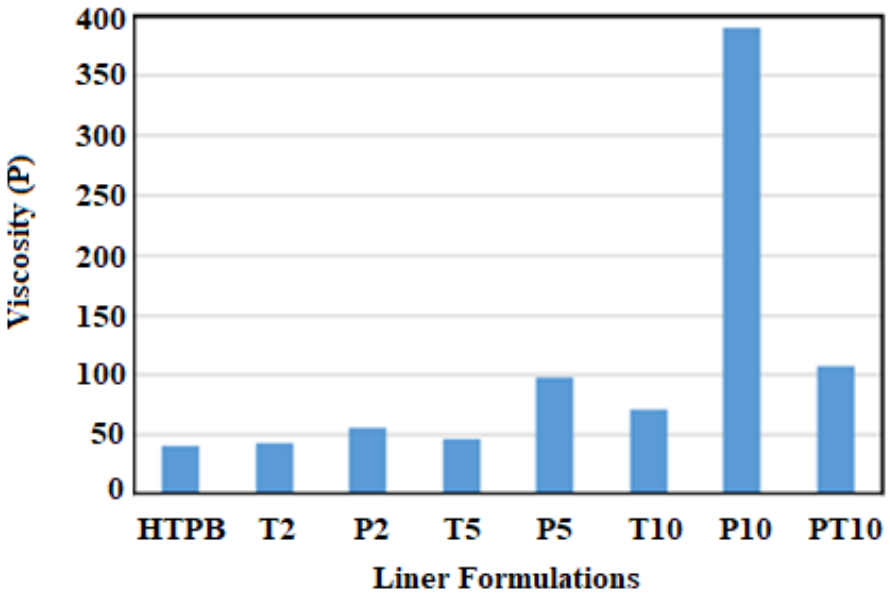

Figure 4-6. The viscosity of CB filled polyurethane liner formulations at 25°C and 20 rpm

As shown in Figure 4-6, the binary mixture led to a moderate effect that the viscosity of PT10 was between the viscosity of P10 and T10. In fact, the average particle size of Printex-U was close to the average particle size of Thermax N991, and particle packing could not be effectively formed. Hence, the addition of Printex-U did not effectively influence the viscosity of the PT10 formulation.

The critical point is to detect the filler loading limit since higher filler loading causes higher viscosity. In fact, the polyurethane liner formulation should be processable and easily applicable. Hence, the limit of the particle loading for Printex-U was selected as 10wt.%. The particle loading upper than 10wt.% was not able to process using a mechanical stirrer due to high torque need during the mixing. Although the particle loading could be increased than 10wt.% for Thermax N991 filled polyurethane liner, it was kept as 10wt.% of filler loading due to observing the effect of particle size on the properties of CB filled polyurethane liner for further studies.

4.2.2 Effect of Dispersing Agents on Viscosity of Carbon Black Filled Polyurethane Liner

The formulations of P10, T10, and PT10 were selected to study the influences of a dispersing agent on the viscosity. P10 and T10 were chosen since they have different particle size distributions. PT10 was chosen to characterize the effect of binary filler content in the polyurethane liner. The carbon black loading was kept constant at 10wt.% for those formulations. Since carbon black powders used in the formulations tend to agglomerate, it is expected that the dispersing agents work more effectively on those samples. The influences of dispersing agent type and concentration on viscosities of the samples are illustrated in Figure 4-7.

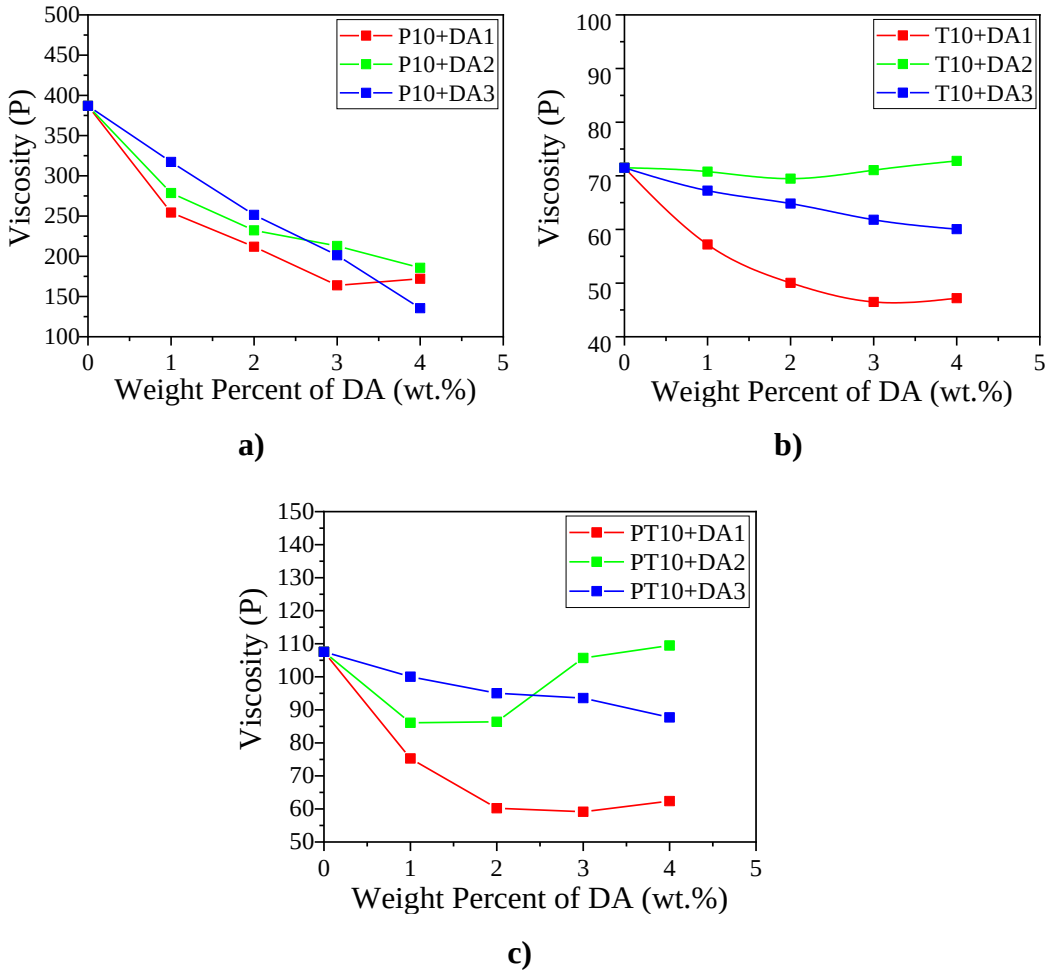

Figure 4-7. Viscosities at 25 °C and sheat rate of 4.3 s^{-1} for the samples: a) P10, b) T10, and c) PT10 containing different dispersing agents

As shown in Figure 4-7, the dispersant DA1 was the most effective dispersant for decreasing the viscosity. The viscosity is also related to the wetting of the CB powders. In fact, the surface tension of the binder must be lower than the surface energy of the pigment to achieve good wetting of pigment agglomerates and primary particles (Pirrung et al., 2002). For the DA1, its affinic groups cause them to be adsorbed onto the CB particle surface. Then, it penetrates into the agglomerates, and therefore HTPB binder wets the surface of the primary particles or aggregates of CB. As a result, the viscosity decreases. Although DA2 has a similar mechanism to DA1, the bi-functional structure of DA1 may provide better wetting. However, DA3 has a

different mechanism compared to DA1. DA3 diffuses on the surface, and its unreacted functional groups cause hydrophilicity enhancement of the surface, and therefore contact angle reduces. The mechanism of surface energy reduction was assumed to be the migration of silicone additive chains to the surface. Although DA3 can not directly interact with carbon black particles, it lowers the surface energy of the CB-filled polyurethane liner and reduces the viscosity.

4.2.3 Rheological Behavior of Carbon Black Filled Polyurethane Liner

The formulations (T10, PT10, and P10) and those containing 2wt.% of DA1 based on the CB were selected. Although 3wt.% of DA1 provides a higher reduction for the viscosity of the CB-filled polyurethane liner, 2wt.% of DA1 was selected due to providing higher mechanical properties (see Chapter 4.3). The samples were measured using spindle speed from 5 rpm to 40 rpm with 5 rpm increment at 25°C, 35°C, 50°C, and 65°C, respectively.

Figure 4-8 shows the viscosities of the formulations (T10, PT10, and P10) at different shear rates and temperatures (**25°C, 35°C, 50°C, and 65°C).**

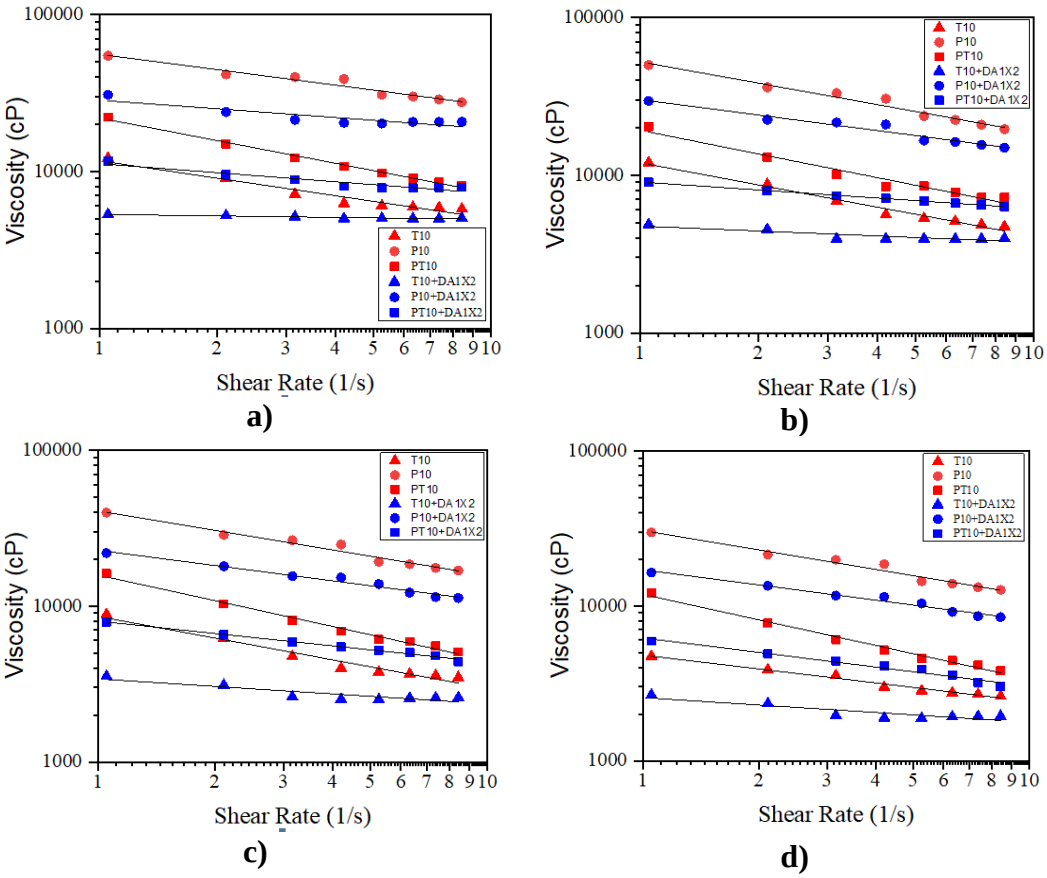

Figure 4-8. The viscosity of the formulations at temperatures of a) 25°C b) 35°C c) 50°C and d) 65°C

Table 4-3 summarizes the consistency index and power-law index values of the samples (T10, PT10, and P10) when the power law is used to represent the viscosity as a function of shear rate (see Equation-3).

Table 4-3. The consistency index and power-law index values of the samples at various temperatures

Samples	25 ºC		35 ºC		50 ºC		65 ºC	
	k (cP)	n	k (cP)	n	k (cP)	n	k (cP)	n
T10	9136	0.812	7783	0.696	5536	0.695	3971	0.601
T10+DA1X2	7901	0.969	6010	0.896	3750	0.841	2657	0.721
P10	53155	0.674	39480	0.550	32623	0.584	19252	0.449
P10+DA1X2	29301	0.772	29375	0.721	21036	0.685	8761	0.583
PT10	13748	0.521	10444	0.420	8433	0.430	5938	0.296
PT10+DA1X2	12076	0.866	10327	0.791	7688	0.724	5449	0.604

As can be seen from Table 4-3, the PT10 samples showed the most shear thinning behavior since the PT10 samples had lower 'n' values, and the T10 samples showed the least shear thinning behavior. It was also observed that the shear-thinning became more significant at higher temperatures. The consistency index of the samples was decreased with the addition of DA1. Furthermore, the power-law index of the samples was increased with the addition of DA1, suggesting less shear rate dependence for the viscosity of samples.

4.3 Mechanical Properties of Carbon Black Filled Polyurethane Liner

The effects of CB particle size and loading on mechanical properties were studied. The mechanical properties are not only affected by filler type or loading but also design parameters such as ratios of NCO/OH, Triol/Diol, and Plasticizer/Polymer. Thus, design parameters were fixed for the CB-filled polyurethane liner formulations. The cured binder was used as a control sample to monitor mechanical property changes. The tensile strength and strain results can be seen in Figure 4-9.

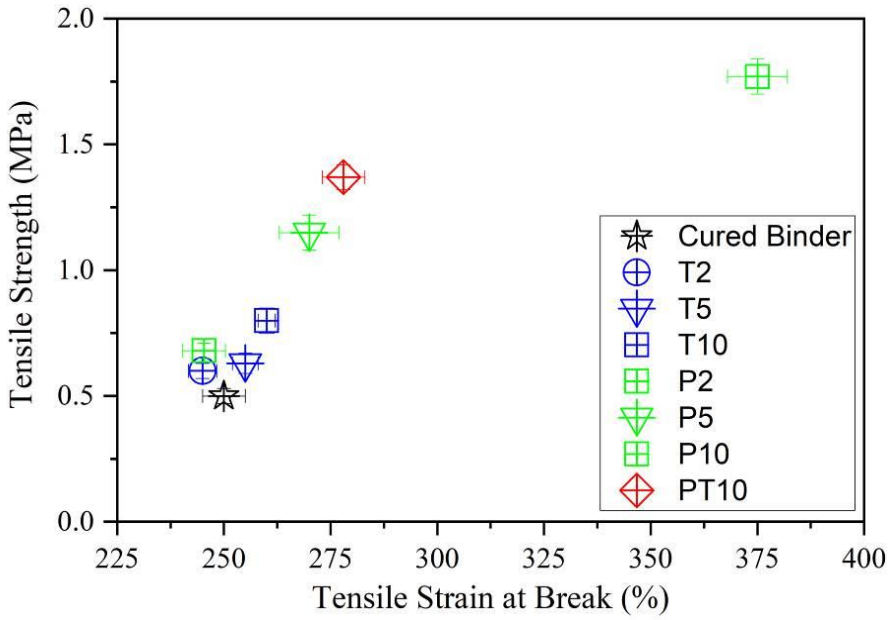

Figure 4-9. Tensile strength and the tensile strain at break results for the CB-filled polyurethane liner formulations consisting of different carbon black loading

Figure 4-9 shows that the tensile strength of the samples was increased with the addition of CB. The addition of 10wt.% Printex-U CB provided the best mechanical properties improvement (i.e., tensile strength and strain). In fact, the surface area of the particles increases with the decreasing particle size. The higher surface area brings about higher adsorption of the binder; therefore, the mechanical properties increase when smaller particles are used. Moreover, the increase of carbon black loading brings about better mechanical properties, as expected.

4.3.1 Effect of Dispersing Agents on Mechanical Properties of Carbon Black Filled Polyurethane Liner

The liner formulations P10, PT10, and T10 were selected to investigate the effects of dispersing agents. Three types of dispersing agents were used in the selected formulations with 1wt.%, 2wt.%, 3wt.%, 4wt.% based on the CB content.

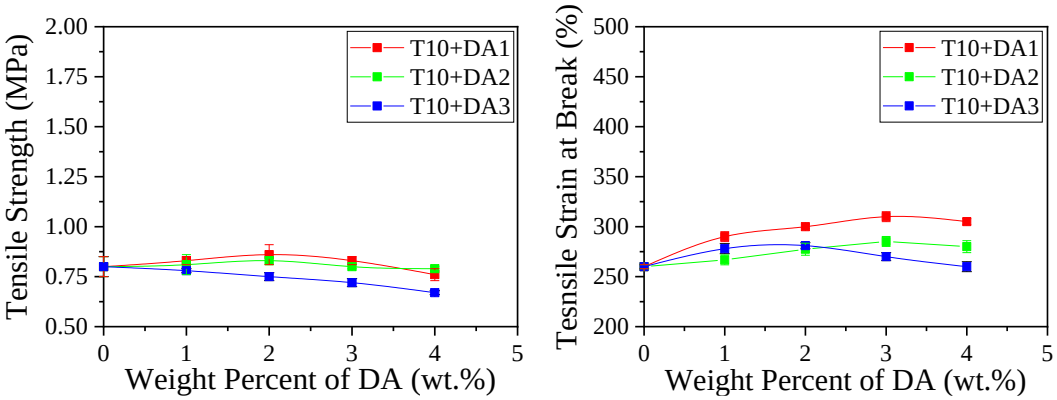

Figure 4-10. The tensile strength and tensile strain at break graphs for the T10 samples containing various dispersing agents with different amounts

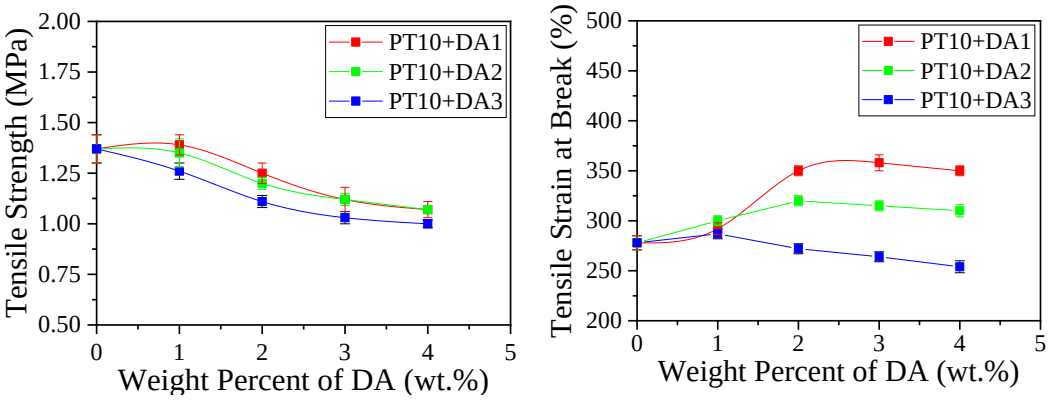

Figure 4-11. The tensile strength and tensile strain at break graphs for the PT10 samples containing various dispersing agents with different amounts

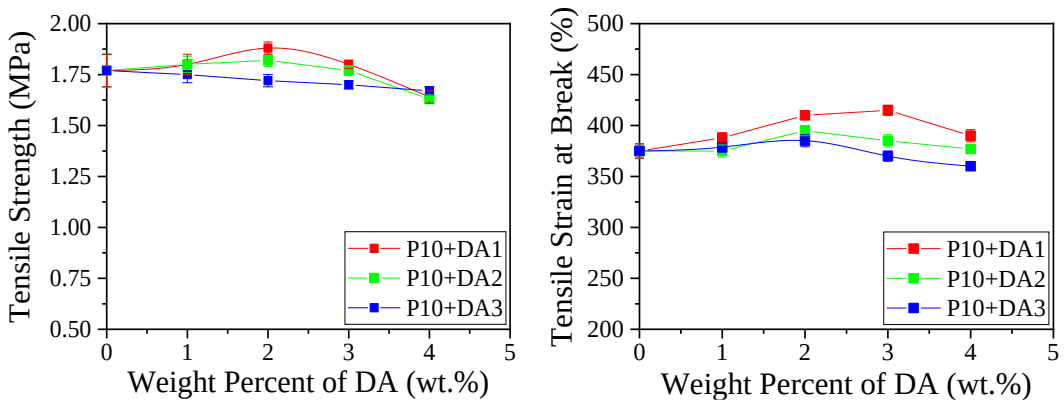

Figure 4-12. The tensile strength and tensile strain at break graphs for the P10 samples containing various dispersing agents with different amounts.

According to Figure 4-10, Figure 4-11, Figure 4-12, DA1 provided the best tensile strength values at 2wt.% of DA1. Moreover, all dispersing agents increase the tensile strain at break values up to 2wt.% use. When the results were compared with standard CB-filled polyurethane liner, a higher improvement was achieved for P10+DA1X2 containing 2wt.% of DA1 based on CB amount in the formulation. The dispersing agents did not show the expected effect on the mechanical properties of T10 and PT10 formulation. By using one of the dispersing agents, it was desired to improve tensile strengths and strains of those formulations better than standard CB-filled polyurethane liner.

The bifunctionality of DA1 provides two sites for interacting with the functional groups (see. Figure 3-1a): one side with the surface of the carbon black and the other side with the –OH groups on the backbone of the HTPB binder chains. Amine functional group holds on the particle surface and leading to the better dispersion of the carbon black and formation of mesoscopic physical networks.

One tail of DA2 has an amine group that is also adsorbed on the CB surface; therefore, interfacial interaction between filler and binder increases. Other tail has polyester-based block copolymer, which forms electrostatic interaction with the binder. Since the bond between the HTPB binder and DA1 was stronger than the

electrostatic interaction between the HTPB binder and DA2, DA1 improved mechanical properties more than DA2. DA3 diffuses on the surface and lowers the surface free energy, which increases the wetting of the particles. Although wetting of the particle may improve the dispersion quality, –OH functional groups of DA3 could react with –NCO groups of the isocyanate. Hence, it may be stated that DA3 affects the reaction stoichiometry between HTPB binder and isocyanate; therefore, it lowers the mechanical properties.

The results also showed that the samples without dispersing agents had a higher standard deviation of tensile strength and tensile strain at the break since the carbon black particles did not disperse effectively. Hence, It can be claimed that all dispersing agents perform their works properly since the standard deviation decreases.

The CB-filled polyurethane liner formulation was also prepared by using the ultrasonication process. The proper ultrasonication parameters were found as 300 W ultrasonication power with 5 minutes duration and 7 seconds/3seconds start/wait period according to Chapter 4.1.1. P10 formulation having 2wt.% DA1 was prepared by using ultrasonication. P10 formulation was selected since Printex-U used in the formulation had a high tendency to agglomerate. Hence, it was necessary to destroy agglomerates using external energy. It was found that ultrasonication and use of DA1 were highly effective in decreasing the particle size of Printex-U CB powder, according to studies in Chapter 4.1. The ultrasonicated sample is indicated as P10+DA1X2-S. The comparative mechanical test results can be seen in Figure 4-13.

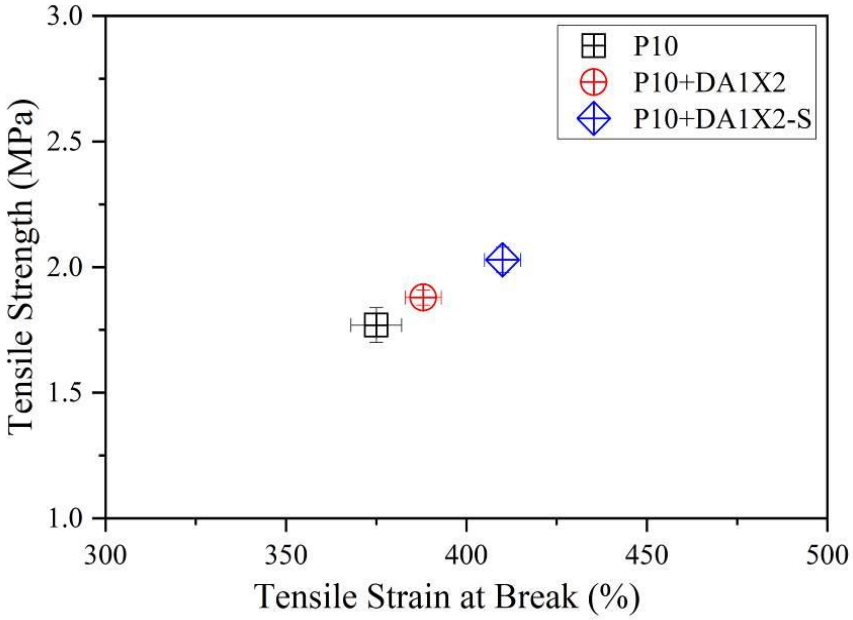

Figure 4-13. Stress-Strain graph of CB filled polyurethane liner formulations P10, P10+DA1X2, and P10+DA1X2-S

The ultrasonication process increased the mechanical properties of the P10 sample since the ultrasonication energy decreased the agglomerate size of the CB powders. Ethyl Acetate solvent was used and then evaporated using a vacuum oven. The solvent must be evaporated effectively; otherwise, the solvent may soften the final CB-filled polyurethane liner and decrease mechanical properties. Ethyl Acetate is used since it can dissolve the HTPB binder, and it has a low boiling point (65°C), which is also the curing temperature of polyurethane liner. Thus, ethyl acetate can evaporate during the curing period. It also provides to handle the sample easily during the solvent evacuation in the vacuum oven and ultrasonication. It must be considered that the temperature of the sample may rapidly increase during ultrasonication. The temperature increase causes faster solvent evaporation and curing reaction; thus, ultrasonication can not work effectively.

Figure 4-13 shows that P10, P10+DA1X2, and P10+DA1X2-S formulations had better tensile strengths and strain properties than the standard CB-filled polyurethane liner. Hence, those formulations were selected for further studies.

4.4 Thermal Properties of Carbon Black Filled Polyurethane Liner

Thermal properties of P10, T10, and PT10 were characterized using a Dynamic Mechanical Analyzer (DMA). The glass transition temperatures are summarized in Table 4-4. The graphs related to Storage Modulus(E'), Loss Modulus(E″), and Tan(δ) are given in Figure 4-14.

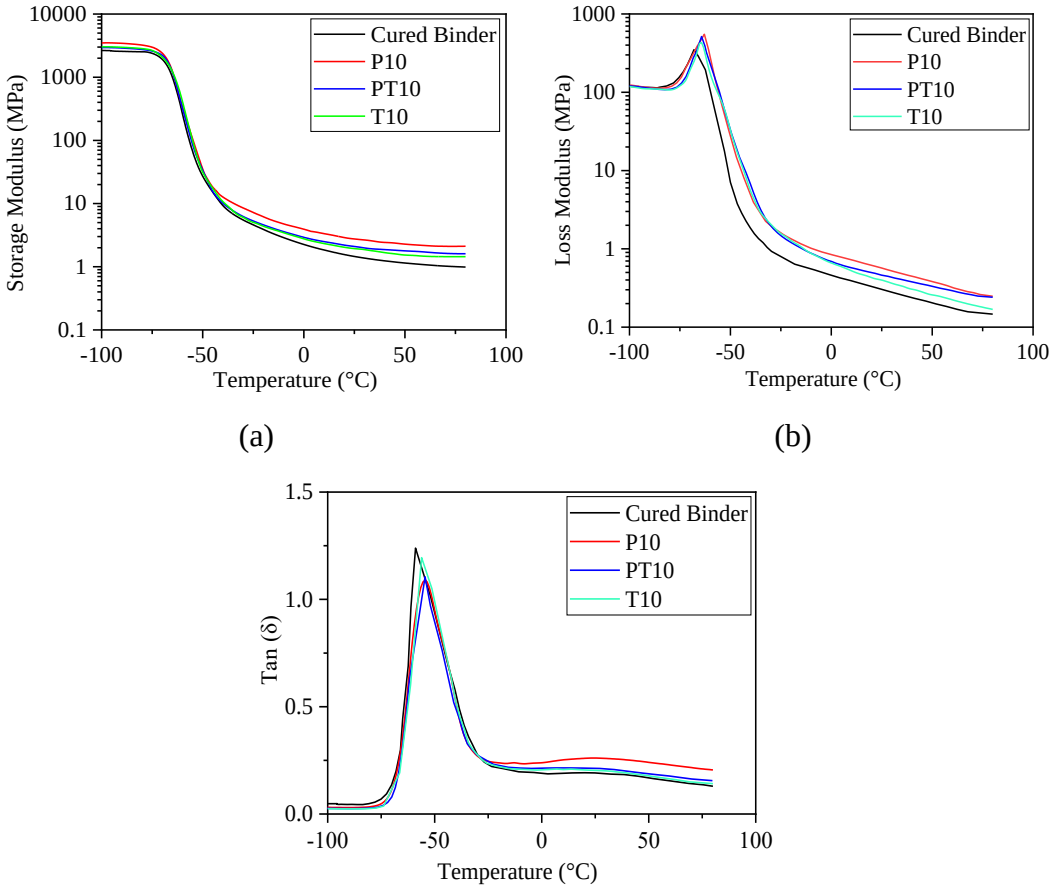

Figure 4-14. DMA results of the samples (a) Storage Modulus (b) Loss Modulus (c) Tan(δ) vs. Temperature

Table 4-4. Summary of the DMA results for CB filled polyurethane liner formulations

Sample	T_g (°C) by E″ Peak	T_g (°C) by Tan(δ) Peak	E'at 25°C (MPa)
Binder	-67.03	-58.96	1.45
T10	-65.28	-56.12	1.92
P10	-62.89	-53.54	2.75
PT10	-64.27	-54.49	2.06

According to Table 4-4, the difference between the glass transition temperatures comes from the free movement of the polymer chain, which is related to Tg. It can be stated that smaller particle size diminishes the chain movement, and therefore, higher Tg is found. The P10 samples had the highest storage modulus (E') at 25 °C, agreeing with the mechanical test results. Since the design parameters were kept constant for all CB-filled polyurethane liner formulations, the crosslink density of those formulations was theoretically equal, and the change in storage modulus was directly related to the particle size of CB used in the polyurethane formulations.

4.5 Effect of Dispersing Agents on Thermal Properties of Carbon Black Filled Polyurethane Liner

The highest improvement was achieved for P10 formulation, and therefore the effect of dispersing agents on the thermal properties of CB filled polyurethane liner was studied using the P10 formulation. The glass transition temperatures are summarized in Table 4-5. The graphs related to Storage Modulus(E'), Loss Modulus(E″), and Tan(δ) are given in Figure 4-15.

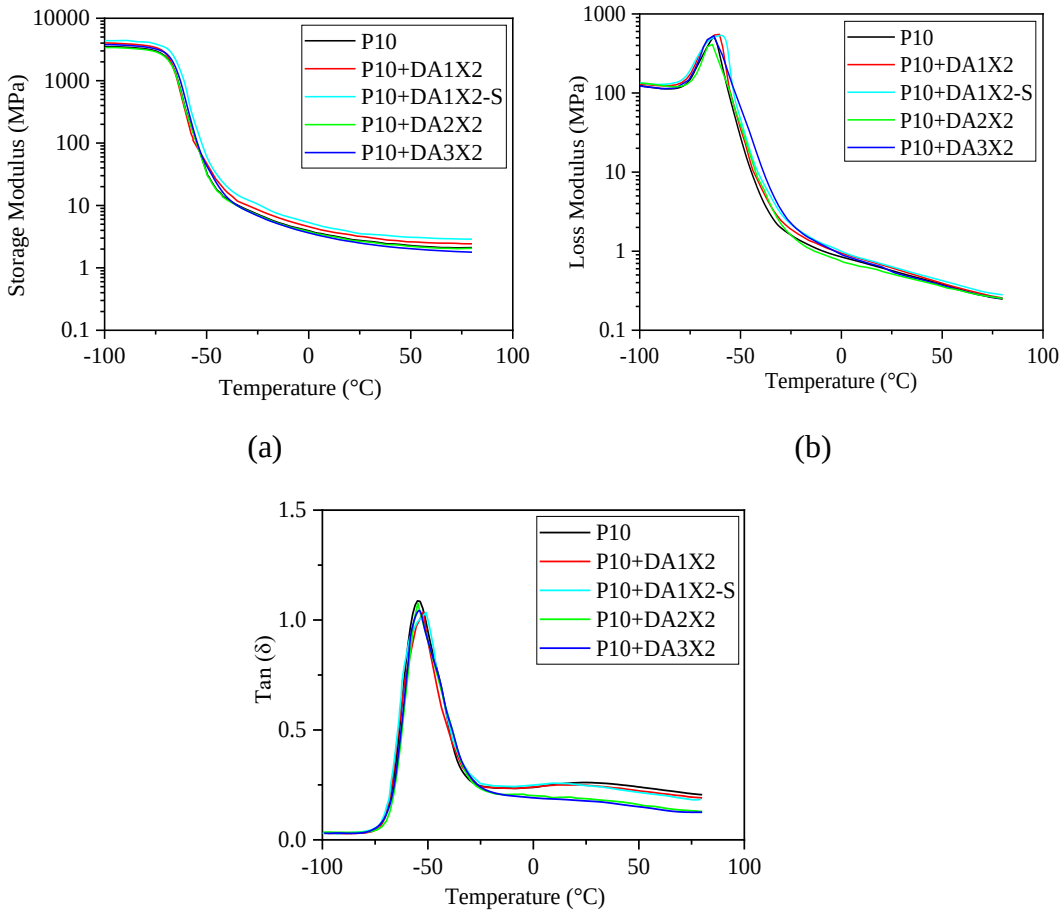

Figure 4-15. DMA results of the samples (a) Storage Modulus (b) Loss Modulus (c) Tan(δ) vs. Temperature

Table 4-5. Summary of the DMA results for liner formulations containing various dispersing agents

Samples	T_g (°C) by E″ Peak	T_g (°C) by Tan(δ) Peak	E'at 25°C (MPa)
P10	-62.89	-53.54	2.75
P10+DA1X2	-60.48	-52.15	3.22
P10+DA1X2-S	-57.86	-50.84	3.54
P10+DA2X2	-63.27	-54.80	2.67
P10+DA3X2	-62.94	-53.81	2.47

The dispersing agents were used as 2wt.% based on carbon black amoun in the P10 formulation. The amount of dispersing agents was selected according to the results of the mechanical properties (see Chapter 4.3). As shown in Table 4-5, DA1 gives better results based on the storage modulus at 25°C. DA1 also slightly increases glass transition temperature (T_g) since DA1 increases polymer-filler interaction and provides decreasing free volume, resulting in less mobility of the macromolecules.

The thermal property of the CB-filled polyurethane liner formulation prepared by ultrasonication (P10+DA1X2-S) is also given in Table 4-5. The results suggested that the ultrasonication process increased mechanical properties based on the storage modulus at 25°C. Tg also increased too when ultrasonication was used. The DA1 can adsorb on the surface of the CB, and then it can change the surface property of the CB filler. Higher DA1 adsorption on carbon black filler provides a high area of filler that polymer interacts. Thus, polymer motion is restricted, and therefore, Tg increases.

4.6 Limiting Oxygen Index (LOI) Analysis

Carbon nanomaterials positively affect the flame retardancy of polymers, especially the geometry of carbon nanomaterials plays a key role (Liu et al., 2018). The carbon black used in this study is considered as a three-dimension structure; therefore, it is

meaningful to explore the flame-retardant behavior with dispersing agents. Materials with LOI values less than %21 are classified as combustible, but those with LOI greater than %21 are classed as self-extinguishing since their combustion can not be sustained at ambient temperature. In general, the higher the value of the LOI, the greater the flame retardancy property.

The CB-filled polyurethane liner formulations P10, PT10, and T10 were used for the LOI test. Dispersing agents were used as 2wt.% based on the CB amount in the formulation. Besides, twenty samples were used for each test. In Figure 4-16, the LOI results are presented. P10, PT10, and T10 samples are demonstrated in the first columns, and the other columns belong to samples containing DA1, DA2, and DA3 with 2wt.% based on CB, respectively.

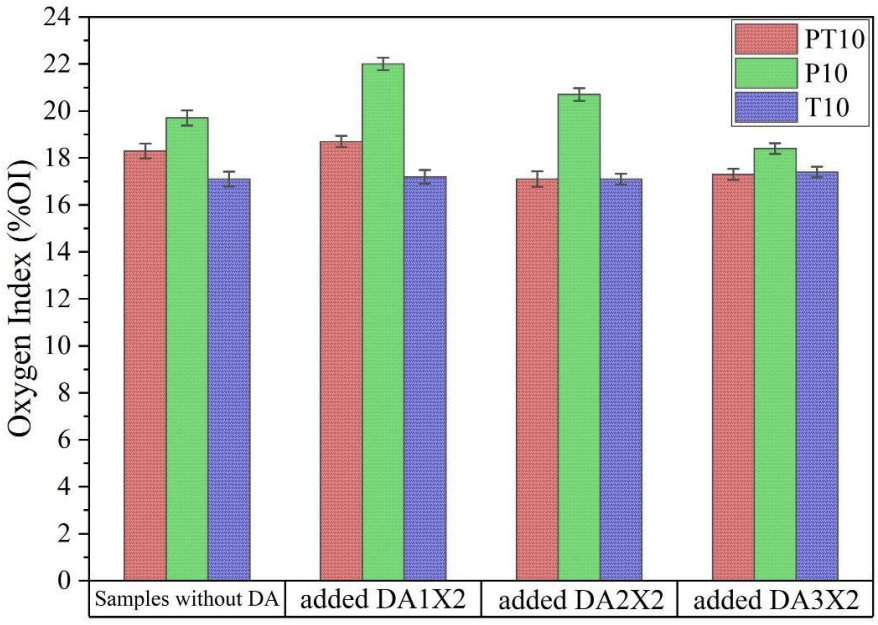

Figure 4-16. LOI Analysis of the samples

The LOI analysis shows that particle size affects the flammability characteristics of the sample. Smaller particle sizes showed lower flame retardancy property. During the combustion process, a heat barrier was formed by carbon black particles. Consequently, the char layer had a more substantial effect on combustion and delayed the temperature increase in the sample. The residual char layer not only acts as the shield for heat transfer but also hinders the migration of volatile decomposition

products and the diffusion of oxygen into the sample (Yang et al., 2017). According to Figure 4-16, the P10 sample had a higher LOI index due to having a smaller particle size. Small particle size enhanced barrier effect due to higher char layer formation directly proportional to particle surface area.

During the combustion process, cracks are formed and propagate into the sample. These crack openings bring about a high mass-loss rate, and this increases thermal degradation. Hence, the sample should be mechanically resistant to crack formation during combustion. Typically, agglomerated particles in the polymer matrix may limit the ability to absorb impact energy because the agglomerates disturb polymer matrix continuity. The stress can concentrate on the agglomerates, and therefore, microcracks may initiate at those points during combustion. Thus, it is essential to decrease agglomeration to obtain high flame retardancy. Takashi et al. demonstrated that forming a network structure of nanoparticles within a polymer matrix can significantly diminish the nanocomposite flammability (Kashiwagi et al., 2008). The use of DA1 increased the LOI index of the P10 liner sample from 19% to 22% since it provided better particle dispersion and improved mechanical properties; thus, the crack formation and initiation during the combustion could be prevented. DA2 and DA3 did not significantly change in flame retardancy of the samples.

4.7 Scanning Electron Microscopy (SEM) Analysis

Scanning Electron Microscopy (SEM) was used to characterize the freeze-fractured surfaces of the CB-filled polyurethane liner samples. The samples containing DA1 were studied since DA1 has provided better results according to previous analysis. The SEM images can be seen in Figure 4-17.

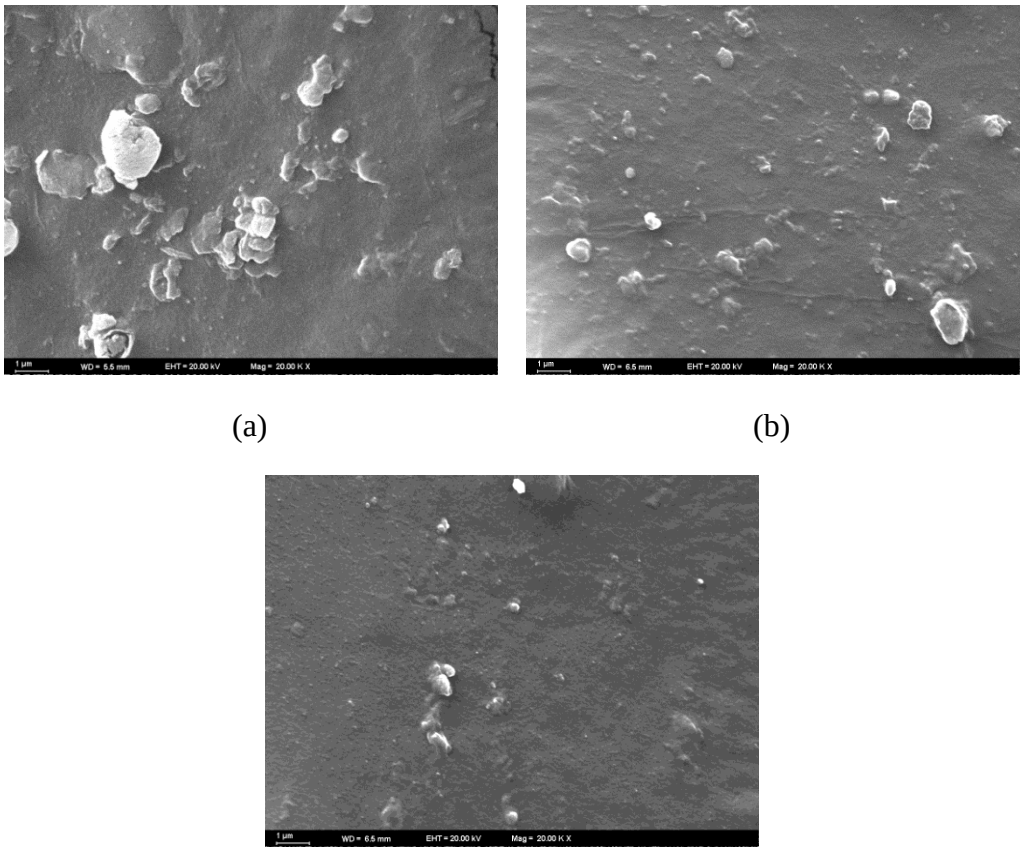

(a) (b)

(c)

Figure 4-17. SEM Image of (a) P10 (b) P10+DA1X2 (c) P10+DA1X2-S

The fracture roughness of the polymer nanocomposites reflects the dispersion level and interfacial interactions of CB particle and polymer. Figure 4-17 shows the smoothness of the samples as follows P10+DA1X2-S > P10+DA1X2 > P10. In other words, that order could be linked with the number of clusters in the samples. The carbon black particles appeared as white dots, and it was hard to detect their primary particle sizes. However, the use of DA1 combining with the ultrasonication process lowered the agglomerate size of carbon black when the clusters of P10+DA1X2-S were compared to other samples. In addition, the clusters were decreased when DA1 was added to the CB-filled polyurethane liner without the use of ultrasonication.

4.8 Mechanical Strength of Liner-Propellant Interface

The bonding performance was investigated using Metal-Insulator-Liner-Propellant (MILP) tensile and shear tests. In this study, the P10 formulation was used since a reasonable improvement was achieved compared to the currently used CB-filled polyurethane liner formulation, referred to as standard liner. Since the addition of 2wt.% of DA1 based on CB improved the properties of the liner, the effect of DA1 usage on the interface properties was investigated in this chapter.

Before the MILP tests, the chemical compatibility of the liner and propellant formulations must be controlled to prevent side reactions at the liner-propellant interface. For this purpose, the Vacuum Stability Test (VST) was done for the propellant and CB-filled polyurethane liner formulations (P10, P10+DA1X2, P10+DA1X2–S). The results and calculations can be seen in Appendix D**,** and it shows that P10, P10+DA1X2, P10+DA1X2–S liner formulations are chemically compatible with the propellant used in this study.

Since DA1 decreased the viscosity of the CB-filled polyurethane liner formulation more effectively, the time to get tacky state could be changed. Tacky state time was determined by curing analysis related to the complex viscosity vs. time graph (see Figure C-1 in Appendix C). For this purpose, the complex viscosity vs. time graph was plotted. Complex viscosity at 10 Pa.s was taken as a reference, and time values were compared for the samples (P10, P10+DA1X2). The results are summarized in Table 4-6. The complex viscosity was determined only for P10 and P10+DA1X2 samples since it was hard to study P10+DA1X2–S due to containing solvent. After P10+DA1X2–S was poured into the DMA instrument holder, the solvent was evaporated, and the level of P10+DA1X2–S sample was below the measurement level, and therefore it caused measurement ambiguity.

Table 4-6. Pot Life of the samples obtained from curing study using DMA

Sample	Pot Life (Second)
P10	~12000
P10+DA1X2	~24000

After the CB-filled polyurethane liner formulation was applied with the thickness of 0.4±0.1mm onto the MILP test samples, it was waited to reach samples tacky-state according to Table 4-6. For the P10+DA1X2–S, it has waited until the sample was considered sticky.

Bonding performance is studied at the point where the fracture occurs from the tensile strength-strain curve. MILP tensile and shear strength depend on both the chemical bonding strength at the liner-propellant interface and migration of the plasticizer species. Chemical bonding at the interface mainly consists of NCO/OH ratios of propellant and liner formulations and the amount of bonding agent in the polyurethane liner that forms bonding with oxidizer particles (i.e., AP) in the propellant. Plasticizer migration occurs from propellant to liner; therefore, it causes a hard layer at the interface. However, this may lead to crack formation at the interface during an aging period of a rocket motor. In this case, the energy absorption of propellant may also decrease at the interface during the operation conditions since the ductility decreases. Thus, plasticizer migration should be minimized.

Two kinds of test specimens were prepared for the MILP tensile and shear tests. The one was tested after the curing was completed, and the others were kept in vacuum bags for six months at room temperature after the curing was completed. The change in tensile strength was discussed using those specimens. The fracture strength results are given in Figure 4-18 and Figure 4-19.

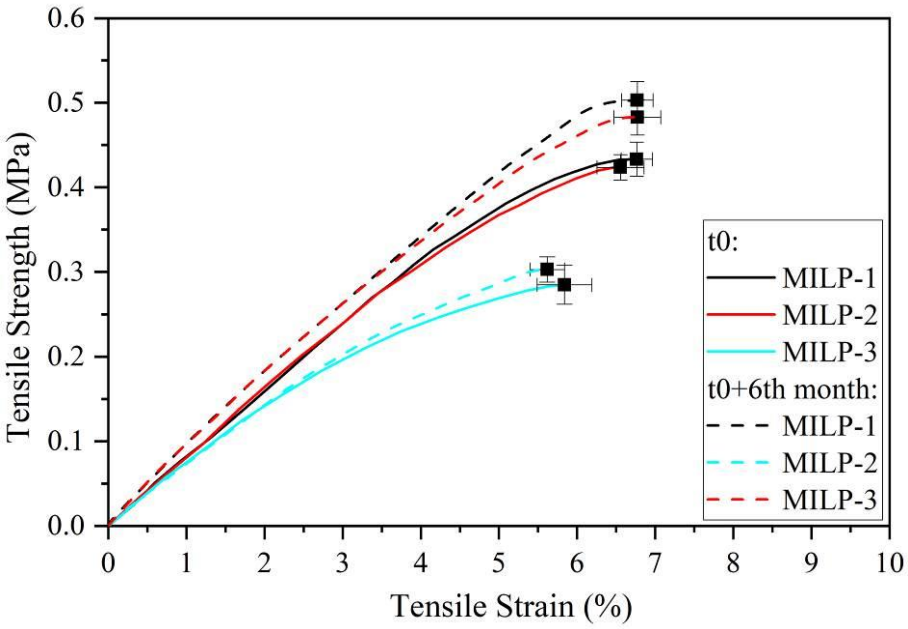

Figure 4-18. MILP Tensile Test results of the samples

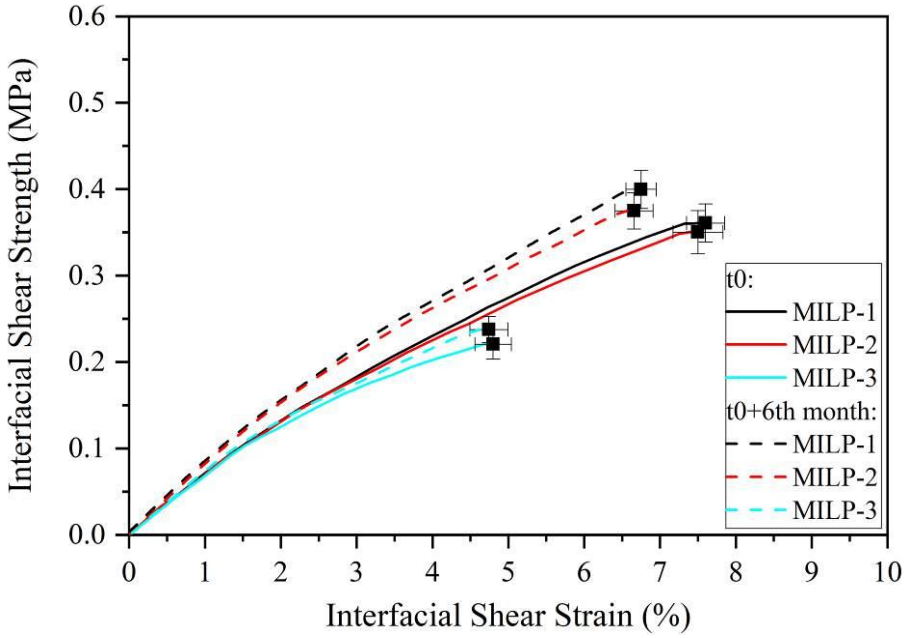

Figure 4-19. MILP Shear Test results of the samples

According to Figure 4-18 and Figure 4-19, it can be stated that the tensile strength increases when the samples are aged for six months due to both plasticizer migration and aging of the propellant. However, the plasticizer migration is a dominant factor

for the interface. The lowest tensile strength value was obtained for MILP-3 due to the existence of the solvent. In other words, the solvent may still exist, even though the sample reaches a tacky state. Although cohesive failures were observed for the MILP-3 sample at the interface, the liner has still existed on the fracture surface of the propellant (see (Figure 4-20a and Figure 4-21a). Hence it could not be interpreted as a totally cohesive failure.

The use of the DA1 slightly decreased the tensile strength of the samples since the dispersing agent constituted van de walls bonds between the HTPB binder and the carbon black particles. It was stated that the functional groups of carbon black might participate in bonding formation due to its –OH or –COOH functional groups (Benli, 1997). Hence, one tail of DA1 interacted with the carbon black surface, and also the other tail also interacted with the HTPB binder; thus, DA1 could decrease the chemical bonding between the liner and the propellant. Moreover, DA1 provided a more regular distribution of CB powders in the polyurethane liner; thus, the plasticizer migration at the propellant-liner interface was limited. Plasticizer migration is discussed in Chapter 4.9. However, the cohesive failure also occurred while DA1 was added to the CB-filled polyurethane liner formulation according to Figure 4-20b and Figure 4-21b.

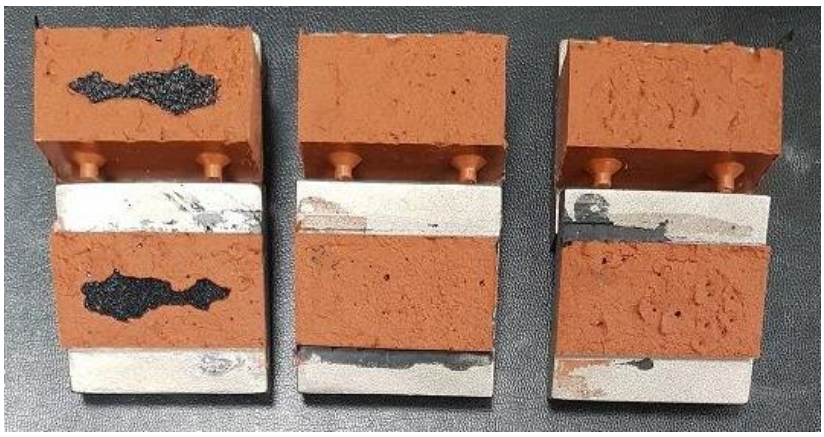

(a) **(b)** **(c)**

Figure 4-20. Failure of MILP Tensile Test specimens kept for 6 months (a) MILP-3 (b) MILP-2 (c) MILP-1

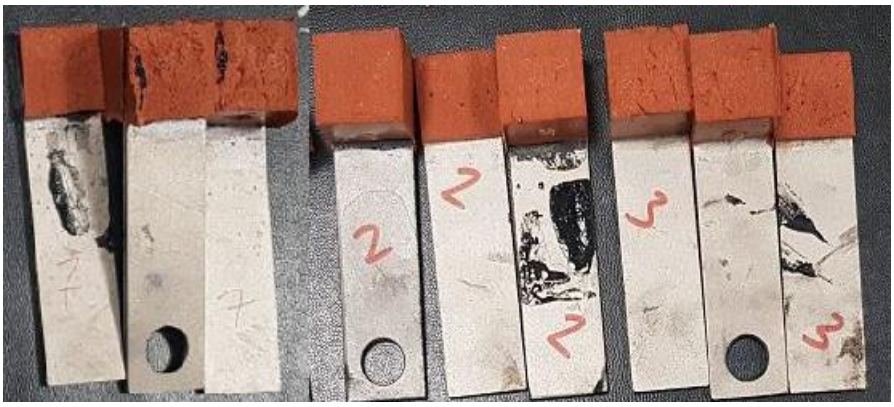

(a) **(b)** **(c)**

Figure 4-21. Failure of MILP Shear Test specimens kept for 6 months (a) MILP-3 (b) MILP-2 (c) MILP-1

Although there were slight differences between the MILP test results of P10 and P10+DA1X2 liner formulation, the statistical tools were used to identify whether the results were significantly different. A T-test was applied for two groups by using Minitab software. A two-sample t-test having a 99.5% confidence level was applied to MILP-1, and MILP-2 samples for both the t0 samples and t0+6months samples since the results were close to each other. A p-value was noted to determine whether the null hypothesis was rejected or not.

P-values were calculated as 0.088 and 0.095 for the t0 MILP tensile and shear test samples, respectively, as 0.075, 0.084 for the MILP t0+6months tensile and shear test samples, respectively. Since all calculated p-values were higher than 0.05, it was stated the null hypothesis was correct. In other words, there was not a significant difference between the means of the two groups: MILP-1 and MILP-2.

4.9 Migration Between Liner-Propellant Interface

The properties of solid propellant may undergo significant change due to the migration of liquid species across the interface between the liner and the solid propellant. The changes may lead to failure in the solid propellant and liner. The

additives with low molecular weight may migrate from high concentration to low concentration. The changes usually occur within the first 5mm of the propellant (Byrd & Guy, 1985). The propellant may become softer or harder due to the migration, and either condition can lead to cracks or failure of the rocket motor. Byrd & Guy states that an excessive amount of bonding agent, isocyanate, and plasticizer may migrate from propellant to liner or vice-versa (Byrd & Guy, 1985). However, Venkatesan et al. claim that plasticizer migration is highly dominant, especially for solid propellant aging (Venkatesan et al., 1993). Hence, the plasticizer migration is discussed in this chapter.

The concentration of additives should be calculated based on the additive/polymer ratio excluding added particles to identify the direction of migration. Solid particles are not considered for the concentration calculations since they are not able to migrate. The polyurethane liner used in this study contains 10wt.% of carbon black, and the propellant contains 86wt.% solid particles such as Ammonium Perchlorate (AP). The polymer concentrations are considered as 90wt.% and 14wt.% for the polyurethane liner and propellant, respectively. The concentration of the plasticizer is calculated using Equation (7).

$$\text{Concentration (wt.\%)} = \frac{\text{Plasticizer (wt.\%)}}{\text{Polymer (wt.\%)}} \times 100 \qquad (7)$$

The migration is illustrated in Figure 4-22, showing that the plasticizer migrates from the propellant to the liner.

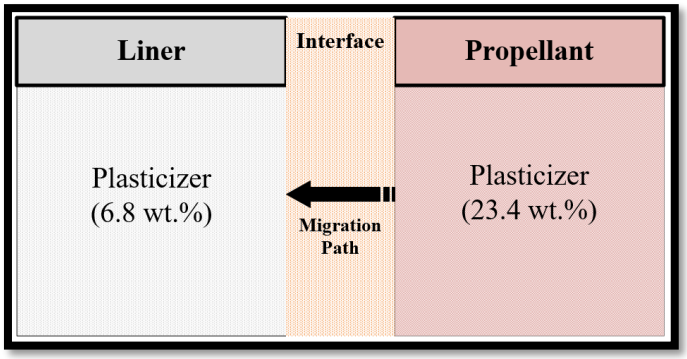

Figure 4-22. Illustration of chemical migration between liner and propellant

The filler in the polyurethane liner formulation has an important role in minimizing migration. Fillers having at least one dimension lower than 100 nm in polymeric matrices achieve a significant decrease in migration compared to the neat matrix by acting as a physical barrier, which has to follow a more tortuous pathway. This phenomenon is called the tortuosity effect. The effect of fillers on barrier properties depends on whether the polymer wets the filler. When the filler is appropriately wetted, permeability decreases; however, if there is a void around each particle caused by poor wetting, a pathway for fast diffusion is provided, leading to a decrease in barrier properties (Rothon, 2017). From the SEM results, DA1 provides better dispersion, and it is expected that the chemical migration may be minimized. P10 and P10+DA1X2 liner formulations were used in the migration study since the P10+DA1X2-S formulation was eliminated due to its low interface strength. TGA and FTIR analysis were used to monitor the plasticizer migration using propellant samples from the different points. The points where the propellant samples were taken, illustrated in Figure 4-23. I-1 and I-2 represent the propellant samples at the liner-propellant interface. I-1 propellant sample was interfaced with the P10 liner, and the I-2 propellant sample was interfaced with the P10+DA1X2 liner. Moreover, RP is the reference propellant sample taken 5 mm away from the interface. The effect of DA1 on migration is discussed comparing with a reference propellant sample (RP).

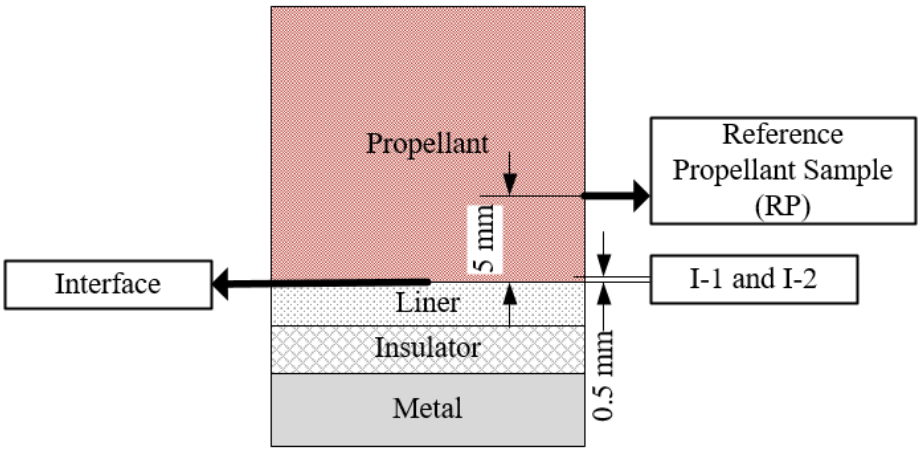

Figure 4-23. Representation of points that propellant was sampled

4.9.1 Thermogravimetric Analysis (TGA)

Isodecyl Pelargonate (IDP) was used as a plasticizer in both propellant and CB-filled polyurethane liner formulation. TGA Analysis was done for RP, I-1, and I-2 samples. The TGA graphs can be seen in Figure 4-24.

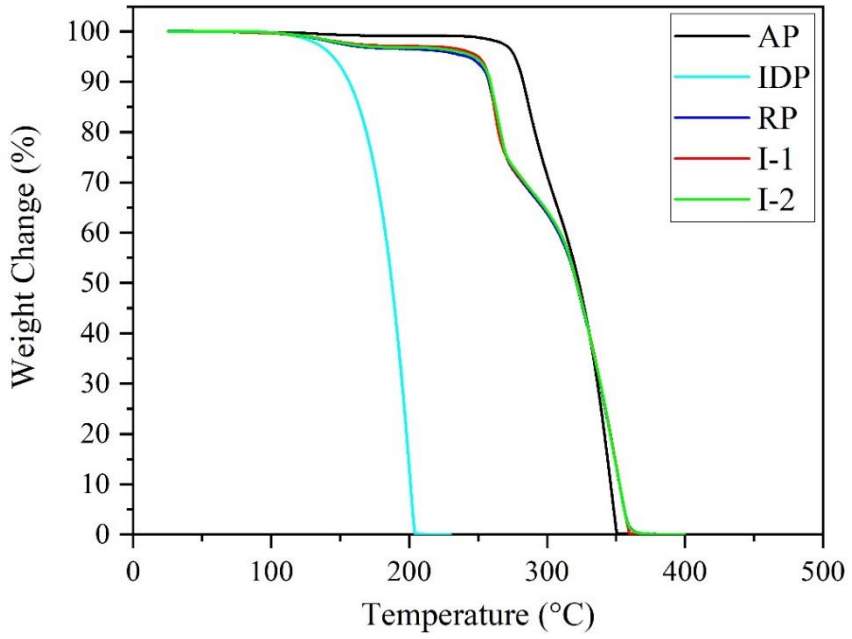

Figure 4-24. TGA curves of the propellant samples (RP, I-1, I-2), IDP, and AP

IDP was degraded between 100°C and 205°C. However, it was degraded until 220°C in the cured propellant since the crosslinked structure of the propellant was delayed the degradation. The decomposition of the binder showed a two-stage degradation. At first, 10–15% mass weight loss occurred during this stage, which was consistent and corresponded to the urethane linkage degradation. In the second step, the degradation of the polymer backbone occurred. At this stage, AP was also degraded up to 360°C.

Figure 4-25 shows the detailed TGA graph between 100°C and 250°C. The weight changes of the propellant samples were calculated between 100°C and 220°C to identify the amount of plasticizer in these samples (see Table 4-7).

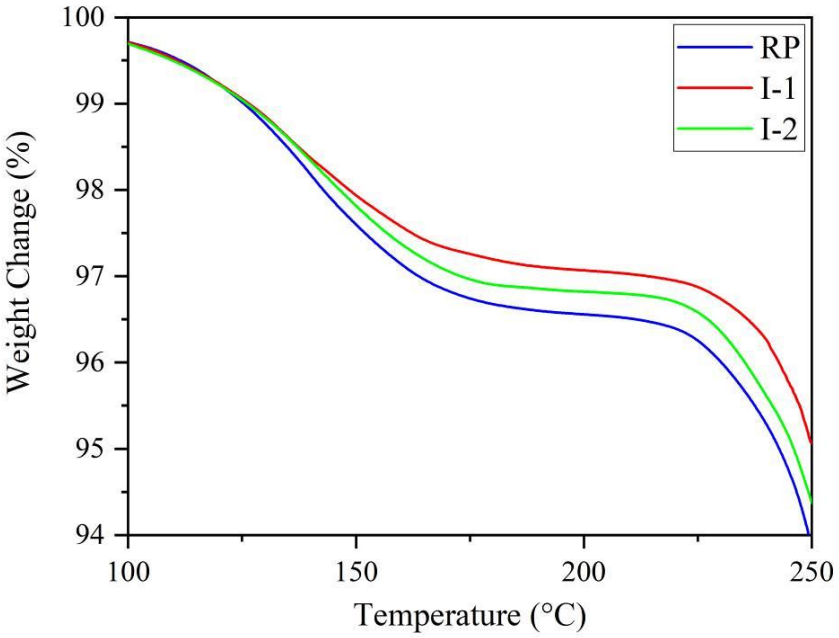

Figure 4-25. TGA curves of the propellant samples (RP, I-1, I-2) between 25°C and 250°C

The amount of IDP was obtained from Figure 4-25 as a % percent of the total propellant formulation. Then, the plasticizer/polymer ratio was also calculated (see Table 4-7) to observe the % percent of plasticizer that has been migrated.

Table 4-7. Weight changes of the propellant samples from 100°C to 220°C

Samples	**Weight Change (wt.%)**	**Plasticizer/Polymer (wt.%)**
RP	3.28	23.4
I-1	2.63	18.8
I-2	3.05	21.8

IDP in the RP sample was found as 23.4 wt.%. Table 4-7 shows that the plasticizer migrates from the propellant to the liner at the interface. The IDP content of the I-1 sample (18.8 wt.%) was lower than that of the I-2 sample (21.8 wt.%) since the carbon black particles in polyurethane liner (i.e., P10+DA1X2) interfaced with I-2

were dispersed better when the DA1 was added. Thus, the more efficient dispersion of carbon black particles made the polyurethane liner less permeable for the plasticizer migration. The mechanism is illustrated in Figure 4-26.

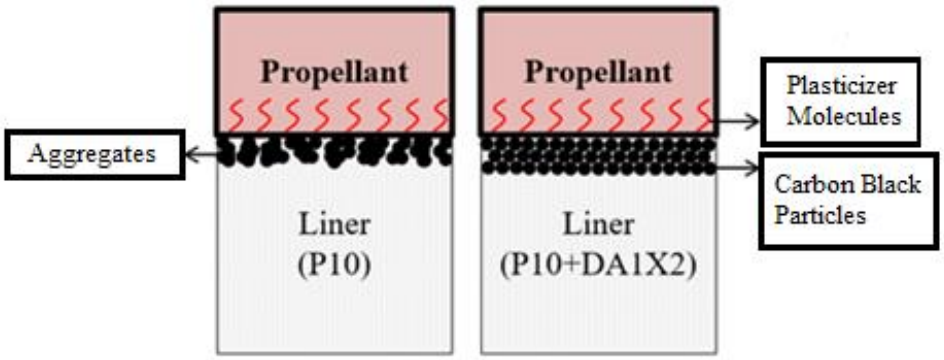

Figure 4-26. Effect of aggregates and well-dispersed particles on the migration at the interface

4.9.2 Attenuated Total Reflectance–Fourier Transform Infrared (ATR-FTIR) Spectroscopy Analysis

The plasticizer migration was also followed by Attenuated Total Reflectance Fourier Transform Infrared Spectroscopy (i.e., ATR-FTIR). The spectrum belonging to RP, I-1, I-2 samples are monitored in FTIR Spectrum (see Appendix E).

From Figure E.1 in Appendix E, the absorption bands of propellant samples in FTIR spectra consist of overlapping peaks. The curve-fitting can be used to separate absorption bands into individual peaks. The Gaussian fitting model was used to separate peaks, and then the peaks of functional groups were identified.

From the spectra Figure E.1, the characteristic spectral absorbance at 1640 cm^{-1} assigned to the C=C bond did not change during the reaction; therefore, the spectra were considered a reference peak. Guo et al. studied HTPB-IPDI curing reaction simultaneously, and they reported that 1640 cm^{-1} peak did not change during the curing reaction (Guo et al., 2018). As shown in Figure E.1, the absorption band around 3300 cm^{-1} assigned as N-H stretching shifted to around 3450 $cm^{-1,}$ and this

peak was to be assigned as NH_3. At the same time, the bending mode of NH became very weak at 1410 cm^{-1}. According to these two facts, the reaction occurred between AP and Bonding Agent in the propellant, which resulted in an ionic bond to play a role to adhere strongly HTPB binder to AP powder (Hori et al., 1985). During the curing reaction, the new absorption peaks appeared around 1700 - 1715 cm^{-1} attributed to polyurethane (-NHCOO-). Since IDP Plasticizer in the propellant formulation had an ester link, carbonyl stretching of ester (-C=O) at 1735 cm^{-1} was prominent. Thus, the absorption bands of polyurethane and carbonyl stretching of ester overlapped, and the peak should be separated (see Figure 4-27).

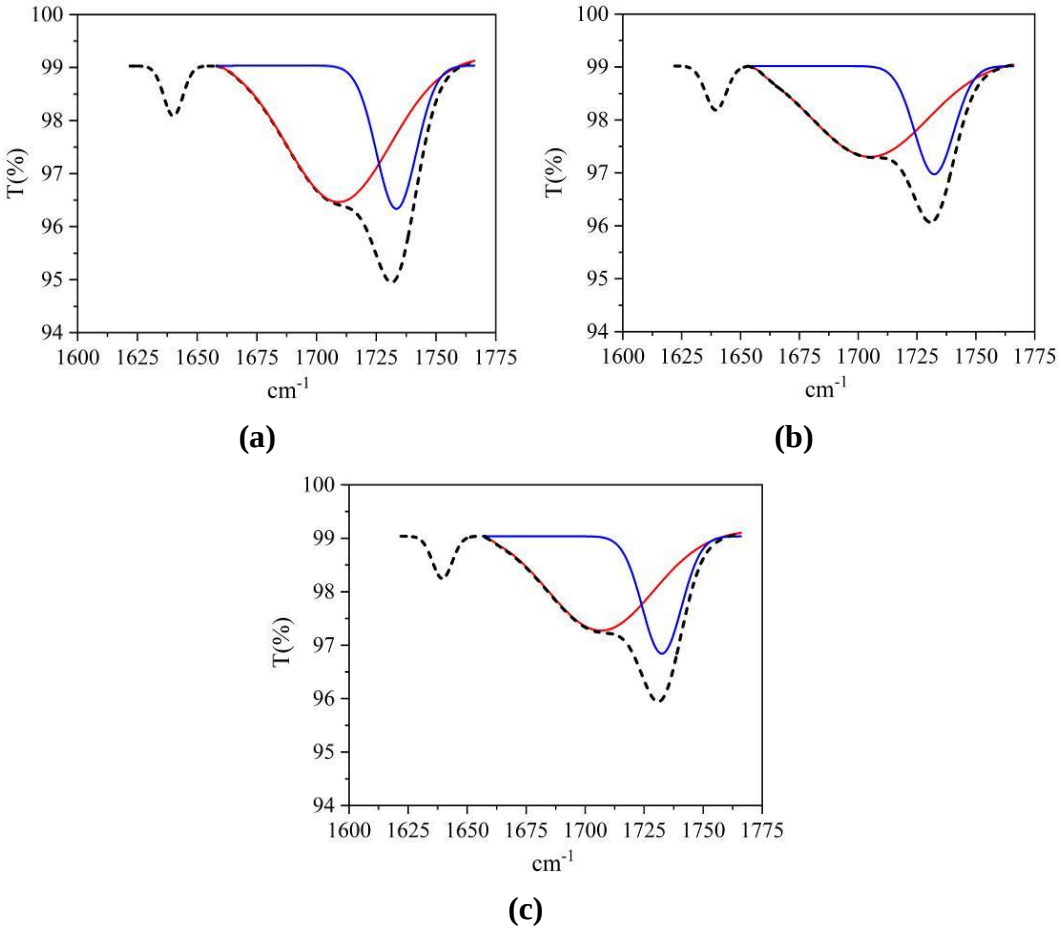

Figure 4-27. Absorption peaks of (a) RP, (b) I-1, (c) I-2 between the 1620 - 1735cm^{-1} spectrum

In Figure 4-27, the dashed line belongs to the original spectra of the samples between the 1620-1765cm^{-1}. Then, the original spectrum was deconvoluted to red and blue lines, which refer to polyurethane (-NHCOO-) and carbonyl stretching of ester (-C=O), respectively. According to Lambert Beer's law, a given peak area is directly proportional to the concentration. Hence, the peak area at 1735 cm^{-1} (i.e., blue curve) was calculated to specify the amount of IDP related to the carbonyl stretching of ester. The area under the 1735 cm^{-1} can be seen in Table 4-8.

Table 4-8. The area under specific peaks at FTIR spectrum.

Samples	**A (1640 cm-1)**	**A (1735 cm-1)**	**A (1735 cm-1)/ A (1640 cm-1)**
RP	9.41	56	5.95
I-1	9.18	45	4.90
I-2	9.89	50	5.09

From Table 4-8, the areas under 1735 cm^{-1} were divided by the areas under 1640 cm^{-1} that was the reference peak. Then, it was found that the IDP content of the RP was higher (i.e., 5.95) than those of the I-1 and I-2 samples (i.e., 4.90 and 5.09, respectively). The result indicated that the plasticizer diffusion occurred at the liner-propellant interface. The plasticizer content of the I-2 sample was higher than that of the I-1 sample since the more efficient dispersion of carbon black particles with the addition of the DA1 was decreased the permeability of the CB-filled polyurethane liner.

CHAPTER 5

CONCLUSION AND FUTURE WORKS

5.1 CONCLUSION

This study aims to improve the mechanical, rheological, and interface properties of the HTPB-IPDI based carbon black (CB) filled polyurethane liner formulation. Mechanical and interface properties are essential parameters since the CB-filled polyurethane liner must endure tensile and shear stresses during the operation condition of a rocket motor. The CB-filled polyurethane liner must also exhibit good adhesion strength related to observing cohesive failure from the propellant. Besides, the liner should have low enough viscosity to be applied easily.

The tensile strength and the elongation at break values of the currently used carbon black filled HTPB-IPDI based polyurethane liner (i.e., the standard liner) is about 1.3 MPa and 270%, respectively. Two types of carbon black powders (i.e., Thermax N-991 and Printex U) were used in this study, and three different dispersing agents (alkylammonium salt of a high molecular-weight copolymer (i.e., DA1), high molecular-weight copolymer with pigment affinic groups (i.e., DA2), and hydroxyl functional silicone modified polyacrylate (i.e., DA3) were used in this study. From the particle size analysis, the DA1 (2wt.% of DA1 based on CB) was the most effective dispersşng agent to reduce the agglomerate size of carbon black powders: the agglomerate size of Thermax N991 was lowered from 521 nm to 392nm, and that of Printex-U was lowered from 550 nm to 263 nm.

Two different types of carbon black with various amounts (2wt.%, 5wt.%, 10wt.%) were used in the polyurethane liner formulations. Then, the polyurethane liner (i.e., PT10) having a 5%+5% mixture of Thermax N991 and Printex-U was also prepared to observe the particle packing effect. First, the viscosity measurement of the CB-filled polyurethane liner formulations was carried out. The CB-filled polyurethane

liner formulations such as P10, T10, and PT10 were selected for further studies due to their proper viscosity value and mechanical properties. Tensile strengths of P10, T10, and PT10 liners were found as 1.77 MPa, 0.77 MPa, 1.3 MPa, respectively, and the elongation at break values were found as %375, %260, %275 for P10, T10, and PT10, respectively. Then, three types of dispersing agents were used to improve the properties of those liner formulations. The various amount of dispersing agents based on carbon black amount (1wt.%, 2wt.%, 3wt.%, 4wt.%) was added to the CB-filled polyurethane liner formulations. The highest improvement was obtained for the polyurethane liner formulation (i.e., P10+DA1X2), consisting of 10wt% of Printex-U carbon black and 2wt% of DA1 based on the Printex-U. The addition of 2wt% DA1 based on the Printex-U in P10 liner formulation increased the tensile strength from 1.77 MPa to 1.88 MPa and enhanced the elongation at break from 370% to 410%. Besides, storage modulus (E') at 25°C was increased from 2.75 MPa to 3.22 MPa. Moreover, the viscosity of the liner was decreased from 390 Poise to 205 Poise when 2wt% of DA1 based on the Printex-U was added to the P10 liner formulation. Thus, DA1 provides the best results in lowering viscosity and increasing mechanical strength due to its amphiphilic structure. While one tail clings to a carbon black surface, the other tail may react with a binder. In addition, DA1 was most effective for polyurethane liner filled with Printex-U CB since the highest surface area of a particle causes more adsorption of the polymer on the surface. SEM Images proved that DA1 effectively decreases the agglomerate size of Printex-U CB in the polyurethane liner. Furthermore, the LOI value was also increased from 19.5% to 22% when 2wt% of DA1 based on the Printex-U CB was used in the polyurethane liner.

The interface properties were related to both adhesion strength and plasticizer diffusion. It was observed that the usage of DA1 in P10 liner formulation did not significantly change the adhesion properties. In fact, the CB-filled polyurethane liner containing 2wt% of DA1 based on the Printex-U CB exhibits cohesive failure from the propellant. Moreover, the adhesion property of CB-filled polyurethane liner prepared using ultrasonication (i.e., P10+DA1X2-S) was the worst since the residual

solvent in this liner softens the liner-propellant interface. Plasticizer migration was observed using TGA and FTIR analysis. The study showed that migration could be lowered by using DA1 in the CB-filled polyurethane liner formulation since it provides more stabilized and well-dispersed particles that constitute an effective physical barrier. The amount of plasticizer was found as 2.63wt.% of total propellant formulation sampled from propellant-liner interface while it was increased to 3.05wt.% by adding DA1 to CB-filled polyurethane liner. FTIR result verified that the use of DA1 in the CB-filled polyurethane liner decreases the migration. Hence, the better dispersion of carbon black particles in the liner limits the plasticizer migration from the propellant. In addition, the crack formation may be prevented at the propellant-liner interface during the aging period of a rocket motor.

Within the scope of this thesis, the mechanical properties of the standard CB-filled polyurethane liner were initially improved using 10wt.% of Printex-U CB as a filler. Then, the use of 2wt% of DA1 based on Printex-U CB improved tensile strength to 1.88 MPa and the elongation at break to 410%. It has been shown that the use of DA1 not only decreases viscosity but also limits plasticizer migration from the propellant to the liner.

5.2 FUTURE WORKS

The study discussed in this thesis indicates many new directions for researchers to pursue further research in this field. Some of them are summarized below:

1. It is necessary to improve the flame retardant properties of the liner. Hence, the flame retardant behavior of carbon black filled polyurethane liner may be further improved using phosphorus, nitrogen, silicon, boron, zinc, iron, and aluminum-based flame retardant additives. The synergetic effect between CB and those additives can be investigated.
2. The processing steps can be improved to decrease the agglomerate size of carbon black powder. Ultrasonication was used in this thesis; however, it was

shown that solvent use may cause interface problems during the process. Thus, the instruments such as basket mills, ball mills, or high shear homogenizers can be used to prepare polyurethane liner.

3. If a carbon black powder with a smaller agglomerate size than Printex-U can be used, the polyurethane liner having better rheological, mechanical, and flame retardant behavior may be obtained. Interface properties should also be studied.

REFERENCES

Agbo, C., Jakpa, W., Sarkodie, B., & Boakye, A. (2017). A Review on the Mechanism of Pigment Dispersion. *Journal of Dispersion Science and Technology*, 1–16. https://doi.org/10.1080/01932691.2017.1406367

Ajaz, A. G. (1994). Hydroxyl Terminated Polybutadiene Telechelic Polymer (HTPB): Binder for Solid Rocket Propellants. *Rubber Chemistry and Technology*, *68*, 481–506.

Benli, S. (1997). *Effect of Fillers on Thermal and Mechanical Properties of Polyurethane Elastomer ¨*. 1057–1065.

Billmeyer, F. W. (1984). Textbook of Polymer Science. In *Kobunshi* (Issue 3). Wiley. https://doi.org/10.1295/kobunshi.12.240

Byrd, J. ., & Guy, C. A. (1985). Destructive Effects Of Diffusing Species In Propellant Bond Systems. *AIAA/SAE/ASME/ASEE 21 St Joint Propulsion Conference*.

Cao, G. (2004). *Nanostructures and Nanomaterials*. Imperial College Press.

Carraher, C. E., & Craver, C. D. (2000). *Applied Polymer Science* (1st ed.). Elsevier.

Chen, G. H., Tian, J., Liu, C., Li, D., & Lu, X. H. (2014). Analysis on the bonding property of the propellant and liner. *Advanced Materials Research*, *912–914*, 44–47. https://doi.org/10.4028/www.scientific.net/AMR.912-914.44

Donnet, J. B., Bansal, R. C., & Meng-Jiao, W. (1993). *Carbon Black: Science and Technology, Second Edition* (2nd ed.). Marcel Dekker, Inc. https://books.google.com/books?id=SPpx6MkRYwMC&pgis=1

Douglass, H. W. (1973). *Solid Propellant Processing Factors in Rocket Motor Design*.

Esfahani, A. R., Katbab, A. A., Dehkhoda, P., Karami, H. R., Barikani, M., Sadeghi, S. H. H., & Ghorbani, A. (2012). Preparation and characterization of foamed polyurethane/silicone rubber/graphite nanocomposite as radio frequency wave absorbing material: The role of interfacial compatibilization. *Composites Science and Technology*, *72*(3), 382–389. https://doi.org/10.1016/j.compscitech.2011.11.030

Esmaeilpour, M., Niroumand, B., Monshi, A., Ramezanzadeh, B., & Salahi, E. (2016). The role of surface energy reducing agent in the formation of self-induced nanoscale surface features and wetting behavior of polyurethane coatings. *Progress in Organic Coatings*, *90*, 317–323. https://doi.org/10.1016/j.porgcoat.2015.11.005

Furnas, C. C. (1931). Grading Aggregates. *Industrial and Engineering Chemistry*, *23*(9), 1052–1058.

Gercel, B. O., Üner, D. O., Pekel, F., & Özkar, S. (2001). Improved adhesive properties and bonding performance of HTPB-based polyurethane elastomer by using aziridine-type bond promoter. *Journal of Applied Polymer Science*, *80*(5), 806–814. https://doi.org/10.1002/1097-4628(20010502)80:5<806::aid-app1158>3.3.co;2-7

Giants, T. W. (1991). Case Bond Liner Systems for Solid Rocket Motors. *The Aerospace Corporation*. http://dtic.mil/dtic/tr/fulltext/u2/a242297.pdf

Guo, J., Chai, T., Liu, Y., Cui, J., Ma, H., & Jing, S. (2018). Kinetic Research on the Curing Reaction of Hydroxyl-Terminated Polybutadiene Based Polyurethane Binder System via FT-IR Measurements. *Coatings*, *8*(175), 1–9. https://doi.org/10.3390/coatings8050175

Hamilton, R., Wardle, R., & Hinshaw, J. C. (1994). *Oxazoline Bonding Agents in Composite Propellants* (Patent No. 5,366,572).

Harbers P. (2020). *Dispersion Technology*. https://www.uniqchem.com/dispersing-technology/

Haska, S. B., Bayramli, E., & Pekel, F. (1996). *Mechanical Properties of HTPB – IPDI-Based Elastomers*. 2347–2354.

Hauptman, N., Gunde, M. K., Kunaver, M., & Bešter-Rogač, M. (2011). Influence Of Dispersing Additives On The Conductivity Of Carbon Black Pigment Dispersion. *Journal of Coatings Technology and Research*, *8*(5), 553–561. https://doi.org/10.1007/s11998-011-9330-5

Hepburn, C. (1992). *Polyurethane Elastomers* (2nd ed.). Elsevier.

Herd, C. R., McDonald, G. C., & Hess, W. M. (1991). Morphology of Carbon Black Aggregates: Fractal Versus Euclidean Geometry. *Rubber Chemistry and Technology*, *65*.

Hori, K., Iwama, A., & Fukuda, T. (1985). On the adhesion between Hydroxyl-Terminated Polybutadiene Fuel-Binder and Ammonium Perchlorate. Performance of bonding agents. *Propellants, Explosives, Pyrotechnics*, *10*(6), 176–180. https://doi.org/10.1002/prep.19850100604

Hui, M., Yu-Cun, L., Tao, C., Tuo-Ping, H., Jia-Hu, G., Yan-Wu, Y., Jun-Ming, Y., Jian-Hua, W., Ning, Q., & Liang, Z. (2017). Kinetic studies on the cure reaction of hydroxyl-terminated polybutadiene-based polyurethane with variable catalysts by differential scanning calorimetry. *E-Polymers*, *17*(1), 89–94. https://doi.org/10.1515/epoly-2016-0245

Kakade, S. D., Navale, S. B., Kadam, U. B., & Gupta, M. (2001). Effect of fillers and fire retardant compounds on hydroxy-terminated polybutadiene-based insulators. *Defence Science Journal*, *51*(2), 133–140. https://doi.org/10.14429/dsj.51.2213

Kakade, S. D., Navale, S. B., & Narsimhan, V. L. (2003). Studies on interface properties of propellant liner for case-bonded composite propellants. *Journal of Energetic Materials*, *21*(2), 73–85. https://doi.org/10.1080/713845500

Kashiwagi, T., Mu, M., Winey, K., Cipriano, B., Raghavan, S. R., Pack, S., Rafailovich, M., Yang, Y., Grulke, E., Shields, J., Harris, R., & Douglas, J. (2008). Relation between the viscoelastic and flammability properties of polymer nanocomposites. *Polymer*, *49*(20), 4358–4368. https://doi.org/10.1016/j.polymer.2008.07.054

Kelsall, R. W., Hamley, I. W., & Geoghegan, M. (2005). *Nanoscale Science and Technology*. Wiley.

Kincal, D., & Özkar, S. (1997). Kinetic study of the reaction between hydroxyl-terminated polybutadiene and isophorone diisocyanate in bulk by quantitative FTIR spectroscopy. *Journal of Applied Polymer Science*, *66*(10), 1979–1983. https://doi.org/10.1002/(SICI)1097-4628(19971205)66:10<1979::AID-APP14>3.0.CO;2-Q

Koo, J. H. (2016). Fundamentals, Properties, and Applications of Polymer Nanocomposites. *In Fundamentals, Properties, and Applications of Polymer Nanocomposites* (pp. 1–270). Cambridge University Press. https://doi.org/https://doi.org/10.1017/CBO9781139342766

Korayem, A. H., Barati, M. R., Chen, S. J., Simon, G. P., Zhao, X. L., & Duan, W. H. (2015). Optimizing The Degree of Carbon Nanotube Dispersion In A Solvent For Producing Reinforced Epoxy Matrices. *Powder Technology*, *284*, 541–550. https://doi.org/10.1016/j.powtec.2015.07.023

Kraus, G. (1977). Reinforcement of elastomers by carbon black. *Die Angewandte Makromolekulare Chemie*, *60*(1), 215–248. https://doi.org/10.1002/apmc.1977.050600109

Krishnamurthy, V. N., & Varghese, T. L. (2017). *The Chemistry and Technology of Solid Rocket Propellants (A Treatise on Solid Propellants)* (p. 326).

Liu, Z. Q., Li, Z., Yang, Y. X., Zhang, Y. L., Wen, X., Li, N., Fu, C., Jian, R. K., Li, L. J., & Wang, D. Y. (2018). A geometry effect of carbon nanomaterials on flame retardancy and mechanical properties of ethylene-vinyl

acetate/magnesium hydroxide composites. *Polymers*, *10*(9). https://doi.org/10.3390/polym10091028

Loos, M. R., Yang, J., Feke, D. L., & Manas-Zloczower, I. (2012). Effect of block-copolymer dispersants on properties of carbon nanotube/epoxy systems. *Composites Science and Technology*, *72*(4), 482–488. https://doi.org/10.1016/j.compscitech.2011.11.034

Mahanta, A. K., & Pathak, D. D. (2012). HTPB-Polyurethane: A Versatile Fuel Binder for Composite Solid Propellant. *Polyurethane*. https://doi.org/10.5772/47995

Manjeet, M., & Raminder, K. (2017). Influence of Aliphatic and Aromatic Isocyanates on the Properties of Polyether-Ester Polyol Based PU Adhesive System. *Society of Plastics Engineers*. DOI 10.1002/pen.24537

Metravib. (n.d.). *Metravib DMA 450+ User Manual*.

Napper, D. H. (1984). *Polymeric Stabilization of Colloidal Dispersions*. Academic Press.

Norouzi, M., Zare, Y., & Kiany, P. (2015). Nanoparticles as Effective Flame Retardants for Natural and Synthetic Textile Polymers : Application, Mechanism, and Optimization. *Polymer Reviews*, *55*(1), 37–41. https://doi.org/10.1080/15583724.2014.980427

Oberth, A. E., & Bruenner, R. S. (1969). *Polyurethane-Based Propellants*. 84–121.

Pegoretti, A., & Dorigato, A. (2019). *Polymer Composites: Reinforcing Fillers* (Issue 1). https://doi.org/10.1002/0471440264.pst130.pub2

Pinto, J. A. R. (2006). *Optimization of Bondline's Properties of Solid Rocket Motors*.

Pirrung, F. O. H., Quednau, P. H., & Auschra, C. (2002). Wetting and dispersing agents. *Chimia*, *56*(5), 170–176. https://doi.org/10.2533/000942902777680496

PubChem. (n.d.). https://pubchem.ncbi.nlm.nih.gov/

Qi, X., Blizanac, B., Dupasquier, A., Oljaca, M., & Li, J. (2013). Understanding the influence of conductive carbon additives surface area on the rate performance of LiFePO 4 cathodes for lithium-ion batteries. *Carbon*, *64*, 334–340. https://doi.org/10.1016/j.carbon.2013.07.083

Rodić, V. (2007). Case Bonded System for Composite Solid Propellants. *Scientific Technical Review*, *LVII*(4), 11–21.

Ross, P., Escobar, G., Sevilla, G., & Quagliano, J. (2017). Micro and nanocomposites of polybutadiene-based polyurethane liners with mineral fillers and nanoclay: Thermal and mechanical properties. *Open Chemistry*, *15*(1), 46–52. https://doi.org/10.1515/chem-2017-0006

Rothon, R. (2017). Fillers for Polymer Applications. In *Springer*. https://doi.org/10.1007/978-3-319-28117-9

Sethi, J. (2014). *Carbon Nanotubes filled Polyurethane Nanocomposites: A Filler Morphology and Surfactant Study*. Tampere University of Technology.

Tang, G., Ranch, S., Scott Joseph, M., & Edward Francis, R. (2014). Method of Mitigating Ice Build-Up On A Substrate (Patent No. 2014/0212584). In *Apparatus and Methods for Controlling and Applying Flash Lamp Radiation* (2014/0212584).

Toulemonde, P. A., Diani, J., Gilormini, P., Desgardin, N., & Nevière, R. (2018). Propellant cohesive fracture during the peel test of a propellant/liner structure. *Journal of Adhesion*, *94*(8), 657–666. https://doi.org/10.1080/00218464.2017.1332999

Ullmann, F. (2016). *Ullmann's Polymers and Plastics* (B. Elvers (Ed.); 7th ed.). Wiley-VCH.

Venkatesan, D., Srinivasan, M., Reddy, K. A., & Pendse, V. V. (1993). The migration of plasticizer in solid propellant grains. *Polymer International*, *32*(4), 395–399. https://doi.org/10.1002/pi.4990320410

Villar, L. D., Cicaglioni, T., Diniz, M. F., Takahashi, M. F. K., & Rezende, L. C. (2011). Thermal aging of HTPB/IPDI-based polyurethane as a function of NCO/OH ratio. *Materials Research*, *14*(3), 372–375. https://doi.org/10.1590/S1516-14392011005000063

Vogelsanger, B., Ossola, B., & Brönnimann, E. (1996). The diffusion of deterrents into propellants observed by FTIR microspectroscopy - Quantification of the diffusion process. *Propellants, Explosives, Pyrotechnics*, *21*(6), 330–336. https://doi.org/10.1002/prep.19960210609

Xia, H., & Song, M. (2005). Preparation and characterization of polyurethane-carbon nanotube composites. *Soft Matter*, *1*(5), 386–394. https://doi.org/10.1039/b509038e

Yadav, A., Pant, C. S., & Das, S. (2020). Research Advances in Bonding Agents for Composite Propellants. *Propellants, Explosives, Pyrotechnics*, *45*(5), 695–704. https://doi.org/10.1002/prep.201900329

Yang, H., Ye, L., Gong, J., Li, M., Jiang, Z., Wen, X., Chen, H., Tian, N., & Tang, T. (2017). Simultaneously improving the mechanical properties and flame retardancy of polypropylene using functionalized carbon nanotubes by covalently wrapping flame retardants followed by linking polypropylene. *Materials Chemistry Frontiers*, *1*(4), 716–726. https://doi.org/10.1039/c6qm00172f

Zhao, Y., & Duan, Y. X. (2007). The Dispersion of MWCNTs within Epoxy by Treatment with Coupling and Dispersing Agents. *Materials Science Forum*, *546–549*, 2307–2312. https://doi.org/10.4028/www.scientific.net/msf.546-549.2307

Zhou, Q. C., Xu, J. S., Chen, X., & Zhou, C. S. (2016). Review of the adhesively bonded interface in a solid rocket motor. *Journal of Adhesion*, *92*(5), 402–428. https://doi.org/10.1080/00218464.2015.1040155

APPENDICES

A. Classification of Carbon Black Particles

Table A-1. Classification carbon black according to ASTM D1765

Name	**Standard Abbreviation**	**ASTM Designation**	**Particle Size (nm)**	**Average N_2 Surface Area (m^2 /g)**
Super Abrasion Furnace	SAF	N110	15–18	124–130
Intermediate SAF	ISAF	N220	20–25	112–115
High Abrasion Furnace	HAF	N330	28–36	76–80
Fast Extrusion Furnace	FEF	N550	39–55	39–41
General Purpose Furnace	GPF	N660	56–70	34–36
Semi Reinforcing Furnace	SRF	N770	71–96	31–32
Fine Thermal	FT	N880	180–200	17–20
Medium Thermal	MT	N990	250–350	7–9

B. Particle Size Analysis

Table B-1. Particle size of the carbon black samples according to ultrasonication parameters.

Sample	**S1**									**S2**								
P	**200 W**									**300 W**								
D	**1 min**			**5 min**			**15 min**			1 min			5 min			15 min		
S	10	9	7	10	9	7	10	9	7	10	9	7	10	9	7	10	9	7
W	0	1	3	0	1	3	0	1	3	0	1	3	0	1	3	0	1	3
D(4:3) nm	558	530	521	420	310	300	636	617	592	362	346	319	308	243	195	706	706	688
D(3:2) nm	448	425	418	358	256	249	511	500	492	290	282	265	255	207	157	567	567	554
Span	0.99	0.99	0.97	1.10	1.07	1.07	1.19	1.16	1.11	1.2	1.0	0.98	1.1	0.99	0.94	1.44	1.39	1.10

Sample	**S3**								
P	**400 W**								
D	**1 min**			**5 min**			**15 min**		
S	10	9	7	10	9	7	10	9	7
W	0	1	3	0	1	3	0	1	3
D(4:3) nm	326	322	322	582	571	439	786	770	655
D(3:2) nm	280	268	268	477	474	368	664	651	553
Span	1.12	1.1	1.1	1.42	1.38	1.3	1.47	1.47	1.44

S: Sample
P: Ultrasonic Power (Watt)
D: Duration Time (minutes)
S/W: Start/Wait Time during ultrasonication (Seconds-Seconds)

C. Curing Analysis

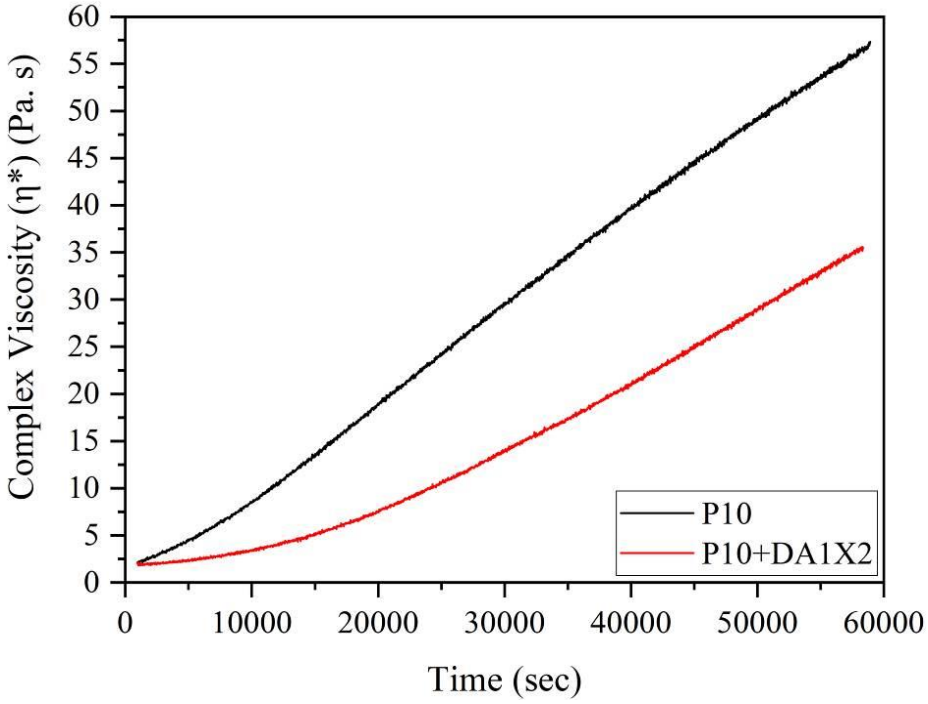

Figure C-1. Complex Viscosity graph of the samples

D. Vacuum Thermal Stability Test (VTS) Results

Table D-1. The samples evolved gas after 48 hours at 100°C

Sample	V (cm^3)
RP	0.455
Liner(P10)	1.1
Liner(P10+DA1X2)	0.898
Liner(P10+DA1X2–S)	0.925
RP+ Liner(P10)	1.721
RP+ Liner(P10+DA1X2)	1.647
RP+ Liner(P10+DA1X2-S)	1.872

According to, Equation 6 is applied to find volume of the gas evolved after the test (see Chaper 3.7).

$$V_{Liner(P10)}=1.721-(1.1+0.455)=0.116<5\ cm^3$$

$$V_{Liner(P10+DA1X2)}=1.647-(0.898+0.455)=0.294<5\ cm^3$$

$$V_{Liner(P10+DA1X2-S)}=1.872-(0.925+0.455)=0.492<5\ cm^3$$

E. FTIR Analysis

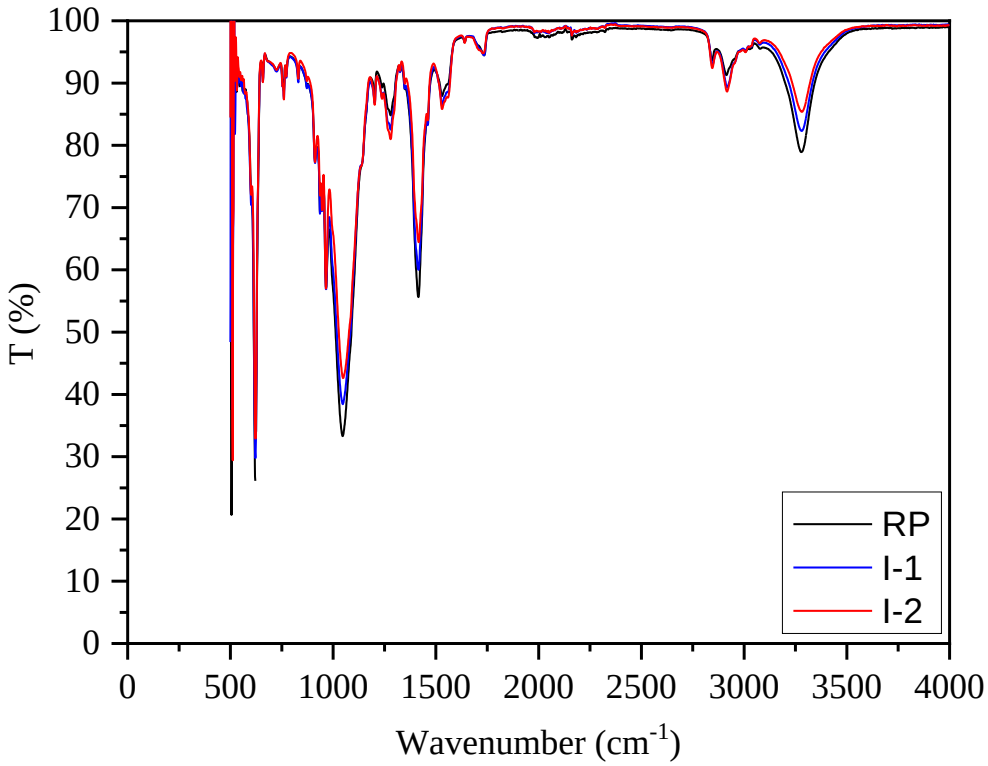

Figure E-1. FTIR Spectrum of the propellant samples RP, I-1, and I-2